AN ABSTRACT OF THE THESIS OF

CARLOS LOPEZ for the degree of MASTER OF SCIENCE

in OCEANOGRAPHY presented on SEPTEMBER 19, 1977

Title: ELEMENTAL DISTRIBUTIONS IN THE COMPONENTS OF METALLIFEROUS SEDIMENTS FROM THE BAUER AND ROGGEVEEN BASINS - NAZCA PLATE

Redacted for privacy

Abstract Approved: _____
Dr. John B. Corliss

Major and trace element analyses were made on biogenic carbonate, silica, and fish debris and on authigenic phillipsite, micronodules, and yellow and brown aggregates recovered from Bauer and Roggeveen Basin metalliferous sediments. Phase components and the bulk samples were analyzed by INAA and AAS methods. Leachates and residues from ammonium oxalate and mild HCl leaches of bulk and fine sediment fractions were also analyzed. The mild acid leach removed fish debris and carbonate, and the oxalate leach dissolved the micronodule phase. Sediments of the Bauer and Roggeveen Basins differ in bulk composition, yet respond to various chemical treatments in similar manner. I interpret this as indicative of a close similarity in the mineralogy of these two areas.

An iron-rich smectite, manganese micronodules, and fish debris dominate the sediment compositions of both basins. The smectite phase concentrates Fe, Si, and Al. Manganese, Co, Ni, Ce, and W are concentrated in the micronodule phase and Ca, Sc, and the lanthanides predominantly in the fish debris component. The trace elements Cu, Zn, As, and Sb are distributed in a complex manner among the three principal phases.

Barium, and some Al and Fe, may be present in small quantities of barite, feldspars, and goethite, respectively. Silica, carbonate, and phillipsite phases exist in such low concentrations that they do not contribute significantly to the bulk composition of the sediments. The response of the various size fractions leached indicates a uniformity of distribution of sediment components from the coarse to the fine fractions.

ELEMENTAL DISTRIBUTIONS IN THE COMPONENTS OF METALLIFEROUS SEDIMENTS FROM THE BAUER AND ROGGEVEEN BASINS - NAZCA PLATE

by

Carlos Lopez

A THESIS

submitted to

Oregon State University

in partial fulfillment of
the requirements for the
degree of

Master of Science

June 1978

APPROVED:

Redacted for privacy

Professor of Oceanography in Charge of Major

Redacted for privacy

Acting Dean of School of Oceanography

Redacted for privacy

Dean of Graduate School

Date thesis is presented September 19, 1977

Typed by Cheryl M. Schurg for Carlos Lopez

TABLE OF CONTENTS

TABLE OF CONTENTS (continued)

LIST OF TABLES

LIST OF TABLES (continued)

LIST OF FIGURES

LIST OF FIGURES (continued)

LIST OF FIGURES (continued)

ELEMENTAL DISTRIBUTIONS IN THE COMPONENTS OF METALLIFEROUS SEDIMENTS FROM THE BAUER AND ROGGEVEEN BASINS - NAZCA PLATE

1.0 INTRODUCTION

Metalliferous sediments characterized by high transition element to aluminum ratios were first reported and described for the South East Pacific by Murray and Renard (1891). These sediments have been found to be widely distributed over the Nazca Plate both as surficial and basal deposits (Bostrom and Peterson, 1966; Sayles et al., 1975; Dymond et al., 1976). The existence of basal metalliferous sediments in other areas of the Pacific Ocean has been documented by the Deep Sea Drilling Project (von der Borch and Rex, 1970; von der Borch et al., 1971; Cronan, 1972). Bonatti (1975) has reported the existance of analagous surface deposits from spreading centers in the Atlantic, Pacific, Indian, and Antarctic Oceans, and the Red Sea. It was, however, the work of Bostrom and Peterson (1966, 1969) and Bostrom et al. (1969) that focused attention on the origin of such sediments and their relationship to the volcanic activity associated with the East Pacific Rise.

The chemical and mineralogical composition of a sediment reflects its genesis and the source of its constituent elements; the unique character of metalliferous sediments has therefore stimulated considerable research directed at understanding the processes of formation of such deposits. The results of such work bear on the economic potential of these deposits and aids in understanding how certain types of ore bodies may form. Extensive chemical analyses by Dymond et al. (1976, 1977) have helped to show that there exist strong similarities

between basal and surficial metalliferous sediment deposits. These authors have shown that hydrothermal sources of metals are important in forming basal and rise crest deposits, as well as in forming the deposits of the Bauer Basin. Sayles et al. (1975) found that the formation of micronodules significantly influences the sediment composition, and Dymond and Veeh (1975) found that the accumulation rates of Fe, Mn, Cu, Ni, and Zn in the Bauer Basin are comparable to those determined for the East Pacific Rise.

Dasch et al. (1971) studying the Sr and Pb isotope ratios of a Bauer Basin sample proposed that Sr was derived from a sea water source while Pb was of mantle origin. Dymond et al. (1973) have shown that metalliferous sediments of the Nazca Plate consist primarily of manganese hydroxides, goethite, and an iron-rich montmorillonite (smectite). They have also shown that the lanthanide element and sulfur isotope compositions of these deposits are similar to those of sea water and are most likely derived from this source. Heath and Dymond (1977) have placed emphasis on describing metalliferous sediments in terms of hydrothermal, detrital, hydrogenous, and biogenic inputs. Individual sediment phases, i.e. fish debris micronodules, todorokite, and smectite grains, have been examined and analyzed by Eklund (1974).

My work deals with the relationship between the bulk chemistry of Bauer and Roggeveen Basin sediments and the chemical composition of individual sediment components. Various types of leaches designed to remove fish debris and carbonate, and/or amorphous iron and manganese oxyhydroxides, were carried out on bulk sediments, as well as on silt

and clay sized sediment fractions. The results indicate that some components account for nearly the total concentration of certain elements, i.e. the lanthanides reside predominantly in the fish debris component, Mn, Ni, Co, Ce, and W are concentrated in the micronodules and Al, Si, and Fe were concentrated in the smectite component. The Roggeveen Basin shows evidence of a separate "excess iron" component, possibly goethite.

From the results of the leach experiments and the chemical composition of individual phases, it was possible to define the phase composition of the sediments from each site and to determine a structural formula for the smectites of each basin.

1.1 Physical Setting

The samples studied were recovered from the Bauer and Roggeveen Basins of the western Nazca Plate. The Bauer Basin is defined by the fossil Galapagos Rise (GR) on the east and the East Pacific Rise (EPR) on the north and west. To the south this basin merges with the Yupanqui Basin. The Roggeveen Basin, separated from the Yupanqui Basin by the Sala y Gomez Ridge, is also bounded by the EPR and GR, and its southern limit is the South Chile Ridge (Figure 1).

Each of the cores studied was recovered during the YALOC 73 cruise conducted as part of the Oregon State University Nazca Plate study program. All are from below the local calcium compensation depth (CCD) (see Table 1). It was found that the sediment cover of the northwestern Nazca Plate is limited in continuity and thickness and that the bathymetry is very rugged (Heath, 1973). In the Roggeveen Basin the sediment cover is

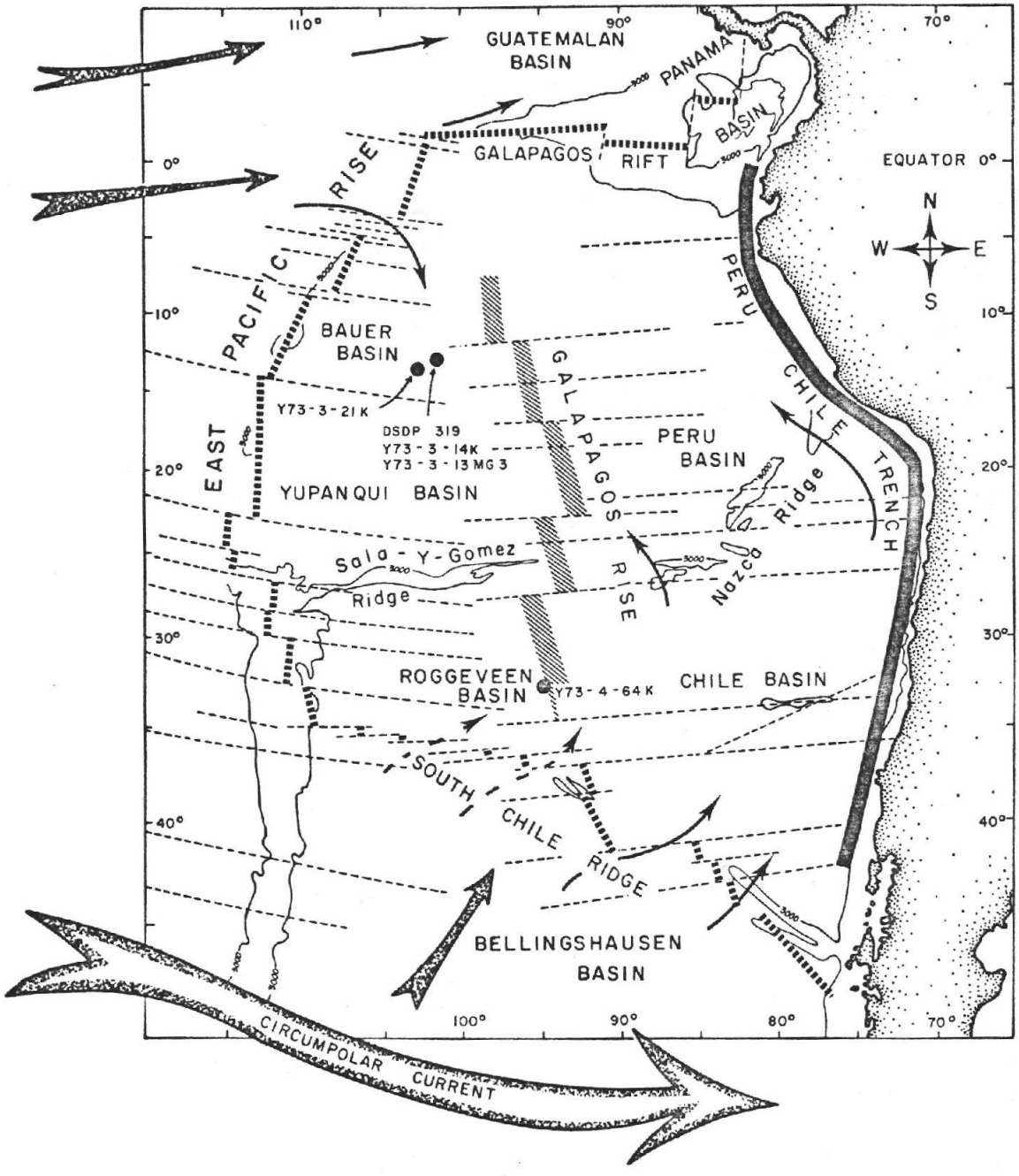

Figure 1. Schematic bathymetric map of the Nazca Plate after Herron (1972). Bottom water flow patterns from Lonsdale (1976).

TABLE 1

Location* of Cores Referred to in this Work

Core I.D.	Latitude	Longitude	Water Depth	Text Designation
Y73-3-14K	13°00.0'S	101°33.0'W	4,290 m.	(BBS) for Bauer Basin Surface Sample
Y73-3-21K	13°37.0'S	102°32.0'W	4,410 m.	(BBD) for Bauer Basin Downcore sample
Y73-4-64K	32°46.0'S	94°42.0'W	4,128 m.	(RBD) for Roggeveen Basin Downcore sample
Y73-3-13 MG-3	12°59.0'S	101°33.0'W	4,318 m.	(BBS-2) for Bauer Basin Surface 2nd Sample
DSDP - 319	13°01.04'S	101°31.46°W	4,296 m.	

* Based on best satellite navigation estimate.

thicker, more uniform, and the topography considerably gentler. Veeh, and Moser (written communications) have both found the sedimentation rate in the Roggeveen Basin to be about twice as high as that of the Bauer Basin.

Lonsdale (1976) has constructed a bottom water circulation pattern over the Nazca Plate from hydrographic data and direct current measurements. In general, bottom waters enter the Bauer Basin from the west through fracture zones in the northern EPR and into the Roggeveen Basin from the south through the fracture zones of the South Chile Ridge.

The cores examined in this work, BBS, BBD, and RBD are from, relatively speaking, analagous settings. They are all: a) below the local CCD, which precludes the accumulation of a significant carbonate component, b) on the western side of the fossil GR and, therefore, effectively protected from important terrigenous influxes of sediments from South America, and c) in the direct path of bottom water flows which recently passed through active fracture zones. Moreover, the samples used in this study are each typical in chemical composition of other metalliferous sediments recovered from the Bauer and Roggeveen Basins. An extensive data set is presently being examined in preparation for a comprehensive study of Nazca Plate metalliferous sediments (Corliss et al., in preparation).

1.2 Core Descriptions

a) Bauer Basin Surface Sample (BBS) - Y73-3-14K

This short Kasten core consisted of some eleven liters of a very

dark brown metalliferous sediment, with light brown mottles. The presence of agglutinated foraminifera, numerous radiolaria, and pelagic foraminifera in a good state of preservation indicate this to be a surface sediment sample.

b) Bauer Basin Down Core Sample (BBD) - Y73-3-21K

The core catcher material from this 160 cm long Kasten core was used. Organic silica was rare, and the biogenic carbonate present severely corroded in this metalliferous sediment sample.

c) Roggeveen Basin Down Core Sample (RBD) - Y73-4-64K

This core also consisted entirely of a dark brown metalliferous sediment and was 180 cm long. As with BBD, the core catcher sample was used. This sample had less organic silica or carbonate than did the BBD sample.

1.3 Methodology

A brief outline of the complete methodology of Appendix I is given here.

Sample BBS was slurried, wet sieved, and washed to provide four size fractions (Figure 2). From these visually pure mineral phases were separated by hand picking under a reflected light bionocular microscope (20-40 x). This yielded seven distinct components, i.e. fish debris, carbonate and siliceous tests, phillipsite, Mn-micronodules, and brown and yellow aggregates (Figure 3). These components were photographed, examined by scanning electron microscopy (SEM), and x-ray

Preliminary Treatment of the BBS (Y73-3-14K) Sample for the Recovery of Individual Sediment Components

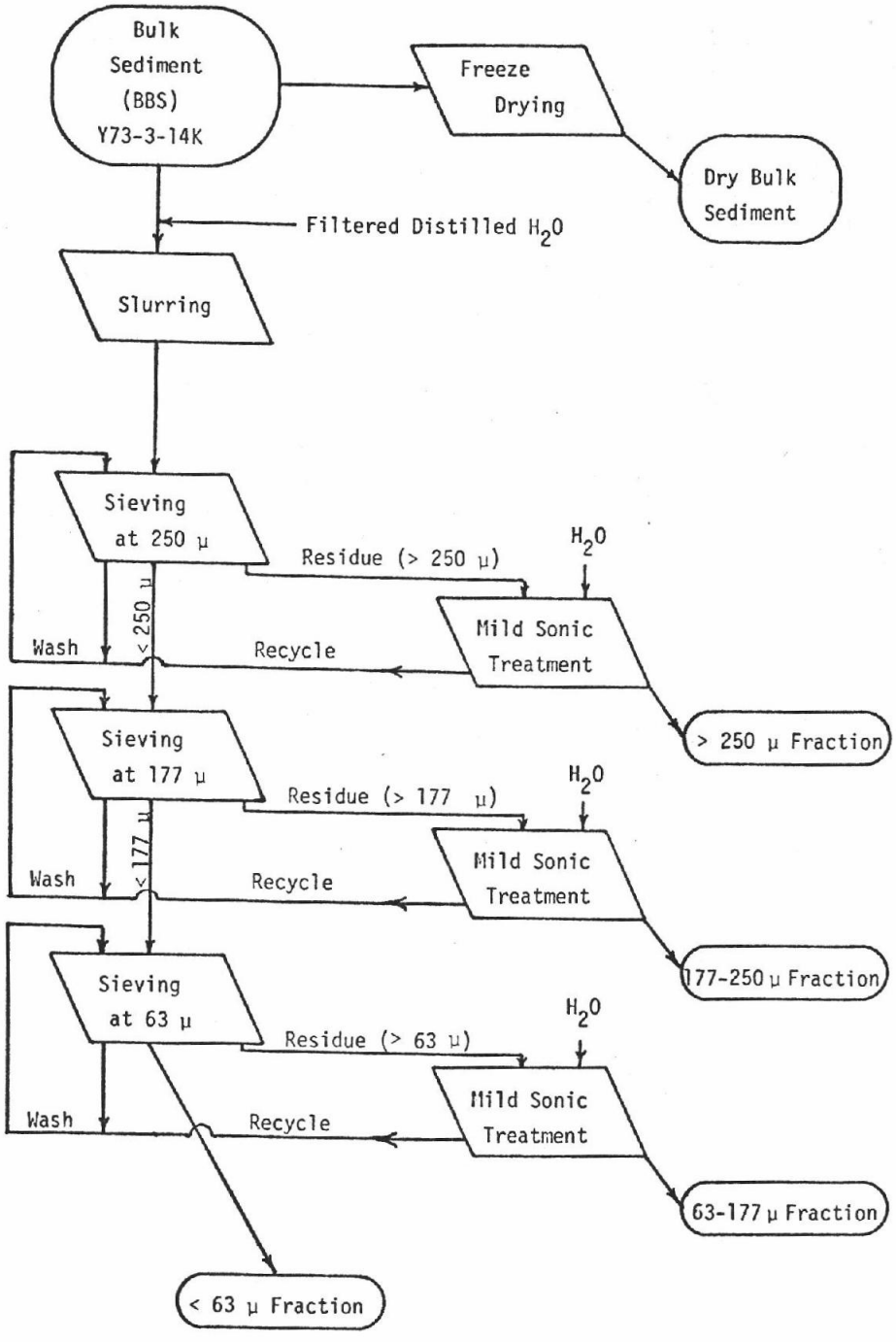

Figure 2

Hand Picking Scheme for the Recovery of Individual Sediment Components from Various Size Fractions of BBS (Y73-3-14K)

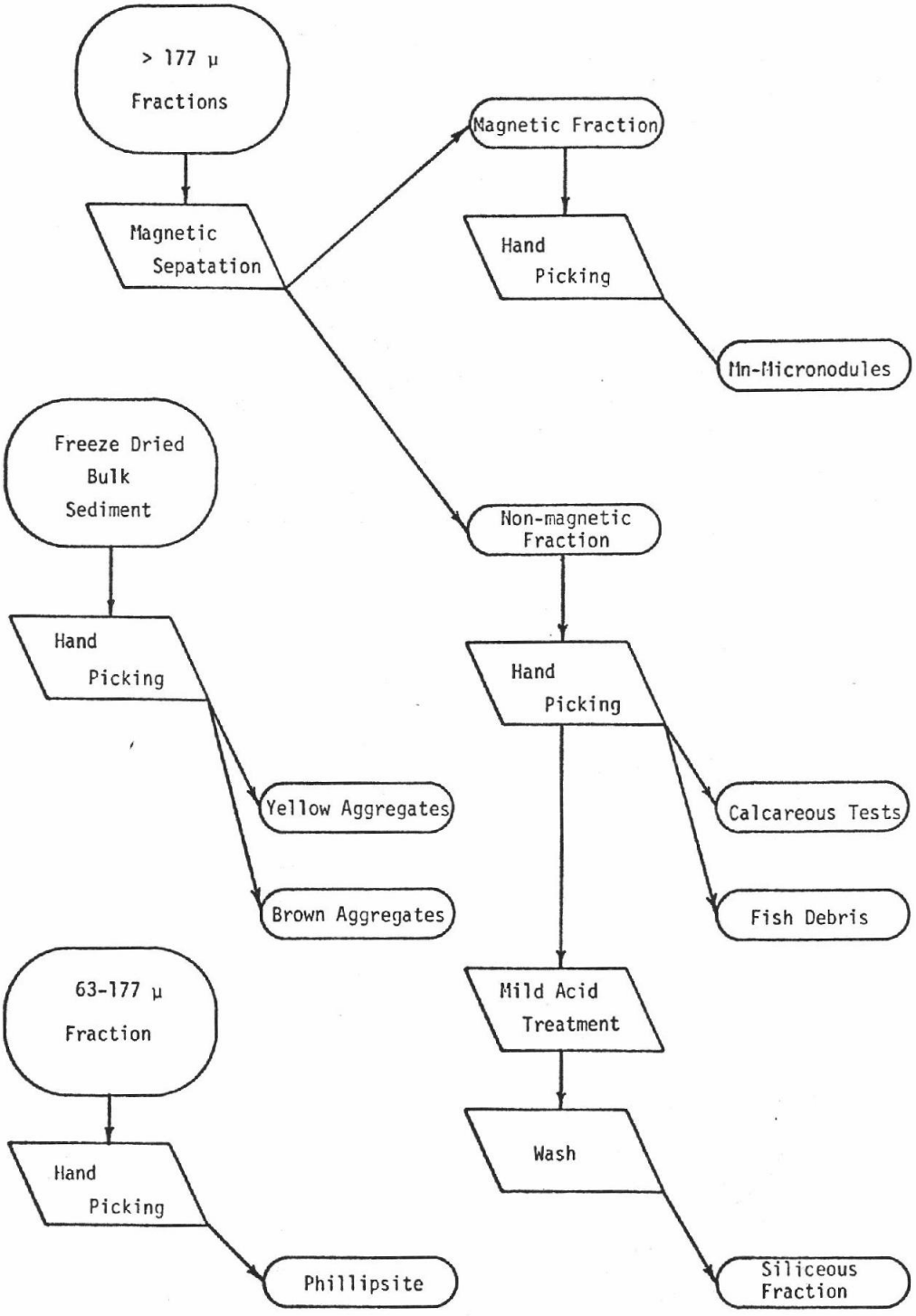

Figure 3

Schematic Outline of Pre-Leaching and Component Separation Work Performed on Bulk Sediment Samples of BBD and RBD (Y73-3-21K and Y73-4-64K)

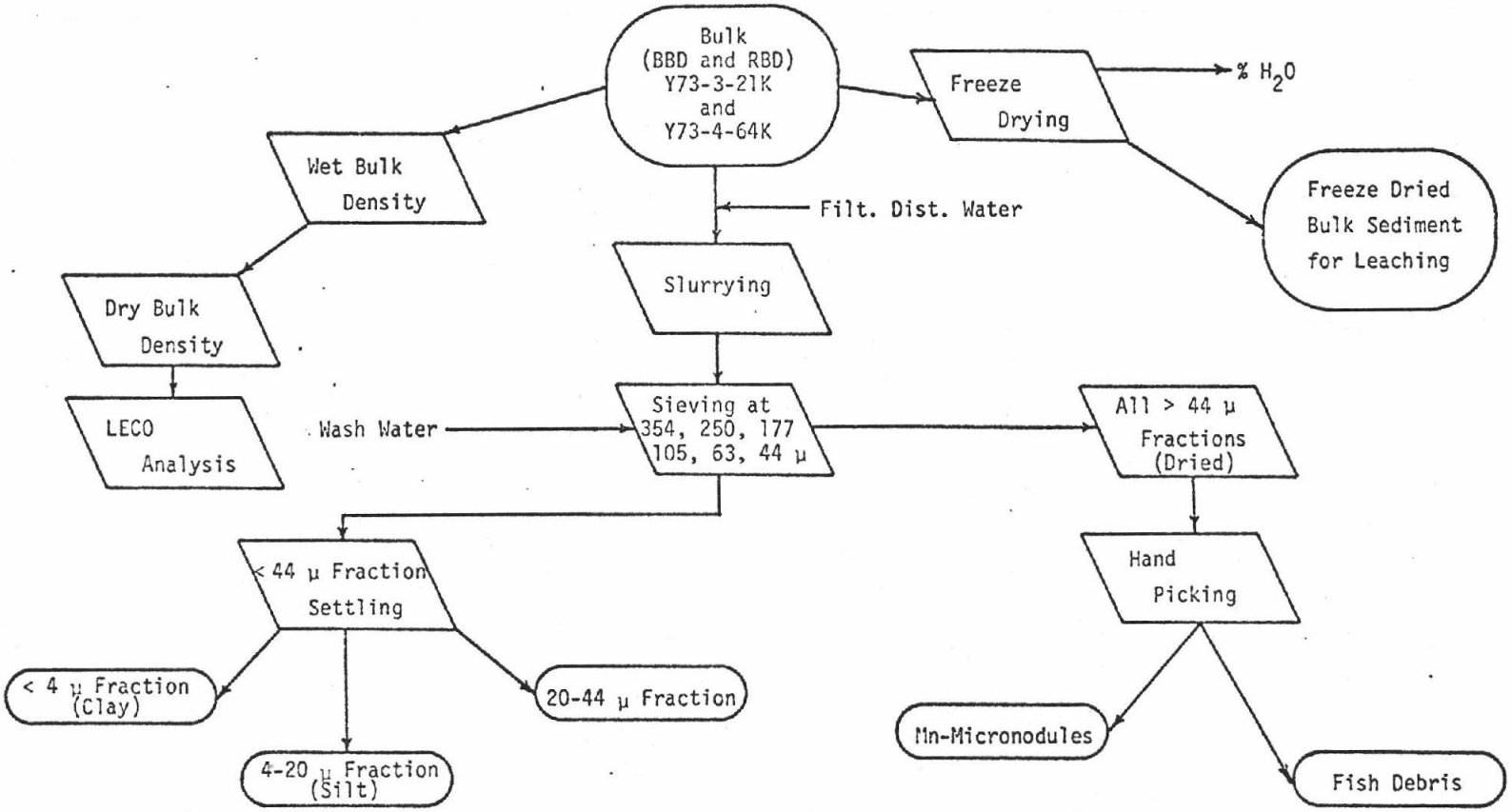

Figure 4

Schematic Outline of the Leaching Experiments and the Subsequent Atomic Absorbtion Spectroscopy (AAS) and Instrumental Neutron Activation Analysis (INAA) Work Performed on BBD and RBD

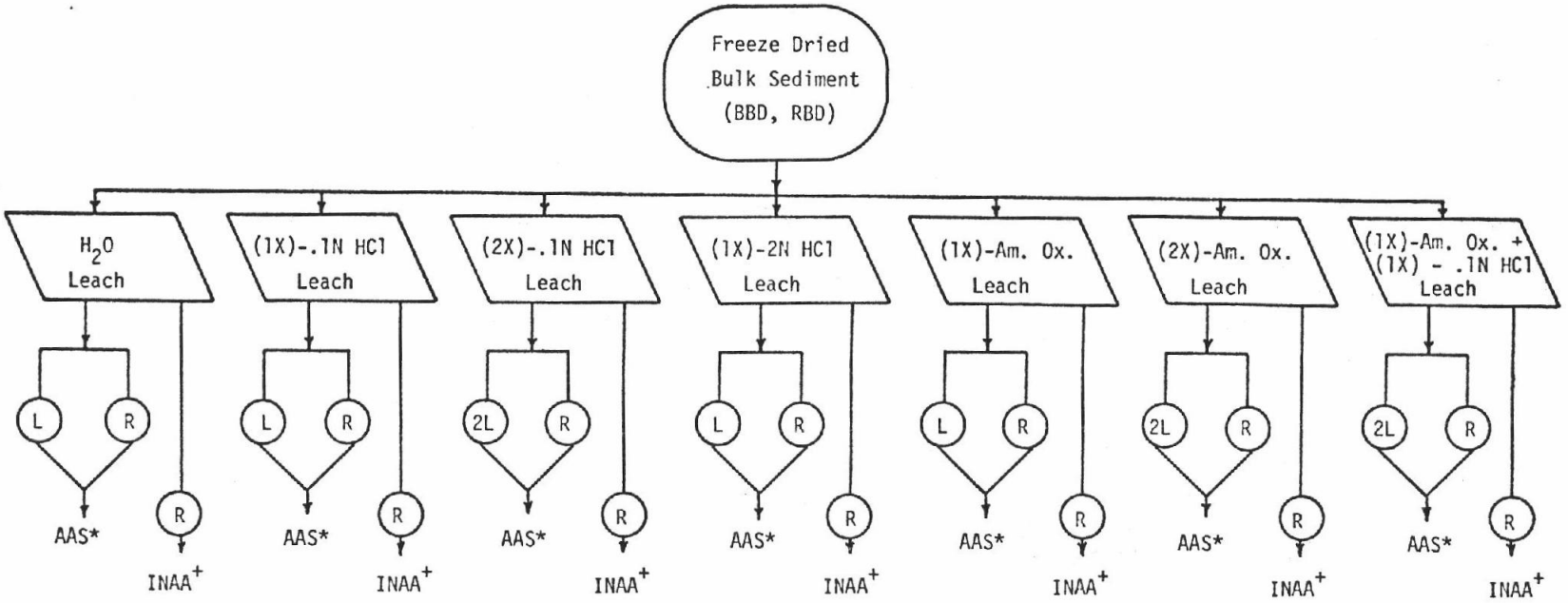

* One (L) or two (2L) leachates and the residue (R) from one experiment were analyzed by AAS (10 leachates and 7 residues each for BBD and RBD).

+ Residues (R) and a second leaching experiment were examined by INAA (7 residues each for BBD and RBD).

Figure 5

Outline of the Leaching Experiments and Subsequent Instrumental Neutron Activation Work Performed on the Bulk, Silt, and Clay Size Fractions of BBD and RBD (Y73-3-21K and Y73-4-64K)

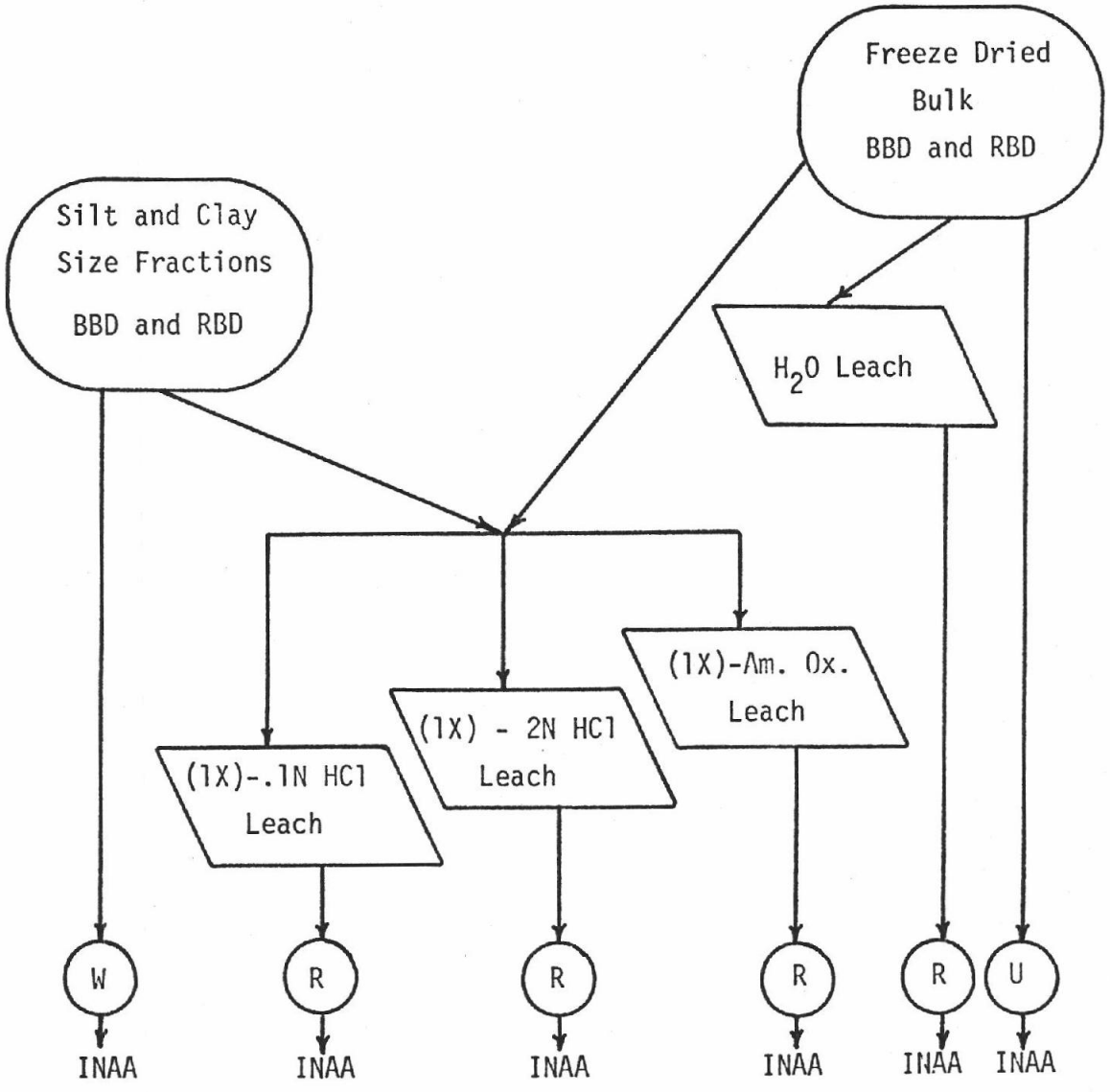

W = Unleached water washed samples of the silt and clay sized fractions of BBD and RBD.

R = Residues of leached samples of the various sized fractions of BBD and RBD.

U = Untreated samples of freeze dried BBD and RBD bulk sediments.

Figure 6

methods, and analyzed by instrumental neutron activation analysis (INAA).

Samples BBD and RBD were similarly handled and two major components, fish debris and micronodules, recovered. Subsamples were taken for wet, and dry bulk density, percent water by freeze drying, percent volatiles, and carbonate determinations. A less than 44 μ sized fraction of BBD and RBD was size settled to recover a clay (< 4 μ) and silt (4-20 μ) sample. These and a salt free bulk sample were subjected to separate leach treatments. An outline of the leaching and analytical scheme for BBD and RBD is given in Figures 4, 5, and 6. The procedure consisted of treating subsamples of each material with various acid, and/or ammonium oxalate solutions and examining the leachates and residues by AAS, or INAA for major and trace elements. The bulk samples were also analyzed by AAS.

2.0 PHASE SEPARATION RESULTS

From the BBS sediment, it was possible to separate out enough biogenic silica, carbonate, fish debris, and authigenic micronodules, and phillipsite to do INAA work on these components. Because of the absence of several components in BBD and RBD, only two phases (fish debris and micronodules) were recovered from these sediments in sufficient quantity to allow INAA work.

The results indicate that:

1) trace element concentrations in the organic carbonate and silica fractions are low, and that these phases are inconsequential contributors to the trace element chemistry of the sediments examined,

2) the lanthanide element and Sc concentrations in the fish debris are significantly higher than in the bulk sediment,

3) manganese, Ni and Co are significantly enriched in the manganese nodule phase,

4) cerium is enriched in the micronodule and depleted in fish debris phases relative to other lanthanides,

5) phillipsite shows an enrichment of Cr and Hf over the bulk sediment but is considered to have little influence on the sediment chemistry due to its low concentration,

6) although the bulk sediment BBS shows a sea water like lanthanide pattern, individual components deviate markedly from such a pattern,

7) in general the composition of the bulk sediment and the individual phases constituting the sediment are distinctly different.

Analytical results and available comparative literature data are given in each section.

2.1 Analytical Results for Components Recovered from BBS, BBD, and RBD

2.1.1 Biogenic Carbonate

A carbonate separate was recovered only from BBS. The tests recovered were primarily those of pelagic foraminifera and were in a good state of preservation (Figure 7). The trace element concentrations for this component were compared to other organic carbonate results for planktonic organisms and the data found to agree quite well (Table 2). To extend the range of possible comparisons trace element data are used for pteropod tests (Turekian et al., 1973), coccolith ooze (Thompson and Bowen, 1969), "biogenic $CaCO_3$" (Spirn, 1965), in addition to the planktonic foraminifera data of Krinsley (1960), Emiliani (1955), and Thompson and Bowen (1969).

An x-ray analysis of the tests indicated a pure calcite pattern. Some contamination of the tests by authigenic deposits cannot be completely excluded. Manganese growths on test fragments was observed (Figure 8) but the contribution of trace elements from such contamination should be minimal, as only the cleanest tests were used for analysis.

The carbonate content of the bulk sediment of BBD is 2.0% and 0.9% for RBD. Considering the low elemental concentrations in this phase, it may be concluded that it is not an important component in determining the composition of the metalliferous sediments of the Bauer or Rog-

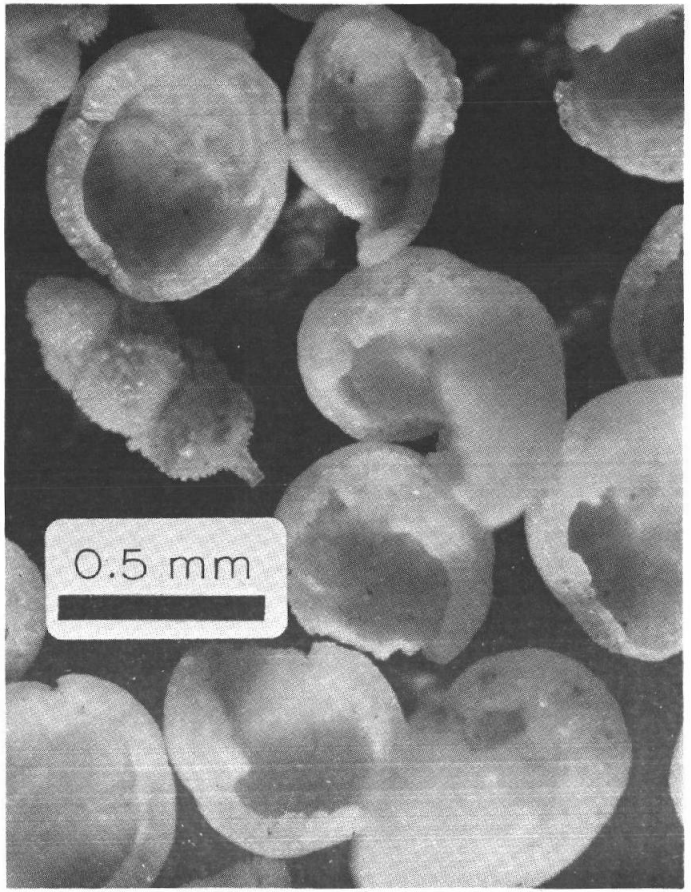

Figure 7. Carbonate tests of planctonic and benthonic foraminifera recovered from BBS for INAA work.

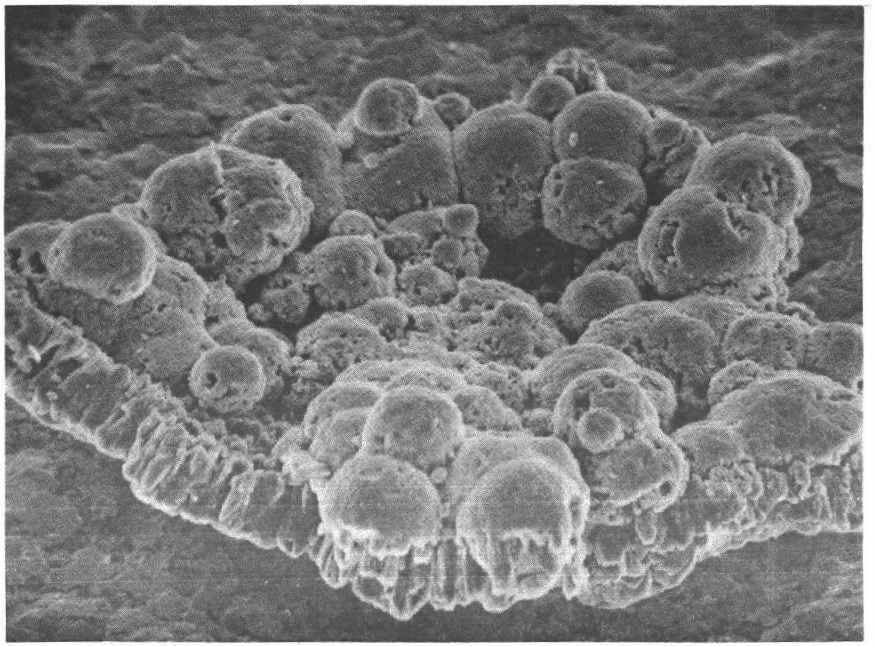

Figure 8. Micronodules growing on a fragment of a carbonate test recovered from BBS (SEM; 700X).

TABLE 2

Elemental Composition of the Biogenic Carbonate Component

Concentration in PPM

Element	BBS	±	Error	(a)	(b)	(c)	(d)	(e)	(f)
Na	3,030		400	n.r.	n.r.	n.r.	n.r.	n.r.	n.r.
K	n.d.		-	n.r.	n.r.	n.r.	n.r.	n.r.	n.r.
Sc	0.40		0.15	n.r.	n.r.	n.r.	n.r.	.03-.25	n.r.
Cr	n.d.		-	n.r.	n.r.	5-6	n.r.	.43-4.91	n.r.
Mn	n.a.		-	n.r.	n.r.	n.r.	n.r.	n.r.	n.r.
Fe	1,300		40	n.r.	500-3,100	~1,000	n.d.-200	49-741	n.r.
Co	1.3		0.4	n.r.	n.r.	3-5	n.r.	.06-1.04	n.r.
As	n.d.		-	n.r.	n.r.	n.r.	n.r.	n.r.	n.r.
Sr	1,010		30	900-1,000	900-1,300	1,430-1,540	800-1,800	n.r.	n.r.
Sb	0.40		0.06	n.r.	n.r.	n.r.	n.r.	n.r.	n.r.
Ba	160		10	n.r.	n.r.	135-195	n.r.	n.r.	n.r.
La	1.88		0.36	n.r.	n.r.	n.r.	n.r.	n.d.-6.09	3.8
Ce	n.d.		-	n.r.	n.r.	n.r.	n.r.	n.d.-3.03	5.5
Nd	n.d.		-	n.r.	n.r.	n.r.	n.r.	n.r.	3.5
Sm	0.46		0.01	n.r.	n.r.	n.r.	n.r.	.04-0.72	.65
Eu	0.17		0.05	n.r.	n.r.	n.r.	n.r.	n.d.-0.12	.15
Tb	n.d.		-	n.r.	n.r.	n.r.	n.r.	n.r.	.11
Yb	n.d.		-	n.r.	n.r.	n.r.	n.r.	n.r.	.28
Lu	0.040		0.002	n.r.	n.r.	n.r.	n.r.	n.r.	.042
Hf	n.d.		-	n.r.	n.r.	n.r.	n.r.	n.r.	n.r.
W	n.d.		-	n.r.	n.r.	n.r.	n.r.	n.r.	n.r.
Th	n.d.		-	n.r.	n.r.	n.r.	n.r.	.01-.15	n.r.

n.r. = not reported
n.d. = not detected
n.a. = not analyzed

(a) Krinsley (1960)
(b) Emiliani (1955)
(c) Thompson and Bowen (1968)
(d) Lipps and Ribbe (1967)
(e) Turekian et al. (1973)
(f) Spirn (1965)

geveen Basins. However, the settling of carbonate tests and their subsequent dissolution on the sea floor can still act as important vertical transport mechanism from the sea surface to the sediment-water interface (Arrhenius, 1963).

2.1.2 Biogenic Silica

The silica fraction recovered from BBS consisted almost exclusively of recent pelagic radiolaria (Figure 9). Comparative literature values are fewer than for the biogenic carbonate phases (Table 3). Some values are given in Martin and Knauer (1973) and a few by Edith M. Stanley (1973; personal communication of unpublished results). Reshetnjak (1971) indicates the presence of Al, Mg, Ca, Na, Fe, Cu, Pb, Ti, Ba, and Ag in the tests of Phaeodasia (an order of radiolaria) but only in a qualitative manner.

The few available data compare reasonably well with the values I have found. As in the case of the carbonate tests, the virtual absence of this phase from the BBD and RBD samples and their low elemental concentrations makes this phase a minor component of the sediment bulk chemistry. Martin and Knauer (1973) have reported Ti, Mn, Fe, Cu, Zn, and Al in the silica frustules of contemporary plankton from the Pacific Ocean. If other sources of an element such as Ti or Al were absent, a vertical transport of these in silica, or other, tests sinking to the sea floor could be an important source of Ti or Al for the sediments.

2.1.3 Fish Debris

Fish teeth were the most common form of fish debris recovered from

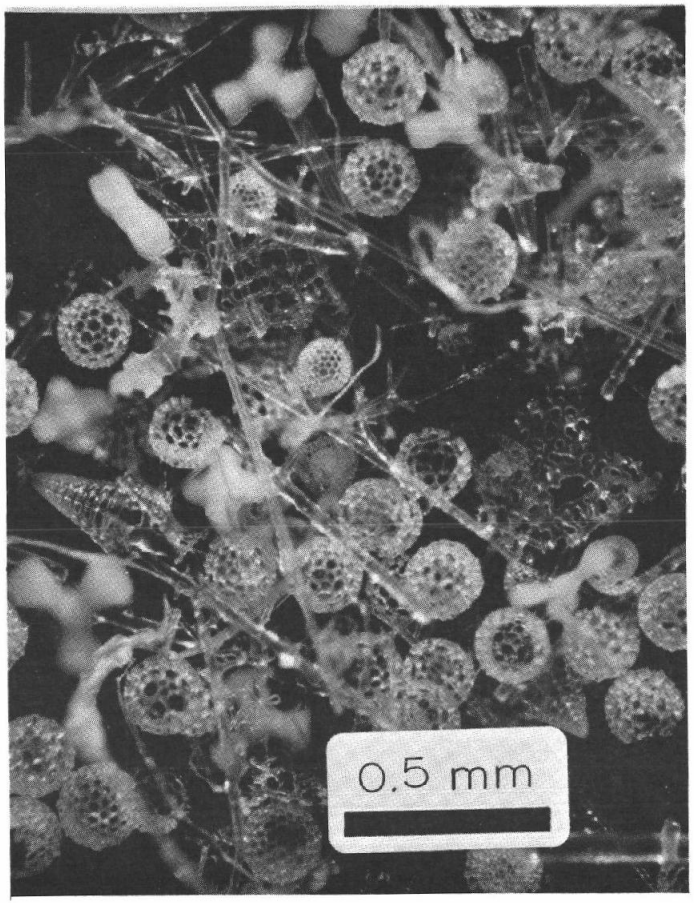

Figure 9. Siliceous component, primarily radiolaria, recovered from BBS, for INAA work.

Figure 10. Fish debris, primarily teeth, recovered from BBS for INAA work.

TABLE 3

Elemental Composition of the Biogenic Silica Component

Concentration in PPM

Element	BBS	±	Error	(a)	(b)
Na	5,680		920	n.d.	n.d.-2,700
K	866		75	n.d.	n.d.-3,200
Sc	0.9		0.4	n.r.	n.r.
Cr	8.9		0.4	n.d.	n.r.
Mn	n.a.		-	n.r.	n.r.
Fe	2,450		380	n.d.-2,815	n.r.
Co	2.7		0.4	n.r.	n.r.
As	n.d.		-	n.r.	n.r.
Sr	n.d.		-	n.d.	n.d.-2,400
Sb	n.d.		-	n.r.	n.r.
Ba	66.4		5.7	n.d.	n.r.
La	1.85		0.31	n.r.	n.r.
Ce	n.d.		-	n.r.	n.r.
Nd	n.d.		-	n.r.	n.r.
Sm	0.45		0.03	n.r.	n.r.
Eu	0.31		0.15	n.r.	n.r.
Tb	n.d.		-	n.r.	n.r.
Yb	n.d.		-	n.r.	n.r.
Lu	0.060		0.003	n.r.	n.r.
Hf	n.d.		-	n.r.	n.r.
W	n.d.		-	n.r.	n.r.
Th	n.d.		-	n.r.	n.r.

n.a. = not analyzed
n.d. = not detected
n.r. = not reported

(a) Martin and Knauer (1973)
(b) Stanley (1973)

BBS, BBD, or RBD (Figure 10). The analytical results show some variability in chemical composition from sample to sample. In general, the data agree reasonably well with available literature values (Table 4). My data for each sample normalized to its corresponding bulk sediment (see section 2.1.6 concerning the normalization of the BBS data) show a marked enrichment in Sc and the lanthanides (Figure 11). The scatter in the normalized Ba values may indicate a substitution of Ba for Ca after deposition of the fish debris. This is suggested by the lack of measureable Ba in the recently deposited fish debris of BBS versus the higher concentrations of Ba found in the older samples recovered from BBD, and RBD.

My lanthanide values are generally lower than those given by Arrhenius and Bonatti (1965) and closer to those determined by Eklund (1974). Herrmann (1972) also indicates that the highest lanthanide concentrations occur on the surface parts of bone tissue in sediments. If, as Arrhenius and Bonatti state:

> "The major process for slow removal of the rare earth ions from solution in sea water was shown... to be surface adsorption in microcrystalline fish-bone apatite..."

then it might be expected that the lanthanide concentrations in fish debris normalized to sea water would approximate a straight line. Figure 12 shows the normalized fish debris data and indicates that there is: a) a similarity in the lanthanide abundance patterns of the samples analyzed in this study, b) a nearly linear pattern for each sample, c) a Ce depletion in the BBS sample (data for BBD and RBD are lacking due to data reduction problems, but an estimate of the Ce con-

TABLE 4

Elemental Composition of the Fish Debris Component

Concentration in PPM

Element	BBS	±	Error	BBD	±	Error	RBD	±	Error	(a)	(b)	(c)	(d)	(e)
Na	10,560		900	n.d.		-	8,600		507	n.r.	4,400-5,420	n.r.	n.r.	n.r.
K	n.d.		-	n.d.		-	n.d.		-	n.r.	330-600	n.r.	n.r.	n.r.
Sc	71.2		3.8	168		3	189		2	150-200	n.r.	n.r.	n.r.	n.r.
Cr	n.d.		-	n.a.		-	n.r.		-	n.r.	n.r.	n.r.	n.r.	n.r.
Mn	n.a.		-	n.a.		-	n.r.		-	n.r.	1,520-2,020	n.r.	n.r.	n.r.
Fe	3,400		1,000	58,000		15,000	n.d.		-	n.r.	1,680-2,520	n.r.	n.r.	n.r.
Co	3.2		1.5	12.2		9.5	48.4		4.0	n.r.	n.d.	n.r.	n.r.	n.r.
As	n.d.		-	n.d.		-	n.d.		-	n.r.	n.r.	n.r.	n.r.	n.r.
Sr	998		54	n.a.		-	n.a.		-	n.r.	n.r.	n.r.	n.r.	n.r.
Sb	n.d.		-	34.0		1.2	247		10	n.r.	n.r.	n.r.	n.r.	n.r.
Ba	n.d.		-	11,650		680	38,500		2,000	n.r.	n.d.	n.r.	n.r.	n.r.
La	740		40	1,887		63	3,280		224	2,600-3,000	1,900-2,600	n.r.	1,500	1,083
Ce	58.2		1.0	(99)		-	(258)		-	1,500-2,800	n.d.	n.r.	2,700	2,263
Nd	791		25	1,250		80	3,410		208	6,800-10,000	n.r.	n.r.	1,500	1,817
Sm	140		3	268		35	782		94	350-450	500-600	n.r.	430	448
Eu	43.6		2.0	91.5		6.5	231		28	~300	n.r.	n.r.	20	n.r.
Tb	33.9		4.7	55.7		1.5	105		3	~0	n.r.	n.r.	30	61
Yb	178		32	370		17	494		27	900-1,100	n.r.	n.r.	100	53
Lu	27.1		1.2	71.7		1.2	89.9		1.3	<50	n.r.	n.r.	n.r.	18
Hf	n.d.		-	n.d.		-	n.d.		-	n.r.	n.r.	n.r.	n.r.	n.r.
W	n.d.		-	n.d.		-	n.d.		-	n.r.	n.r.	n.r.	n.r.	n.r.
Th	4.9		0.1	n.d.		-	32.3		2.5	n.r.	n.r.	60-230	n.r.	n.r.

( ) = estimated values
n.a. = not analyzed
n.d. = not deleted
n.r. = not reported

(a) Arrhenius and Bonath (1965)
(b) Eklund (1974)
(c) Bunat et al. (1970)
(d) Kochenov and Zinov'ev (1960)
(e) Blokh (1961)

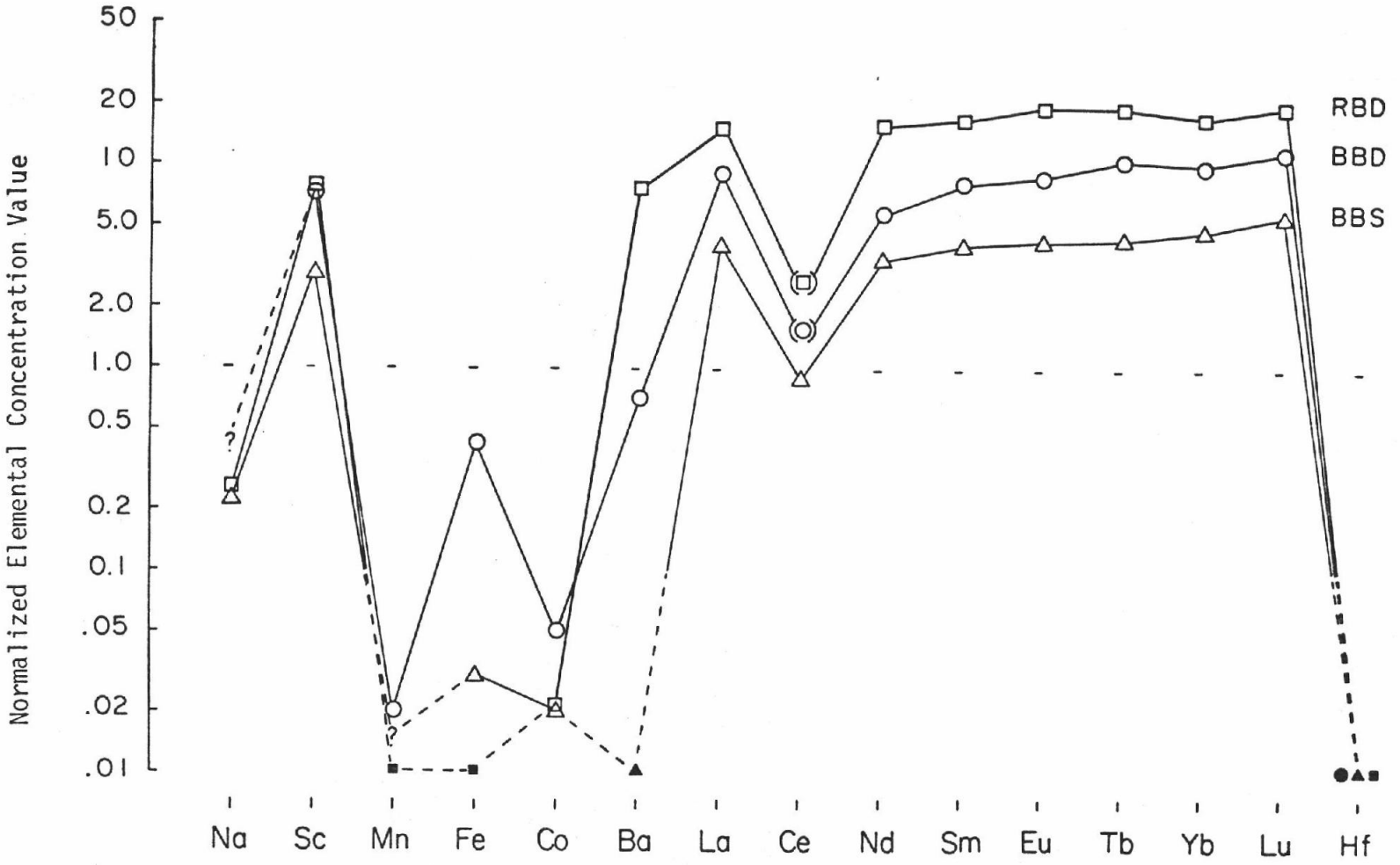

Figure 11. Elemental concentrations in the fish debris in BBS, BBD, and RBD normalized to the corresponding bulk sediment concentration. Values in ( ) are estimated. Solid figures represent values less than 0.01.

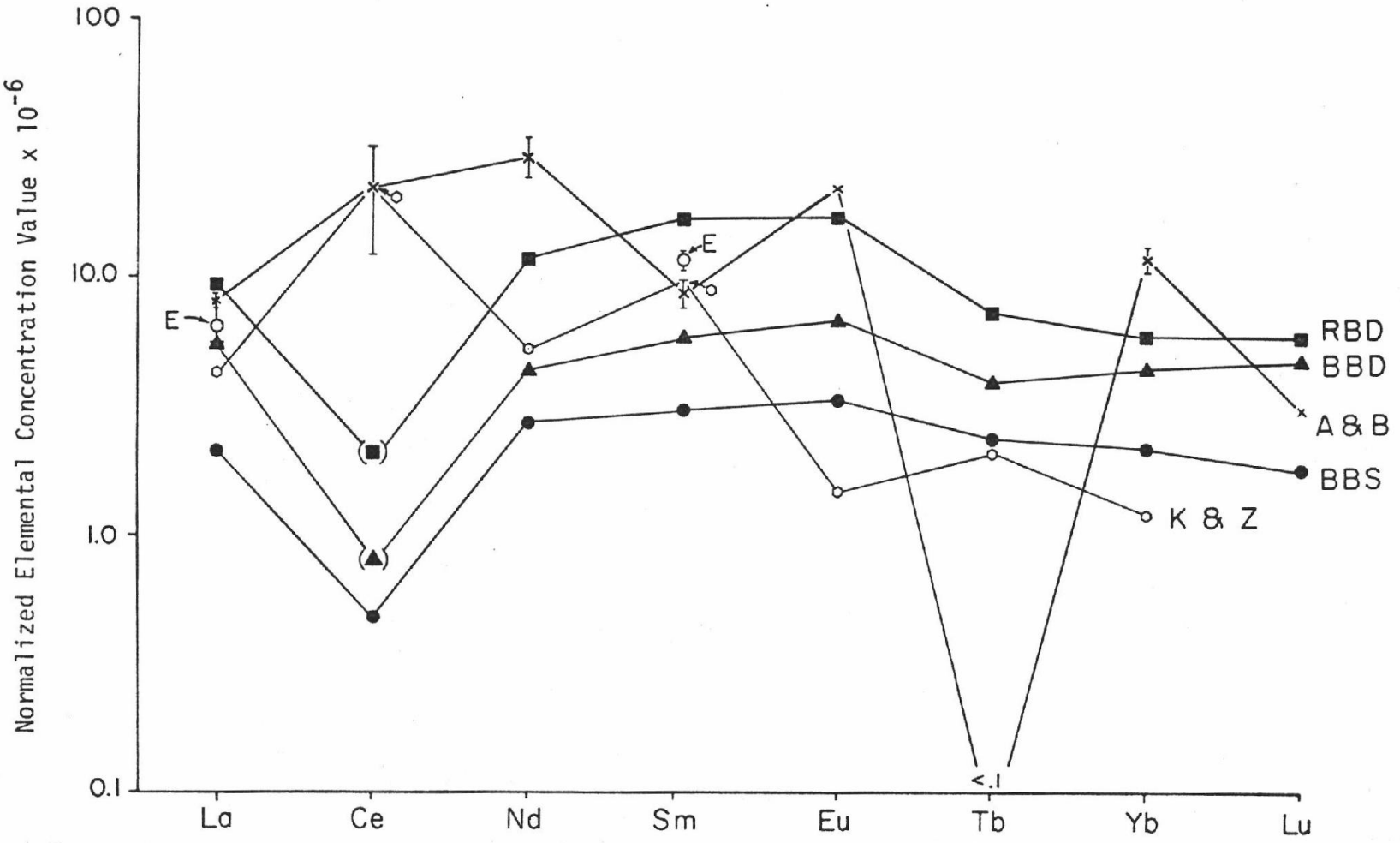

Figure 12. Lanthanide element concentrations in the fish debris from BBS, BBD, RBD, A and B (Arrhenius and Bonatti (1965)), K and Z (Kochinov and Zinovev (1960)), and E (Eklund (1973)) normalized to sea water. Values in ( ) are estimated.

centration in these samples was made based on the similarity of the ratios of the elements to each other in all of my samples), d) no Ce anomaly for the data of Arrhenius and Bonatti, and a positive Ce anomaly in the data of Kochenov and Zinovev (1960), and e) a marked deviation from a straight line pattern in the data of Arrhenius and Bonatti, and Kochenov and Zinovev.

The discrepancy between my data and that of other authors may be due to differences in the provenance of the samples or to the analytical methods used. Because of the limitations of comparative literature data a range of trace element values in fish debris cannot be ascertained. Arrhenius and Bonatti, moreover, do not indicate where their samples came from or how the lanthanide values were determined. The anomalous behavior of Ce will be treated later.

A visual examination of the samples showed fish debris to be common. As this component has such high lanthanide concentrations, it might play an important role in the lanthanide chemistry in metalliferous sediments of the Bauer and Roggeveen Basins. The parallelism between the P and lanthanide contents of pelagic North Pacific sediments (Volkov and Fomina, 1973) indicates that phosphatic fish debris may play an important role in the trace element chemistry of pelagic sediments in general.

2.1.4 Phillipsite

Phillipsite was recovered from only one sample (BBS). The concentration of this component in BBD and RBD was too low to permit hand picking. The BBS sample was x-rayed and the diffractogram compared

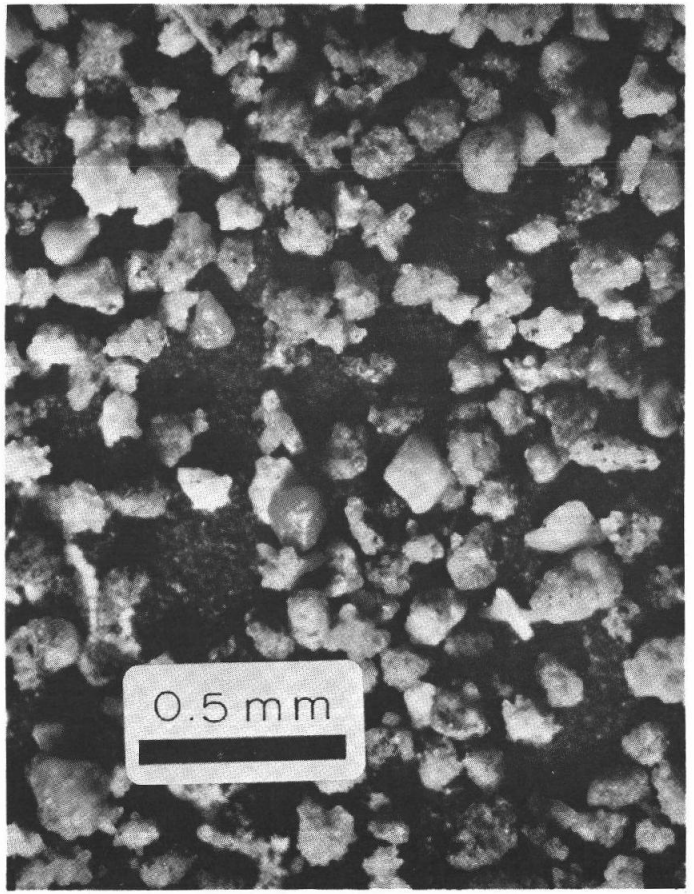

Figure 13. Phillipsite component, showing twinned crystals and rounded grains, recovered from BBS, for INAA work.

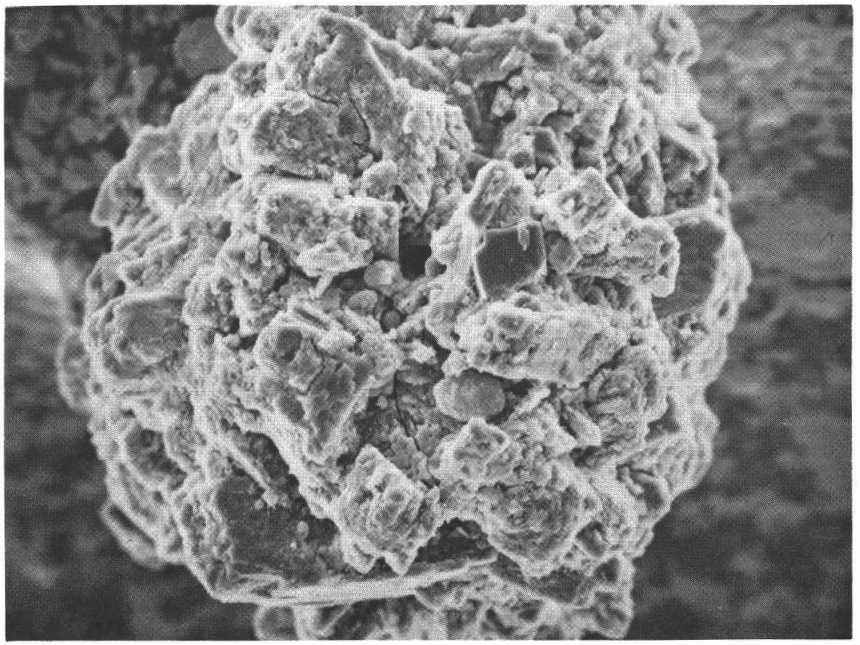

Figure 14. Rounded phillipsite grain showing numerous juxtaposed crystal faces (SEM; 700X).

well with that of a marine phillipsite obtained from J. Dymond (personal communication). The main peaks corresponded to those shown in Dymond et al. (1973) for this mineral. Available phillipsite analyses report mainly major element concentrations and therefore the compositional comparison is limited to a few elements. Except for the higher Fe in my sample, the comparison is quite good (Table 5).

The rather significant amount of iron noted in this sample (10.1%) may reflect its development in a high iron metalliferous sediment environment. The open silicate structure of this zeolite is capable of accommodating a wide variety of cations, and of intergrowing with nontronite (an iron rich smectite) (Riley and Chester, 1971), as well as with palagonite (a high iron basaltic glass) (Bonatti, 1963, 1965). Murray and Renard (1891) reported 3.8 to 4.3% Fe for untreated phillipsite crystals and Sheppard et al. (1970) reported 0.03 to 3.3% Fe. This latter author, however, attributed the iron to contamination in the form of iron oxide coatings.

The existence of phillipsite in the surface sample (BBS) but not in the downcore sample (BBD) may either indicate that there are marked local variations in the formation of phillipsite in the Bauer Basin or that this phase is metastable. The rounded edges of the crystal grains seen in Figure 14 indicate that this phase is in the process of dissolving. Bernat and Goldberg (1969) concluded from a downcore study of the Th content of North Pacific phillipsite samples that there is a continuous growth of this phase within the sedimentary column.

Phillipsite however may not be durable in a metalliferous environment giving way eventually to more stable components such as Fe-smectite

TABLE 5

Elemental Composition of the Phillipsite Component

Concentration in PPM

Element	BBS	± Error	(a)	(b)	(c)	(d)	(e)	(f)
Na	29,200	970	9,300-48,000	54,900	55,000	n.r.	n.r.	n.r.
K	35,800	1,400	44,900-72,300	49,800	51,000	n.r.	2,000-59,000	n.r.
Sc	14.1	1.4	n.r.	n.r.	n.r.	n.r.	n.r.	n.r.
Cr	37.9	0.4	n.r.	n.r.	n.r.	n.r.	n.r.	n.r.
Mn	5,250	110	n.r.	n.r.	n.r.	n.r.	n.r.	n.r.
Fe	101,000	8,700	300-33,100	350	n.r.	n.r.	n.r.	n.r.
Co	21.9	1.8	n.r.	n.r.	n.r.	n.r.	n.r.	n.r.
As	64	15	n.r.	n.r.	n.r.	n.r.	n.r.	n.r.
Sr	n.d.	-	n.r.	n.r.	n.r.	n.r.	n.r.	n.r.
Sb	4.8	0.5	n.r.	n.r.	n.r.	n.r.	n.r.	n.r.
Ba	3,930	500	n.d.-7,200	n.r.	n.r.	n.r.	n.r.	n.r.
La	86.7	4.9	n.r.	n.r.	n.r.	n.r.	n.r.	167
Ce	17.9	3.3	n.r.	n.r.	n.r.	n.r.	n.r.	54.7
Nd	121	7	n.r.	n.r.	n.r.	n.r.	n.r.	169
Sm	16.1	1.0	n.r.	n.r.	n.r.	n.r.	n.r.	32
Eu	4.8	0.7	n.r.	n.r.	n.r.	n.r.	n.r.	7.5
Tb	3.67	0.71	n.r.	n.r.	n.r.	n.r.	n.r.	6.6
Yb	13.0	2.7	n.r.	n.r.	n.r.	n.r.	n.r.	21.3
Lu	2.2	0.2	n.r.	n.r.	n.r.	n.r.	n.r.	3.6
Hf	5.1	0.6	n.r.	n.r.	n.r.	n.r.	n.r.	n.r.
N	n.d.	-	n.r.	n.r.	n.r.	n.r.	n.r.	n.r.
Th	1.40	0.06	n.r.	n.r.	n.r.	2.95-13.2	0.6-8.3	n.r.

n.a. = not analyzed
n.d. = not detected
n.r. = not reported

(a) Sheppard et al. (1970)
(b) Rex (1967)
(c) Goldberg (1961)
(d) Bernat and Goldberg (1969)
(e) Bernat et al. (1970)
(f) Piper (1974)

and micronodules.

2.2.5 Manganese Micronodules

Micronodules were recovered from each of the three samples BBS, BBD, and RBD. Because of the limited number of available micronodule analyses in the literature, I have compared my data to that of available macronodule analyses and found reasonable agreement (Table 6). The data of Eklund (1974) and Lyle (written communication) are of greatest interest since both refer to micronodules from the Bauer Deep cores. The physical aspect of the samples examined is similar to that recorded by Friedrich (1976); sub-rounded to elongate grains with botryoidal surface features (Figures 8, 15, and 16). Macronodules show very similar structural features (Fewkes, 1973), implying a close relationship in their manner of formation.

The micronodule data of each sample normalized to the corresponding bulk sediment (Figure 7) show that the samples are markedly enriched in Mn and Co, and to a lesser degree in Ce. RBD shows an enrichment of Ba, Lu, and Hf relative to the bulk sediment not seen in BBS or BBD.

The very open surface texture of micronodules (Figure 15) would allow the incorporation of significant amounts of foreign matter into their structure. Riley and Sinhaseni (1958) found an average of 30.3% insoluble silicates in the nodules they examined. Variations in the amount and type of foreign particles incorporated into the micronodules may, therefore, be the cause of some of the compositional variability observed in my samples.

TABLE 6

Elemental Composition of the Micronodule Component

Concentration in PPM

Element	BBS	±	Error	BBD	±	Error	RBD	±	Error	(a)	(b)	(c)
Na	17,800		3,200	790		180	2,970		170	700-2,500	n.r.	n.r.
K	n.a.		-	n.d.		-	n.d.		-	900-3,900	n.r.	n.r.
Sc	7.2		1.2	3.4		0.2	7.6		0.2	n.r.	n.r.	n.r.
Cr	13.3		0.5	n.a.		-	n.a.		-	n.r.	n.r.	5-31
Mn	262,800		4,700	326,900		5,900	245,500		5,400	99,700-254,800	281,300-312,200	135,600-223,300
Fe	104,300		9,800	121,200		5,000	105,100		1,000	75,400-100,600	105,900-149,200	54,300-141,600
Co	861		54	1,077		86	620		25	220-900	450-840	700-7,250
As	72.6		9.6	n.d.		-	n.d.		-	n.r.	n.r.	n.r.
Sr	n.d.		-	n.a.		-	n.a.		-	n.r.	n.r.	n.r.
Sb	38.0		1.6	22.0		1.0	40.6		7.7	n.r.	n.r.	n.r.
Ba	5,930		500	9,750		680	8,500		1,000	2,800-5,700	4,720-5,220	690-2,600
La	72.2		2.9	44.3		1.3	n.d.		-	n.d.-344	n.r.	n.r.
Ce	121		14	89.1		4.3	102.2		7.1	85-510	n.r.	n.r.
Nd	79.4		7.4	n.d.		-	n.d.		-	n.r.	n.r.	n.r.
Sm	11.2		0.3	4.7		1.6	22.8		1.8	170-780	n.r.	n.r.
Eu	3.2		0.5	1.2		0.2	4.5		0.5	n.r.	n.r.	n.r.
Tb	2.4		0.4	n.d.		-	2.9		0.2	n.r.	n.r.	n.r.
Yb	9.0		1.0	n.d.		-	n.d.		0.2	n.r.	n.r.	n.r.
Lu	1.4		0.2	1.9		0.1	5.9		0.3	n.r.	n.r.	n.r.
Hf	3.0		0.9	3.0		0.2	9.6		0.5	n.r.	n.r.	n.r.
W	60.4		8.5	n.a.		-	n.a.		-	n.r.	n.r.	n.r.
Th	4.8		0.1	15.3		1.0	n.d.		-	n.r.	n.r.	n.r.

n.a. = not analyzed
n.d. = not detected
n.r. = not reported

(a) Eklund
(b) Lyle (1975, unpublished data)
(c) Cronan and Tooms (1969)

TABLE 6 (continued)

Element	(d)	(e)	(f)	(g)	(h)	(i)
Na	16,900-21,200	n.r.	14,100-38,200	n.r.	n.r.	n.r.
K	n.r.	n.r.	5,200-12,800	n.r.	n.r.	n.r.
Sc	6.4-13.5	n.r.	n.r.	n.r.	n.r.	n.r.
Cr	17-26	n.r.	n.r.	8.9-26.7	n.r.	n.r.
Mn	176,000-259,000	n.r.	50,570-243,400	181,000-336,000	n.r.	352,000-354,000
Fe	70,000-135,000	n.r.	8,500-194,400	128,400-162,400	n.r.	22,000-80,000
Co	480-1,030	n.r.	n.d.-15,200	2,320-2,940	n.r.	n.d.
As	n.r.	n.r.	n.r.	n.r.	n.r.	n.r.
Sr	n.r.	n.r.	n.r.	n.r.	n.r.	n.r.
Sb	38-50	n.r.	n.r.	n.r.	n.r.	n.r.
Ba	n.r.	n.r.	9,800	n.r.	n.r.	n.r.
La	113-235	227	n.r.	n.r.	n.r.	n.r.
Ce	n.r.	735	n.r.	n.r.	n.r.	n.r.
Nd	n.r.	272	n.r.	n.r.	n.r.	n.r.
Sm	23-42	51	n.r.	n.r.	n.r.	n.r.
Eu	5.7-10.8	n.r.	n.r.	n.r.	n.r.	n.r.
Tb	4.1-8.4	8.1	n.r.	n.r.	n.r.	n.r.
Yb	n.r.	19.2	n.r.	n.r.	n.r.	n.r.
Lu	n.r.	3.2	n.r.	n.r.	n.r.	n.r.
Hf	4.9-9.6	n.r.	n.r.	n.r.	n.r.	n.r.
W	n.r.	n.r.	n.r.	n.r.	n.r.	n.r.
Th	14-27	n.r.	n.r.	n.r.	2.8-154	n.r.

(d) Rancitelli and Perkins (1973)
(e) Piper (1974)
(f) Skornyakeva et al. (1962)
(g) Glasby (1972)
(h) Ku and Broecker (1969)
(i) Friedrich (1976)

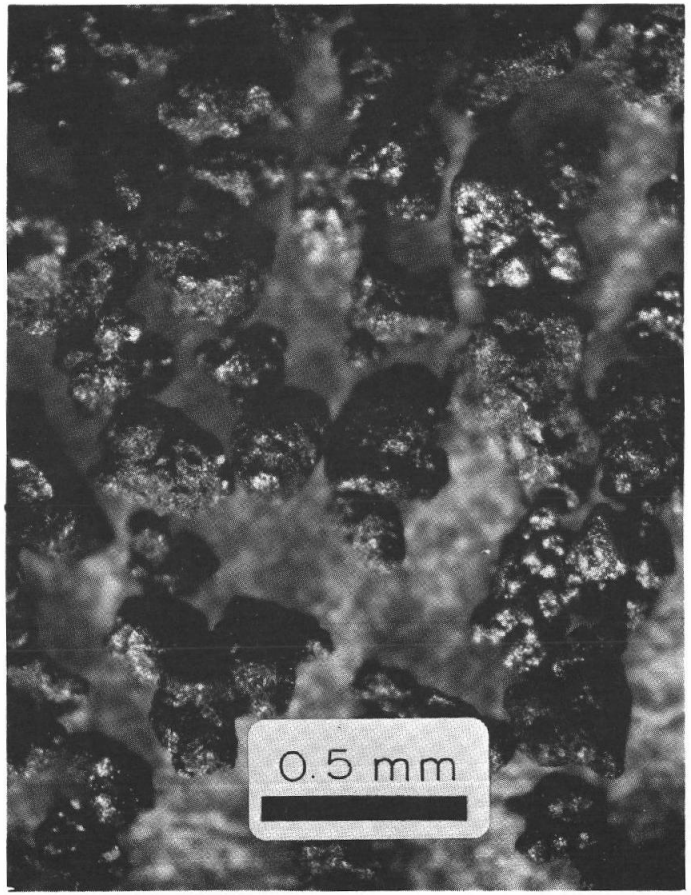

Figure 15. Manganese micronodules recovered from BBS for INAA work.

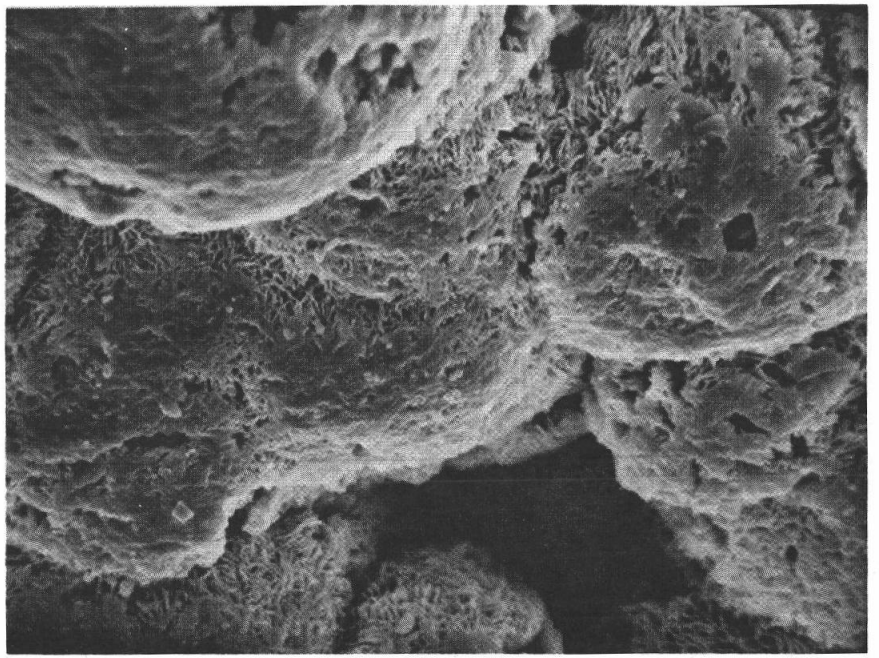

Figure 16. Details of the surface structure of micronodules recovered from BBS (SEM; 3000X).

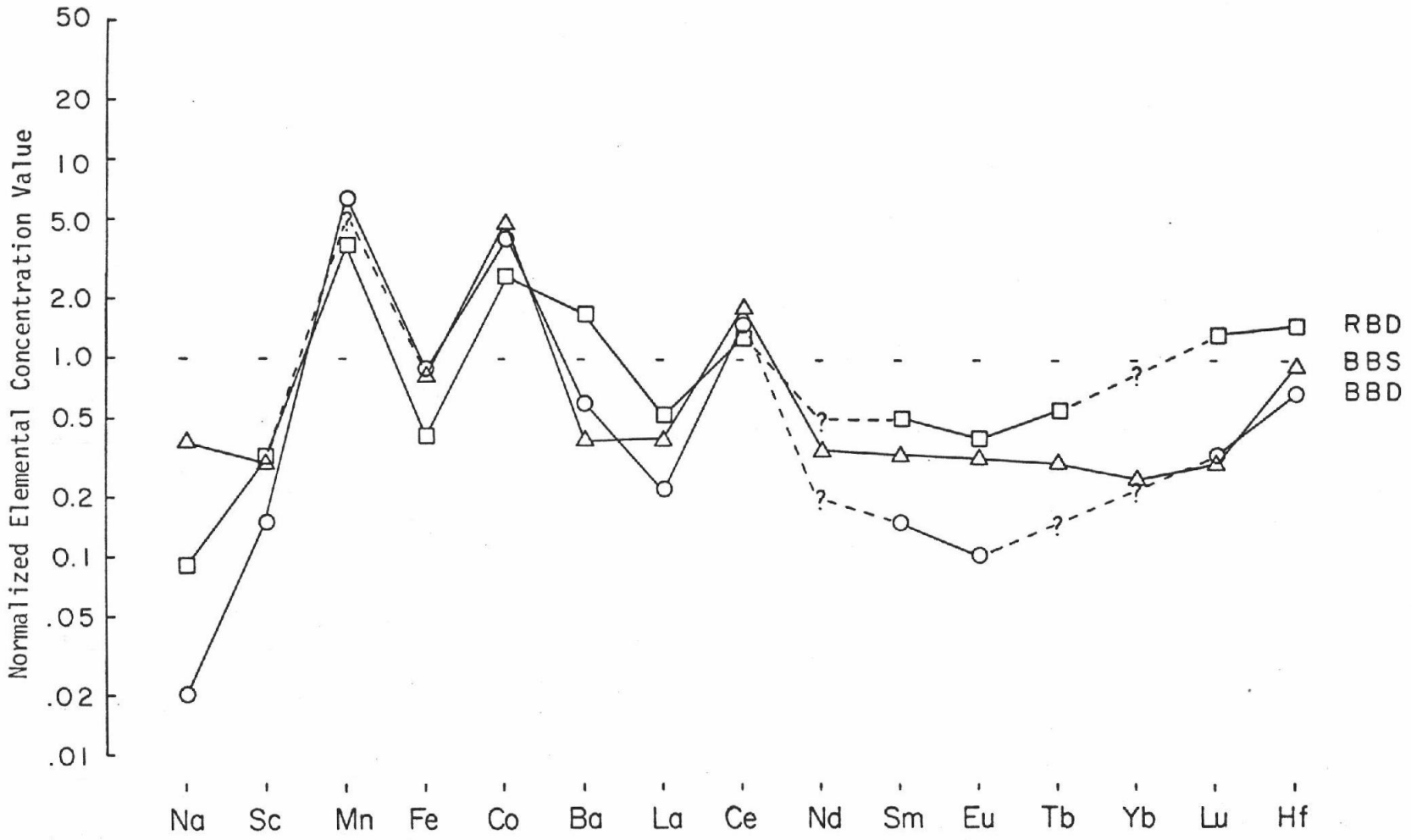

Figure 17. Elemental concentrations in the Mn-micronodules in BBS, BBD, and RBD normalized to the corresponding bulk sediment.

2.1.6 Authigenic Yellow and Brown Aggregates

The freeze dried bulk BBS sediment consisted primarily of a medium brown material with rare aggregates of a light yellow color. The shape of some of the light yellow aggregates (Figure 18) suggests they might be fecal pellets (Cloud, 1965). Dymond (personal communication) suggested these aggregates might be a form of phillipsite. The x-ray pattern of these aggregates, gave a pattern with no identifiable peaks. Most of this material is irregular and angular in shape and resembles, in general, the surrounding mass of brown aggregates.

The yellow aggregates show a lower Mn, Co, and Na content and a higher Ba, Cr, Fe, and Hf content than do the brown aggregates (Table 7). The color difference and lower Mn and Co contents of the yellow aggregates may be due to the presence of organic matter producing a microenvironmental reducing condition. Under reducing conditions, the Mn^{+4} ion would convert to Mn^{+2} and migrate away from the site to precipate further on under oxidizing conditions (Stumm and Morgan, 1970). Cobalt, which is closely associated with Mn in these sediments, may be removed from the yellow particles due to this same mechanism. Price (1977) for example has noted the covariance of Zn, Ni, Cu, and Co with the concentration in anoxic sediments. The presence of a higher Ba concentration may result from the precipitation of $BaSO_4$ in these yellow aggregates. The association of barite with areas of high productivity and the decomposition of organic matter have been shown by Goldberg and Arrhenius (1958) and Church (1970). Barite was identified as a minor constituent in the Bauer Basin sample BBD (x-ray analysis).

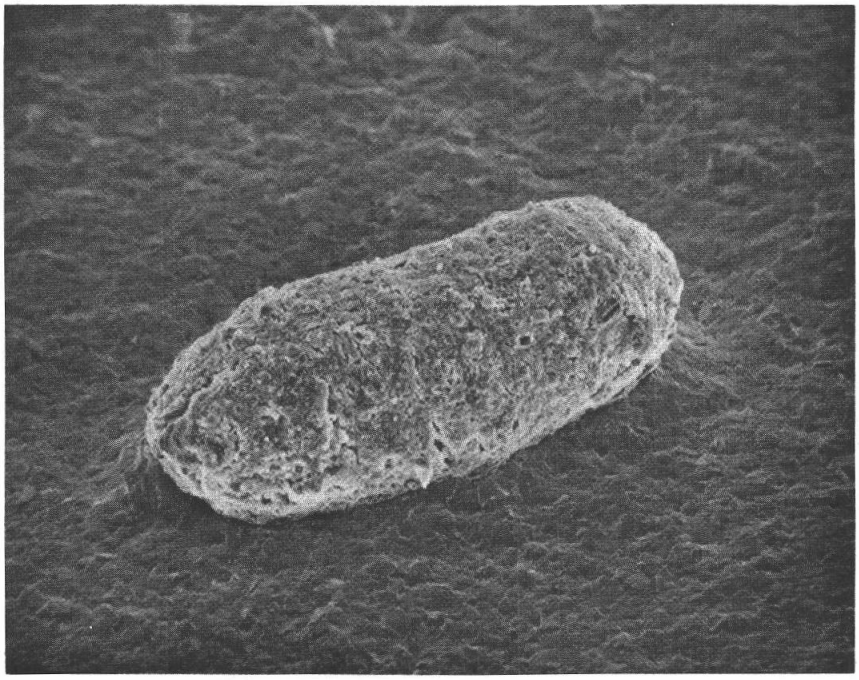

Figure 18. Pale yellow-orange fecal-pellet-like particle recovered from BBS (SEM; 200X).

TABLE 7

Elemental Composition of the Yellow and Brown Aggregate Components

Concentration in PPM

Element	BBS (Yellow Agg.)	± Error	BBS (Brown Agg.)	± Error	BBS - 2 (Bulk Sed.)	± Error
Na	20,300	1,500	47,300	5,300	42,800	2,400
K	11,600	1,300	n.d.	-	n.d.	-
Sc	27.4	2.1	24.3	1.6	24.3	0.2
Cr	48	14	26.0	9.5	n.r.	-
Mn	12,720	230	33,350	730	32,290	350
Fe	160,000	6,100	116,800	6,400	109,600	1,200
Co	35.7	1.2	176	10	191	2
As	82	13	63.4	6.9	n.r.	-
Sr	n.d.	-	747	57	n.r.	-
Sb	9.9	0.5	9.3	1.9	10.2	2.2
Ba	20,400	1,200	15,100	1,600	14,800	410
La	227	11	180	13	185.6	9.1
Ce	54.1	3.8	64.9	3.6	60.1	1.2
Nd	264	19	225	16	n.r.	-
Sm	37.4	1.3	34.1	0.8	33.9	0.6
Eu	11.4	1.5	10.0	1.4	10.8	0.5
Tb	8.1	1.5	7.8	1.1	6.1	0.1
Yb	40.1	8.2	35.8	9.2	32.8	1.8
Lu	5.70	0.28	4.60	0.27	5.1	0.9
Hf	6.3	0.5	3.2	0.2	3.8	0.2
N	n.d.	-	n.d.	-	n.r.	-
Th	3.6	0.2	4.0	0.1	3.8	0.1

n.a. = not analyzed
n.d. = not detected
n.r. = not reported

Comparing the composition of the brown aggregates with that of the top (5-10 cm) of a core (BBS-2) taken 200 meters from the site of BBS shows the samples to be almost identical (Table 7). This indicates that the brown aggregates, in fact, represent the bulk composition of BBS. The brown aggregate composition has, therefore, been used in normalizing the fish debris and micronodule compositions in sections 2.1.3 and 2.1.5.

3.0 CHEMICAL LEACHING RESULTS

In leaching samples of BBD and RBD, it was found that:

1) the elements in both BBD and RBD responded in very similar manner to the various leaches used,

2) the elements in the clay, silt, and bulk fractions responded to the leach treatments in similar manner,

3) the acid leached fraction could be assumed to be fish debris primarily, and that the oxalate leached fraction was quite similar to the micronodule composition,

4) the sediment residue after removal of the fish debris and micronodule phases showed a strong resemblance to marine nontronites,

5) the Roggeveen Basin residue indicated the presence of separate iron component.

6) it is possible to calculate a structural smectite formula from the residue compositions, and

7) the bulk sediment composition could be described as a mixture of iron rich smectite, micronodules, fish debris, a small amount of barite, and in RBD a separate iron oxyhydroxide component.

3.1 Chemical Leachings Used

The freeze dried bulk sediments of BBD and RBD were treated with various chemical leaches in order to separate them into their major components - fish debris, micronodules, and iron rich smectite. In the listing below, each treatment was carried out twice on separate subsamples of both BBD and RBD (Figure 5), a total of 14 separate treatments.

Leachates and/or residues were subjected to AAS and INAA analyses. The results are given in Appendix II. The designation (1X) refers to a single treatment with the designated leach and (2X) means the same sample was treated twice with the same leach.

Leach Treatments Used

a) (1X) - double distilled water

b) (1X) - 0.1N HCl

c) (2X) - 0.1N HCl

d) (1X) - 2N HCl

e) (1X) - acidified ammonium oxalate

f) (2X) - acidified ammonium oxalate

g) (1X) - acidified ammonium oxalate + (1X) - 0.1N HCl

The mild acid treatment was designed to remove the fish debris and carbonate fraction of the samples and the oxalate leach to remove amorphous ferric oxyhydroxides and poorly crystalline ferromanganese components (Landa and Gast, 1973). This treatment should not affect crystalline goethite or iron-rich smectite (Heath and Dymond, 1977). Table 8 shows the effect that each of the leaches had on specific sediment components.

Table 9 gives the percent weight loss results for leachings of the freeze dried bulk sediments of BBD and RBD. These values are average values based on two or more similar chemical treatments of the same material. The manner of calculation of the given values is given in

TABLE 8

Effect of Various Leaches on Components
Separated from BBS (Y73-3-14K)

	Effect Observed With		
Component	0.1N HCl	2N HCl	am. ox.
Bulk Sediment	small amount of gas generated	gas generated	color change to pale yellow*
$CaCO_3$ Tests	dissolution	dissolution	no effect
Fish Debris	dissolution	dissolution	no effect
"Phillipsite"	no visible effect	slight degree of attact on some grains	no effect visible
Mn-Micronodules	no effect	no visible effect on nodules solution yellowed somewhat	dissolution leaving small amount of gray "ash" behind

* Effects apply to brown aggregates; yellow aggregates showing little or no color change with am. ox. treatment.

TABLE 9

Weight Losses Experienced by Bulk BBD and RBD Subjected to Various Leaches

Chemical Treatment	% Weight Loss - BBD (Y73-3-21K)				% Weight Loss - RBD (Y73-4-64K)			
	$\underline{T}$	$\underline{L_W}$	$\underline{L_1}$	$\underline{L_2}$	$\underline{T}$	$\underline{L_W}$	$\underline{L_1}$	$\underline{L_2}$
H_2O Leach	15.5±0.6	15.5±0.6	- -	- -	9.7±1.0	9.7±1.0	- -	- -
(1X) .1N HCl Leach	28.2±0.1	"	12.7±0.7 (15.0)	- -	18.2±0.9	"	8.5±1.9 (9.4)	- -
(2X) .1N HCl Leach	31.3±0.6	"	"	3.2±1.3 (4.5)	19.3±0.4	"	"	1.1±2.3 (1.4)
(1X) am. ox. Leach	33.8±1.0	"	18.2±1.6 (21.5)	-	38.7±0.7	"	29.0±1.7 (32.1)	- -
(2X) am. ox. Leach	35.3±0.5	"	"	1.6±2.1 (2.5)	44.5±0.3	"	"	5.8±2.0 (9.5)
(1X) am. ox. + (1X) .1N HCl Leach	46.8±1.6	"	"	13.1±3.2 (19.1)	45.0±0.6	"	"	6.3±2.3 (10.3)
(1X) 2N HCl Leach	43.5±2.6	"	28.0±3.2 (33.1)	- -	36.3±1.9	"	26.6 (29.5)	- -

T = Total average weight loss. Based on the average of 2 or 3 similar treatments.

L_W = Weight loss due to removal of "salts" by water. In each case it is assumed to be constant.

L_1 = Weight loss due to the HCl or am. ox. of the first leach. $L_1 = T - L_W$

L_2 = Weight loss due to the HCl, or am. ox. of the 2nd leach. This assumes that the water base of the 2nd leach does not remove any additional material from the sample. $L_2 = T - L_1 - L_2$

Note: Figures in parentheses represent the L_1 or L_2 weight loss values above recalculated to a salt free sediment.

detail in Appendix 1, subsection 1.10.

As a result of mechanical losses, the weight changes shown in Table 9 are maximum values; the actual change probably being about 2% lower. An estimate of this difference may be made by comparing the percent weight loss value listed under L_W with the calculated salt content of the sample, as estimated from the water content of the samples (Table 10). These results are shown below:

Sample	Salt	L_W	$\Delta(L_W$ - % Salt)
BBD	13.3%	15.5%	2.2%
RBD	7.4%	9.7%	2.3%

Table 10 also presents some of the physical and chemical properties of the bulk sediment referred to later in the development of this work.

In the case where the treatments are dissimilar, the second leach has a noticeable effect. This indicates that each leach is affecting distinct fractions of the sediment.

3.2 Chemical Effects of Leaching BBD and RBD

Leach data for the major elements Al, Ba, Ca, Fe, K, Mg, Mn, Na, and Si and the trace elements As, Co, Cr, Hf, Ni, Sb, Se, Th, W, Zn, and the lanthanides are given (Figures 19 to 23). It was found that:

1) the lanthanide concentrations of both samples are markedly reduced by acid treatment but not by the oxalate treatment;

2) Co, Mn, Ni and W (in RBD) in the samples are strongly depleted by the oxalate treatment but not by the mild acid treatment;

TABLE 10

Physical and Chemical Properties of BBD and RBD Including Water and Salt Content, Wet and Dry Bulk Densities, Carbonate and Volatile Contents

Determination	BBD - Core - Y73-3-21K	RBD - Core - Y73-4-64K
% H_2O[1]	79.2 ± 0.1%	68.0 ± 0.1%
% Salt[2]	13.3%	7.4%
Wet Bulk Density[3]	1.148 ± 0.007 gm/cm^3	1.310 ± 0.009 gm/cm^3
Dry Bulk Density[4]	0.239 ± 0.001 gm/cm^3(wet volume)	0.420 ± 0.003 gm/cm^3(wet volume)
% Carbonate-Bulk Sed.[5]	2.0%	0.9%
% Carbonate-Salt Free Sed.[6]	2.3%	1.0%
% Volatiles[7]	10.3%	13.3%

1) average of two weight loss determinations per sample by freeze drying
2) based on a bottom water salinity of 34.8 PPT
3) average of three measurements
4) based on the results of 1) and 3)
5) by LECO 714 carbon analyzer
6) % carbonate corrected for the calculated % salt content
7) from LECO analysis - % weight loss of dry sample 500°C for two hours

3) cerium acts independently of the other lanthanides in its response to acid or oxalate treatment;

4) the Fe content of both samples is affected to about the same degree (i.e., 58-72% unleacheable iron) by the oxalate treatment;

5) aluminum and Ba were subject to noticeable degrees of leaching by both acid and oxalate treatments;

6) silica was affected only by the strong acid leach and then only to a slight degree;

7) many trace elements such as As, Cu, Hf, and Th showed a complex pattern of response to the treatments; and

8) in general, both BBD and RBD responded in similar manner to the various leaches.

3.2.1 Leach Effect on the Lanthanide Elements

The lanthanide elements which were found to be concentrated in the fish debris fraction of the sediments (section 2.1.3) are markedly depleted by the mild acid treatment. Up to 90% removal was found (Figure 19). This same treatment removes a maximum of 19.5% of BBD and 10.8% of RBD (based on the salt free weight losses from (1X) and (2X) mild acid treatments - Table 9). The lanthanides present in the sediments are then concentrated in a fraction which constitutes 10 to 20% of the salt free sediment. This is interpreted to mean that the small percent of fish debris present in the samples dominates the sediment lanthanide content.

Direct observations of the samples BBD and RBD indicate that 10 to 20% may not be unreasonably high fish debris concentrations in these

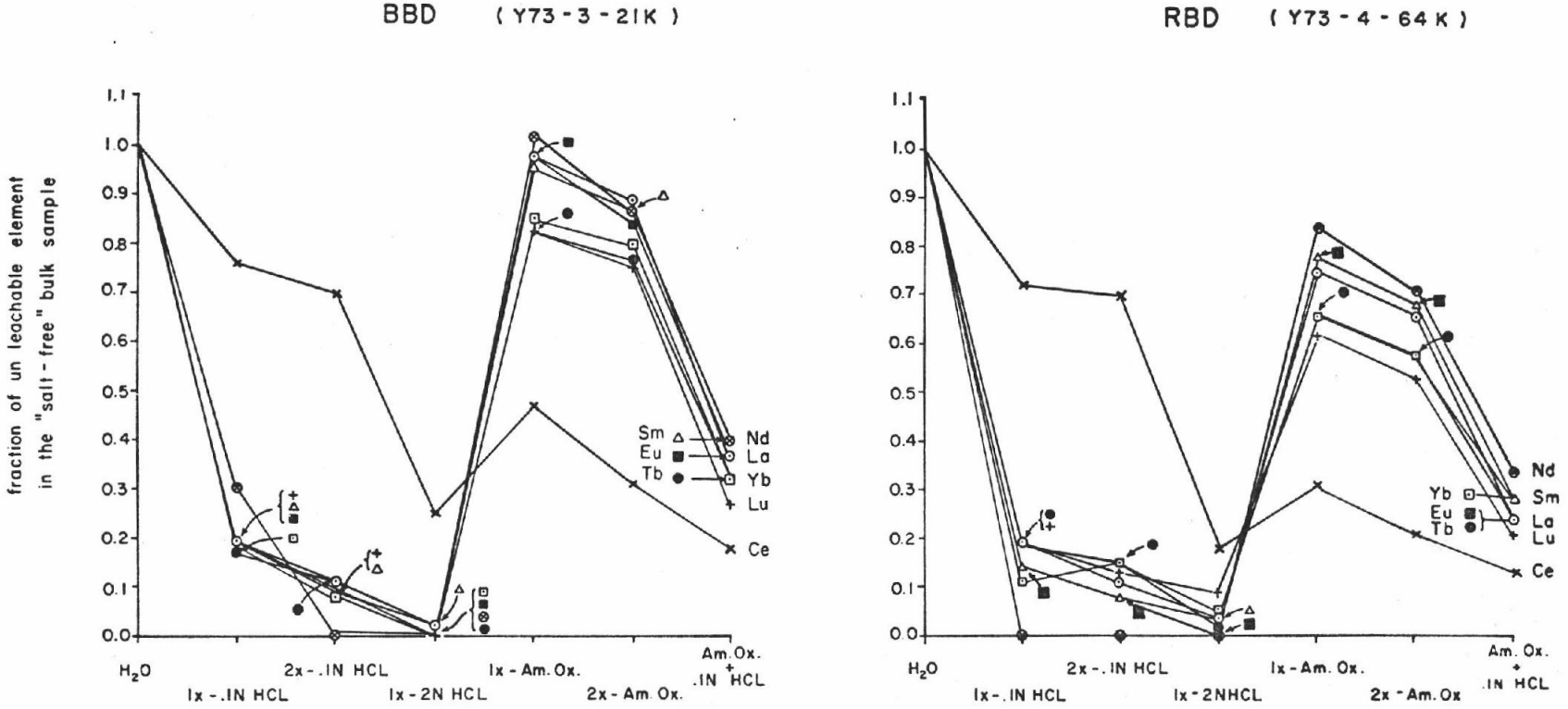

Figure 19. Leach effects on the lanthanide element concentrations in BBD and RBD - bulk sediment.

sediments. Visual estimates for fish debris made on the bulk of each sample indicated some 5-8% fish debris in BBD and 3-6% in RBD. Since the density of this phase is considerably higher than that of the mass of clays which make up the samples, these values can easily be twice as high on a per weight basis.

The oxalate leach effect on the lanthanides is minor (~10% removal) in BBD but significant in RBD (~30% removal). It is evident that an important fraction of the lanthanides in the Roggeveen Basin are associated with an amorphous component. The reduction of the lanthanide concentration to nearly zero by the strong acid leach indicates that these elements are not strongly associated with a detrital or other acid resistant phases of the sediments, i.e. smectite or micronodules. Ce, however, is not totally removed by the strong acid leach, suggesting that the residue (smectite) contains a small fraction of the element.

3.2.2 Leach Effects on Cerium

The response pattern of Ce to the various leaches is noticeably different from that of the other lanthanides. Cerium is only partially reduced by the mild acid treatment and significantly reduced by the oxalate leach. This response agrees well with the fact that Ce is depleted in the fish debris phase and enriched in the micronodule phase (sections 2.1.3 and 2.1.5).

A double leach of 0.1N HCl removes 30% of the Ce, and a double ammonium oxalate leach releases 69%. For RBD the figures are 30% and 79%, respectively, for the same leaches. The two phases, fish debris and oxalate leacheable fraction (micronodules), then appear to monopolize

the total Ce content of each sample.

3.2.3 Leach Effects on the Elements Co, Mn, Ni, and W

Cobalt, Mn, and Ni (and W in RBD) respond to the various leach treatments in similar manner (Figure 20). Each of these elements is strongly reduced by the oxalate leach, while being only slightly affected by the mild acid leach. Nickel is more susceptible to acid leaching than the other elements of this group and may be associated with the fish debris phase. Tungsten (W) was detected only in the RBD sediments.

From the analyses of phases separated from BBS, it is known that Mn, Co, and W are concentrated in the Mn-micronodule phase, and nickel is known to be an important component of manganese nodules (Raab, 1972). Moreover, the calculated composition of the oxalate leached fraction of the sediments is quite similar to the composition of micronodules recovered from BBD (Table 13). Micronodules appear to be the stable component in metalliferous sediments dominating the concentration of Mn, Co, Ni, and W, as well as a major fraction of the Ce.

3.2.4 Leach Effect on Fe, As, Sb, Th, and Hf

Each of the elements Fe, As, Sb, Th, and Hf respond in similar manner to the various leaches (Figures 20 and 21). The concentrations of these elements are not markedly affected by the mild acid leaches but show significant dissolution under oxalate treatment. Iron shows the least degree of depletion by the oxalate treatment (25-30% leachable). This indicates that the major fraction (>70%) of the Fe in the sediments

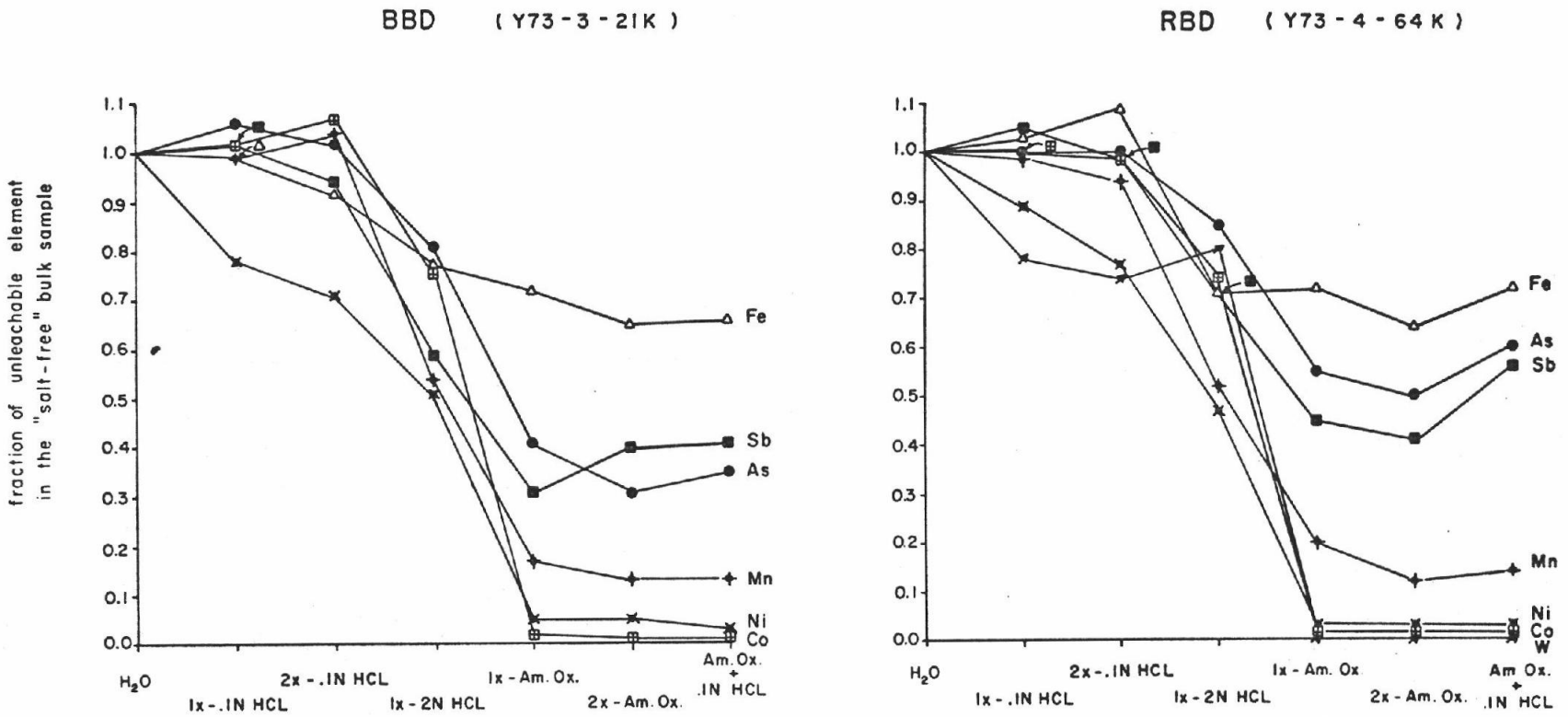

Figure 20. Leach effects on the arsenic, cobalt, iron, manganese, nickle, antimony, and tungsten concentrations in BBD and RBD - bulk sediments.

is in crystalline phases such as goethite or an iron rich smectite which constitute the major fraction of metalliferous sediments (Sayles et al., 1975).

It will be proposed later that the residue of the oxalate + mild acid treatment of the sediments bears a strong resemblance to known iron rich smectites (nontronite). Assuming this residue to be nontronite and using the fractions of unleachable elements from Figures 20 and 21, it is estimated that the following fractions of Fe, Sb, As, Th, Hf, and Mn in the salt free bulk sediment reside in the smectite phase:

Element	BBD	RBD
Fe	68%	68%
Sb	36%	43%
As	36%	53%
Th	64%	30%
Hf	50%	41%
Mn	15%	15%

All of these elements have been reported in authigenic nontronites from the Galapagos Hydrothermal Area (Corliss et al., 1977, in preparation). The remaining fraction of these elements is concentrated in the oxalate leached fraction best represented by the micronodule composition. A small fraction of the Mn in the sediments also exists in the unleached smectite phase.

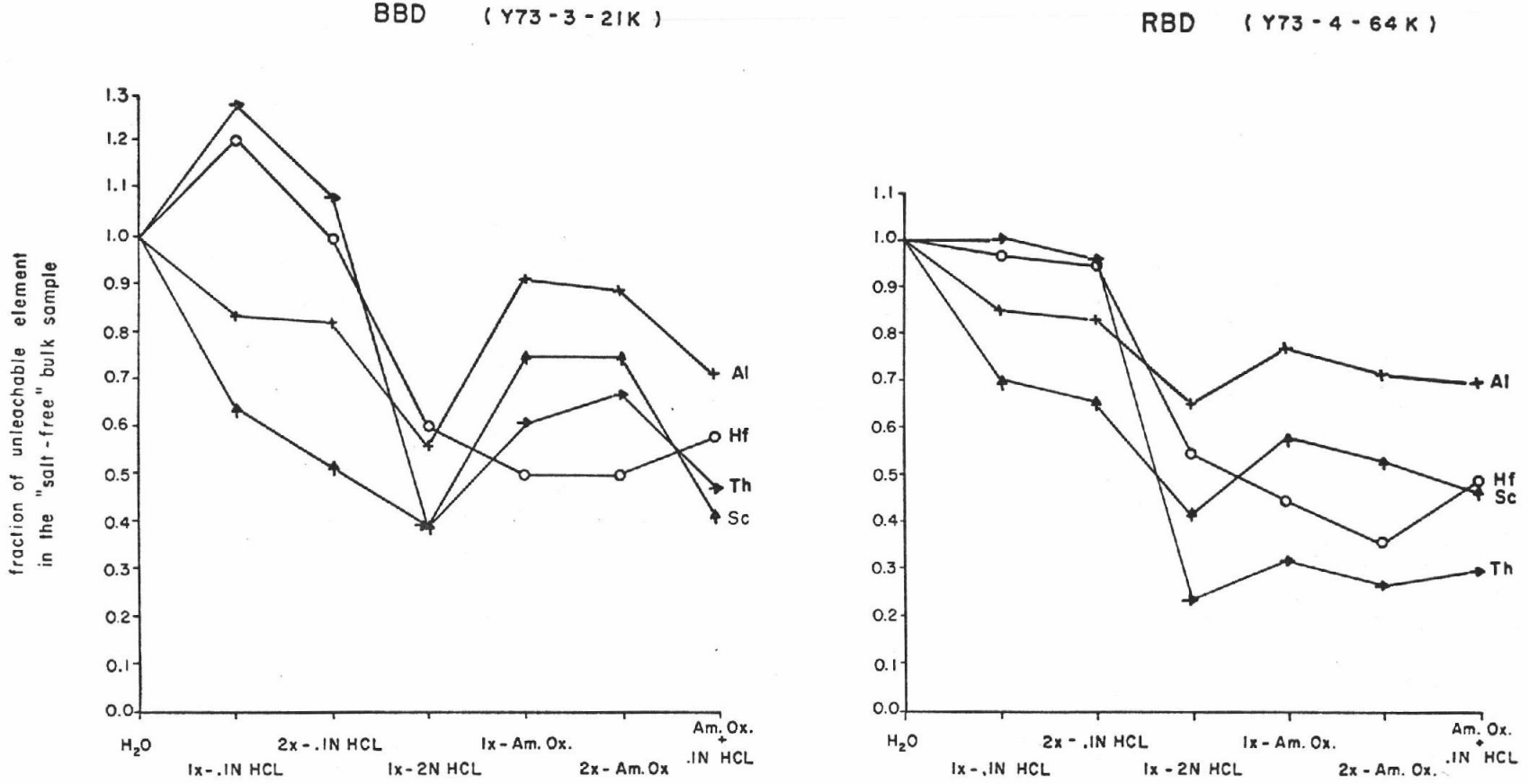

Figure 21. Leach effects on the aluminum, hafnium scandium, and thorium concentrations in BBD and RBD - bulk sediment.

3.2.5 Leach Effects on Al, Sc, Mg, Cu, and Zn

Each of these elements shows a significant degree of leaching by both a mild acid or oxalate leach. The response of these elements to leaching (Figure 22) is not as ameanable to interpretation as were those of the other elements. Of the elements listed, only Sc is known to be concentrated in the fish debris phase (section 3.1.5). All others have been identified as trace components in this phase, i.e. Th, Hf (this work); Cu, Zn, Al, and Mg (Eklund, 1973).

As these elements are also considerably reduced by the oxalate leach, it is assumed that the mild acid leach is actually removing elements loosely adsorbed on the surface of amorphous components or perhaps Mn-micronodules. An estimate of the fraction of these elements which reside in the smectite phase may be made, as was done in section 3.2.4.

Element	BBD	RBD
Al	70%	68%
Sc	42%	47%
Mg	60%	50%
Cu	48%	48%
Zn	44%	60%

Al, usually assumed to be present as a detrital component, should not be leachable. The significant percent of Al which is leachable implies that some Al derives from other than detrital sources.

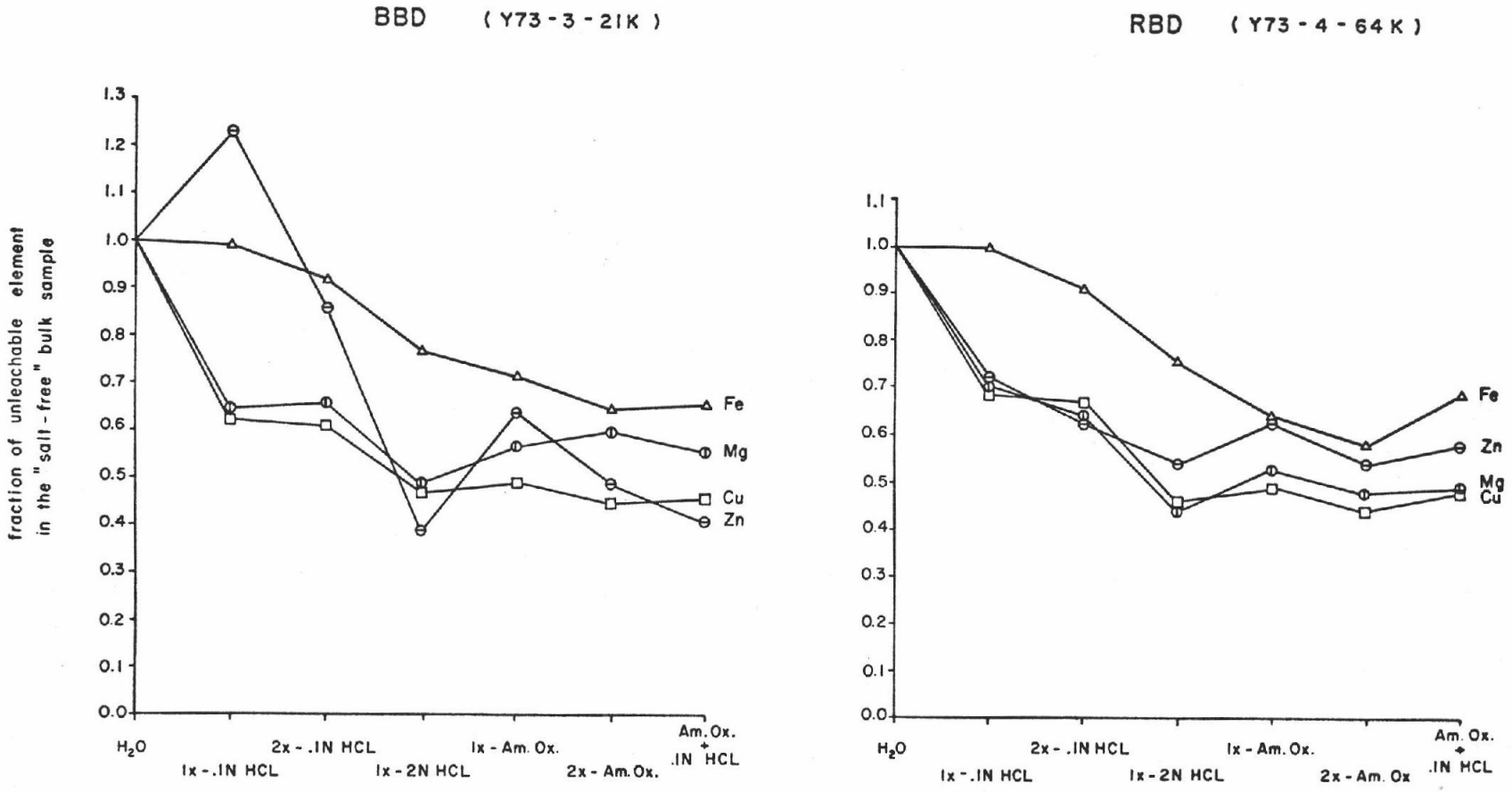

Figure 22. Leach effect on the copper, iron, magnesium, and zinc concentrations in BBD and RBD - bulk sediment.

3.2.6 Leach Effect on Si

Of the elements treated, Si is the least susceptible to any type of leaching. This element remains unaffected by the mild acid leach, and suffers only a 2-3% decrease when RBD and BBD, respectively, are treated with the oxalate leach. Since there is no evidence of siliceous tests or of an important detrital component in either sample, it is assumed that most of the Si is in the Fe-smectite present. Some leachable Si exists in the micronodule component, which contains 4-7% of this element (Table 12).

3.2.7 Leach Effect on K and Na

These two very similar elements respond in quite parallel fashion in the leaching experiments. Between 55 and 65% (Figure 23) of these elements is remobilized by the chemical treatment of BBD (including a strong acid leach) while only 25 to 35% is remobilized by similar treatments of RBD. Glover (1977) has shown Na and K to be important constituents of micronodule birnessite. This may explain why significant amounts of these elements are affected by the oxalate leach. On the other hand, Na, K, and Mg are certainly present as charge balancing ions in the smectite clays which constitute such a significant fraction of these sediments. As such, they could easily be replaced by H^+ ions in the acid leaches. This replacement may also occur to some degree with NH_4^+ ions in the oxalate leach solutions.

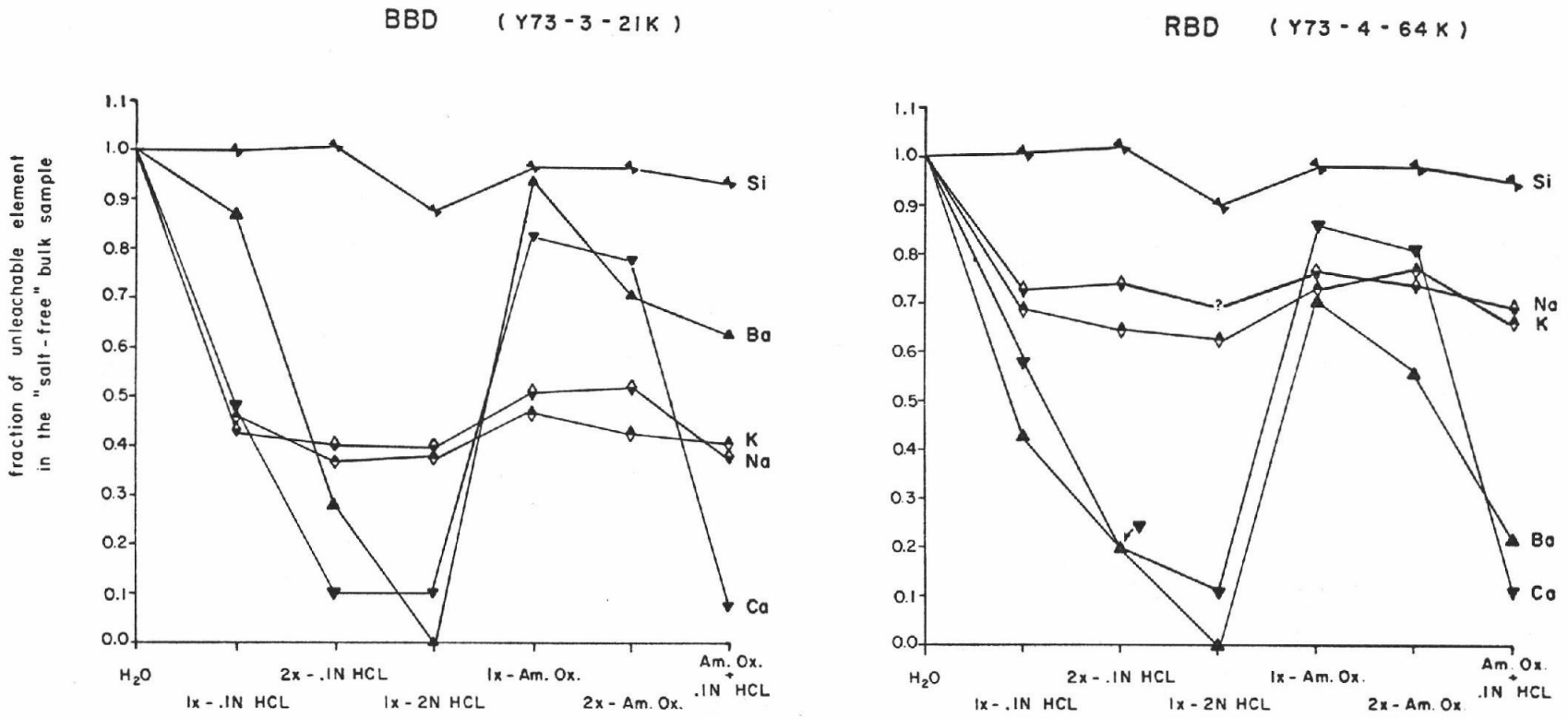

Figure 23. Leach effects on the barium, calcium, potassium, sodium, and silicon concentrations of BBD and RBD - bulk sediments.

3.2.8 Leach Effect on Ca

Calcium dissolves readily when treated with mild acid, a fact which is consistent with its being concentrated in fish debris. Even a strong acid treatment will not, however, reduce a Ca concentration by over 90%, indicating that about 10% exists in a stable, possibly detrital, phase. Calcium shows a degree of susceptibility to leaching with ammonium-oxalate. Since this treatment should only affect the Mn-micronodules, and amorphous oxyhydroxides, the implication is that some Ca is associated with these phases. This is consistent with the AAS Ca data Mn-micronodules from BBD which show that this phase contains about 20,000 ppm Ca. Glover (1977) has also found Ca to be important in micronodule birnessite. The oxalate leach data for calcium may be biased by the formation of an insoluble Ca-oxalate.

3.2.9 Leach Effect on Barium

The response of Ba to the various leaches is confusing in that it should not be leachable if it is present in the sediments, primarily as highly insoluble barite. Barite was noted in the x-ray diffractogram of BBD and some may be present in RBD. The peaks in the RBD diffractogram are, however, not well defined. The fraction of Ba removed by the acid leaches (up to 80% by .1N HCl, and 100% by 2N HCl) is very high and may indicate that Ba is present in other than a barite component. The dissolution of Ba by the oxalate treatment indicates it to be present in the amorphous fraction of the sediment. Ba was measured in the micronodule components (Table 6).

As in the case of Ca, the formation of a Ba-oxalate compound may bias the oxalate leach data.

3.2.10 Bulk Sample Effects - Summary

It was found that treating a sample twice with the same leach had little effect on the total percent removal of any given element. As such, it is possible to classify elements, as being unaffected $\leq$ 5%, slightly affected 5-15%, moderately affected 15-50%, strongly affected 50-85%, and depleted $\geq$ 85%, based on the average percentage of the element removed by the single and double leaches.

The classification of elements as shown in Table 11, in conjunction with a perusal of the preceeding graphs, show that the elements in both BBD and RBD, respond in very similar manners to the various leaches used. Most obvious of all is the depletion of lanthanides (except Ce) by the mild acid leachings. Arsenic, Co, Fe, Hf, Mn, Sb, Si and Th are unaffected by this leach. The elements Ce, Cu, K, Mg, Na, Ni, and Sc are moderately affected, and Ca and Ba are moderately to strongly affected by this same treatment.

The response of the elements to leaching with ammonium oxalate is more complex. Cobalt, Mn, Ni, and W (in BBD) are depleted by oxalate leaching and Si is unaffected. Lanthanides in BBD are only slightly affected, but in RBD are moderately affected. Again Ce is an exception. Cerium, Cu, and Sb are strongly affected and most other elements, in RBD particularly, are moderately affected by treatment with ammonium oxalate.

TABLE 11

Elements Classified According to the Degree to Which They are Leachable by 0.1N HCl and Ammonium Oxalate

Treatment	Core	Sample Weight Loss*	Unaffected <5%	Slightly Affected 5-15%	Moderately Affected 15-50%	Strongly Affected 50-85%	Depleted >85%
0.1N HCl	BBD	15.0-19.5%	As, Co, Cr, Fe, Hf, Mn, Sb, Si Th, Zn	Al	Ba, Ce, Cu, K, Mg, Na, Ni, Sc	Ca	Lanthanides
	RBD	9.4-10.8%	As, Co, Fe, Hf, Mn, Sb, Si, Th	Al, Cr, W	Ca, Ce, Cu, K, Mg, Na, Ni, Sc Zn	Ba	Lanthanides
Ammonium Oxalate	BBD	21.4-24.0%	Cr, Si	Al, Sc Lanthanides	Ba, Ca, Fe, Hf, Mg, Na, Th, Zn	As, Ce, Cu, K Sb	Co, Mn, Ni
	RBD	32.1-41.6%	Cr, Si		Al, As, Ba, Ca Fe, Hf, Mg, Na Lanthanides Sc, Th, Zn	Ce, Cu, Sb	Co, Mn, Ni, W

* given on salt free basis; first figure represents loss for single leach, second figure equals loss from first plus second leach.

3.3 Silt and Clay Size Fraction Leach Effects

Samples of BBD and RBD were sieved to remove the > 63 μ size fraction for the purpose of recovering micronodules and fish debris for INAA analysis. The < 63 μ size fraction was sampled by wet splitting and the remainder sized settled to recover a silt size fraction (4-20 μ), and a clay sized fraction (< 4 μ). Various leaches (.1N HCl, 2N HCl, and am. ox.) were conducted on the bulk, silt and clay size fractions and the residues subjected to INAA analyses.

The response of Mn, Fe, Co, La, Ce, Yb, and Lu in the bulk, silt, and clay sized fractions of BBD, and RBD were found to be quite similar (Table 12 and Figure 24). The results also compare quite well with the more complete leach results described in previous sections. The lanthanides are strongly reduced by the acid treatments; Ce is more strongly reduced by the am. ox. treatment than by the mild acid treatment; iron is not affected by mild acid, and only moderately affected by the oxalate treatment.

The observed similarity of response of the above elements in the three size fractions can best be interpreted as due to a general uniformity in phase composition of the sediments from the coarsest to the finest size fractions. This means that micronodules, fish debris components are not restricted to the larger than sand (> 63 μ) size fraction of these samples. This reassures one that by studying the composition of the sand sized components (micronodules, biogenic carbonate, and silica, fish debris, smectite grains, etc.) it is possible to draw meaningful conclusions about the finer fractions of metalliferous sediments.

TABLE 12

Unleachable Elemental Ratios in Various Sediment Size Fractions of BBD and RBD

Element	Core	Size Fraction	.1N HCl*	2N HCl*	Am. Ox.*
Mn	BBD	Bulk	1.14	0.86	0.02
	"	20/4	1.10	0.77	0.02
	"	4	1.09	0.68	0.02
	RBD	Bulk	1.09	0.88	0.04
	"	20/4	1.13	0.95	< 0.01
	"	4	1.09	0.83	0.04
Fe	BBD	Bulk	1.15	(1.05)	0.90
	"	20/4	1.02	0.96	0.86
	"	4	1.08	1.05	0.88
	RBD	Bulk	1.04	1.06	0.82
	"	20/4	1.07	1.06	0.87
	"	4	1.05	1.06	0.82
Co	BBD	Bulk	1.14	(0.79)	0.01
	"	20/4	1.08	0.80	0.02
	"	4	1.23	0.78	0.01
	RBD	Bulk	1.17	0.97	0.03
	"	20/4	1.12	0.90	0.03
	"	4	1.14	1.09	0.04
La	BBD	Bulk	0.36	(0.05)	1.23
	"	20/4	0.27	0.08	1.22
	"	<4	0.28	0.01	1.19
	RBD	Bulk	0.22	-	1.27
	"	20/4	0.17	0.05	1.29
	"	<4	0.24	0.09	1.19
Ce	BBD	Bulk	0.80	(0.26)	0.53
	"	20/4	0.82	0.23	0.41
	"	<4	0.85	0.29	0.51
	RBD	Bulk	0.81	0.25	0.35
	"	20/4	-	0.26	0.40
	"	<4	n.d.	n.d.	n.d.
Yb	BBD	Bulk	0.32	-	1.03
	"	20/4	0.25	-	0.67
	"	<4	0.23	-	0.67
	RBD	Bulk	-	-	0.80
	"	20/4	-	-	0.80
	"	<4	0.44	-	0.75
Lu	BBD	Bulk	0.35	-	1.07
	"	20/4	0.23	-	0.66
	"	<4	0.19	-	0.52
	RBD	Bulk	0.23	-	0.71
	"	20/4	0.24	-	0.67
	"	<4	0.26	-	0.64

* Values found in each column represent:

.1N HCl: elemental fraction in the salt free sample which is unleachable with a (1X) - .1N HCl treatment

2N HCl: elemental fraction in the salt free sample which is unleachable with a (1X) - 2N HCl treatment

am. ox.: elemental fraction in the salt free sample which is unleachable with a (1X) - am. ox. treatment

n.d. = not detected
( ) = estimated values
- = missing values

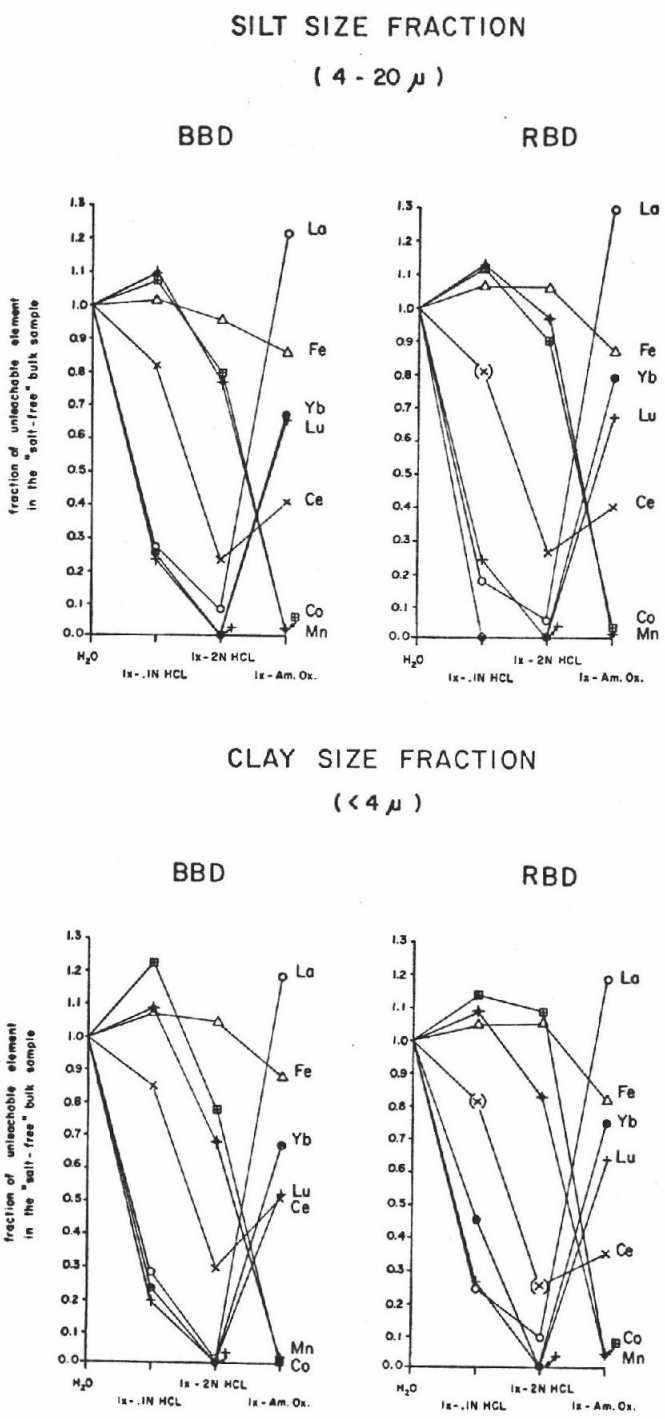

Figure 24. Leach effects on the cerium, cobalt, iron, lanthanum, lutecium, manganese, and ytterbium concentrations in BBD and RBD - silt and clay size sediment fractions.

3.4 Comparison of the Acid and Oxalate Leached Fraction with Known Fish Debris and Micronodule Compositions

In order to test the assumption that the fish debris phase is removed by the mild acid leach, and the micronodule phase by the oxalate leach, the compositions of the leached fractions are compared to known fish debris, and micronodule compositions (Table 13, Figures 25 and 26). As it was not feasible to recover enough fish debris or micronodule material to do both AAS and INAA analyses, comparisons for major elements and some minor elements are based on the calculated composition of the leached fraction. These compositions are based on the AAS leachate analyses corrected for salt content contributions for the elements Ca, K, Mg, Ba, and Si.

The composition of the .1N HCl leached fraction shows marked deviations from the fish debris composition given by Eklund (1974). Except for a similarity in the Ca values, all other elements in the leached fraction show much higher values than those determined by Eklund. It is evident that the mild acid leach removes some fraction of elements from other phases as well as dissolving the carbonate and fish debris fractions.

The discrepancy in the calculated .1N HCl leached fraction and the observed fish debris composition of Eklund (1974) may be due to higher concentrations of the elements considered in my samples than in Eklund's. Eklund's analyses are based on just five individual fragments of fish debris. Some of the elements considered may also have been removed from interstitial sites in the clays of the sediment (Mg and K), or have existed in part in an amorphous condition (Fe, Mn, Al, Si, Cu, Zn, and

TABLE 13

Elemental Concentrations in the Leached Fractions of BBD and RBD

	0.1N HCl Leached Fraction			Ammonium Oxalate Leached Fraction			
Element	BBD	RBD	(a)	BBD	RBD	(b)	(c)
Mg	33,900	60,000	4,100	21,100	21,300	20,100	n.r.
Al	40,600	56,700	1,100	11,700	22,500	9,200	11,600
Si	16,000	31,600	330	36,700	24,500	70,600	39,800
K	60,600	38,300	500	41,300	9,300	2,400	n.r.
Ca	213,800	288,000	322,900	n.d.	2,100	14,700	21,400
Mn	11,700	17,600	2,100	264,300	224,700	229,000	296,500
Fe	74,000	146,300	2,200	252,300	271,600	178,000	131,700
Co	n.d.	n.d.	n.d.	1,200	700	1,000	600
Ni	1,900	3,600	n.d.	3,500	3,800	4,800	5,900
Cu	2,800	6,500	200	2,700	3,000	1,700	5,600
Zn	1,000	2,200	n.d.	1,000	800	1,700	1,100
Ba	31,400	37,700	n.d.	8,700	5,100	9,100	4,900

n.d. = not detected

n.r. = not reported

(a) = Eklund (1973) average value for phosphatic fish debris

(b) = Eklund (1973) average value for microlaminated iron rich grains

(c) = Lyle (O.S.U. Geochem. Data Bank) average values for Mn micronodules from BBD core

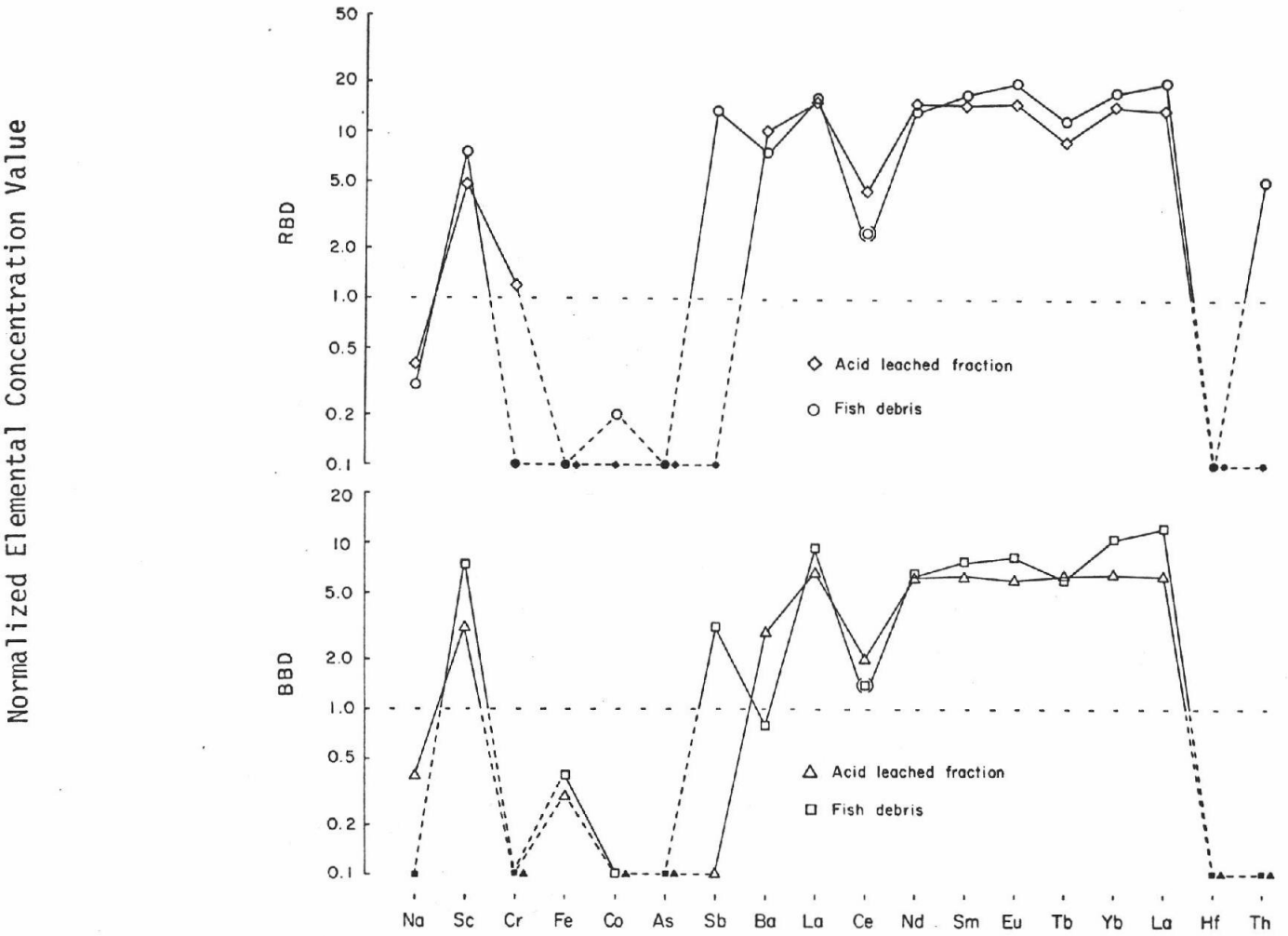

Figure 25. Acid leached sediment fraction and fish debris composition compared by normalizing to the corresponding bulk sediment - BBD and RBD. Values in ( ) are estimated. Solid figures represent values less than 0.1.

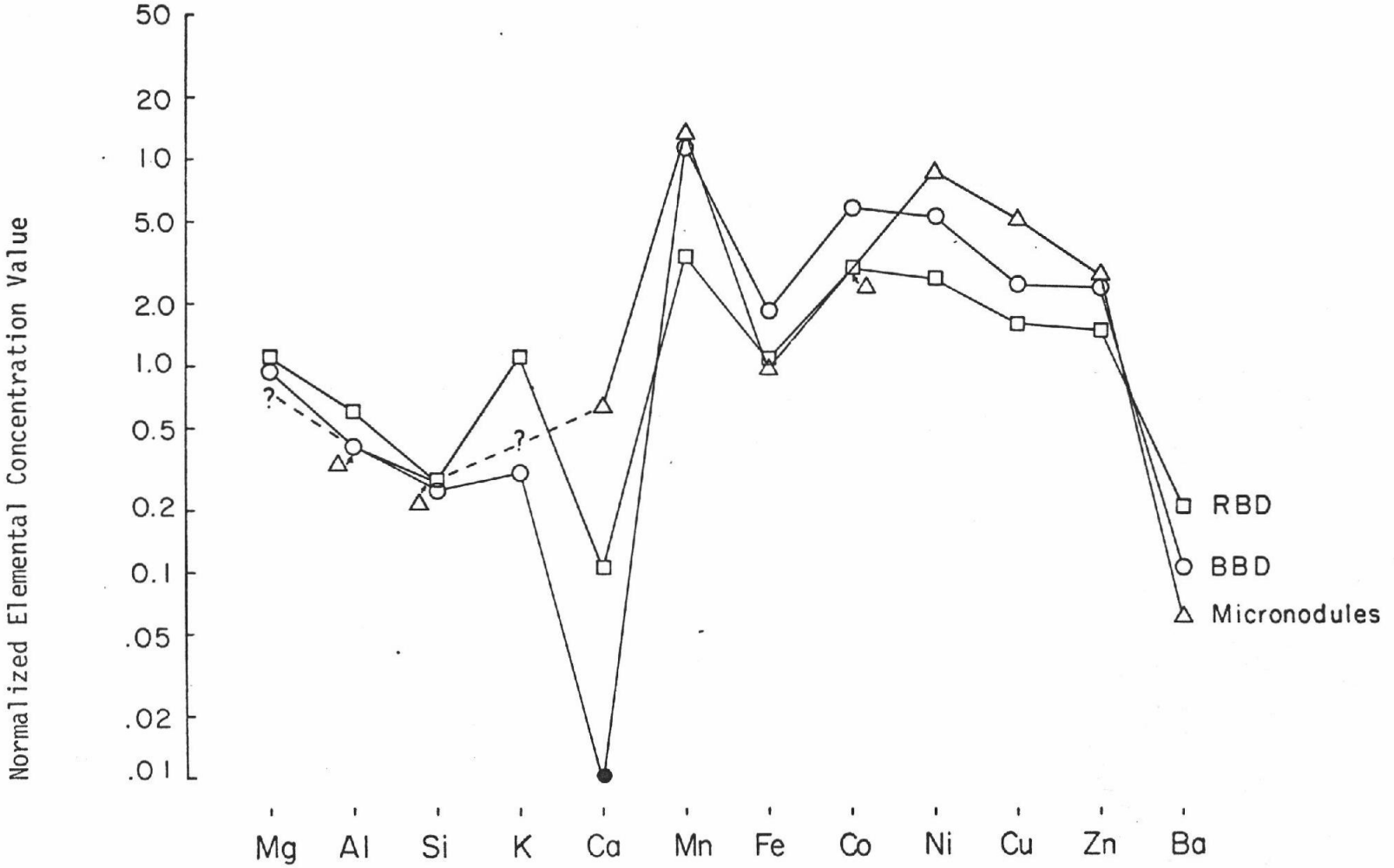

Figure 26. Oxalate leached sediment fraction and Mn-micronodules compositions compared by normalizing to the corresponding bulk sediment. Solid figure represents a value less than 0.1.

Ni). The solution of this problem requires further work on the major and trace element chemistry of the fish debris component.

The trace element composition of the mild acid fraction was calculated and compared to the measured fish debris composition by normalizing to the bulk sediment. These results are shown in Figure 25 and indicate that the calculated and measured trace element compositions resemble each other reasonably well. The lanthanide elements show particularly coherent patterns. These results support the idea that the acid leach removes the fish debris as well as the carbonate contents, along with a small fraction of other acid soluble components.

Comparison of the oxalate leached fraction to known micronodule compositions (Eklund, 1974; Lyle, written communication) show excellent agreement for most elements (Table 13, Figure 26). Several elements show significant discrepancies. The low Ca values for the oxalate fraction is probably due to the precipitation of Ca-oxalate during leaching. The higher K may be due to the removal of this ion from interstitial charge balancing positions in clays. The high iron content of the leached fraction can be attributed to the dissolution of any amorphous iron oxyhydroxide component by the oxalate solution.

In Figure 26, the micronodule data of Lyle were normalized to the bulk sediment composition of BBD, since the micronodules analyzed were recovered from this same core. The similarity of the oxalate leached patterns to that of the micronodules indicates that the fraction of a metalliferous sediment susceptible to leaching by ammonium oxalate is well represented by micronodule compositions.

3.5 Comparison of Residue Compositions to Smectite Compositions

If the sediments treated are a mixture of phases susceptible to specific leaching by acid and ammonium oxalate, then the residue of such leaching experiments should be compositionally similar to some, perhaps well known, chemical entity. It has been postulated that Fe-rich smectite (nontronite) composes a large fraction of the bulk metalliferous sediments (Sayles and Bischoff, 1973). This mineral is known to be resistant to oxalate leaching (Heath and Dymond, 1977). It is also possible that detrital basalt could form the major part of the leach residues. The major element chemistry of the BBD and RBD residues is compared (Table 14) to the corresponding chemistry for smectite grains (Eklund, 1974) and oceanic basalts from the Nazca Plate (Corliss et al., 1976). The BBD and RBD residues compared are those treated with both an oxalate leach (amorphous oxyhydroxides and micronodules removal) and a mild acid leach (carbonate and fish debris removed). The residues compare most favorably with the average smectite composition of Eklund (1974) and deviate quite markedly from the composition of the basalts. The number of published marine nontronite analyses available is limited. It is, therefore, difficult to attribute compositional differences between BBD and RBD and between these and Eklund's compositions to variations in the compositions of the smectites themselves or to contributions from non-smectite components.

The Al content of the BBD and RBD residues is higher than that of the smectite reported by Eklund and could be due to the presence of a detrital feldspar phase (labradorite-bytonite). In this case, however,

TABLE 14

Composition of Leached Residues of BBD and RBD Compared to Known Smectite and Basalt Compositions

Oxide	BBD*	RBD*	Smectite(1)	Basalt(2)
Na_2O	0.29 ± 0.01+	0.38 + 0.01+	0.60	2.80
MgO	3.26 ± 0.03	2.57 ± 0.03	6.10	6.70
Al_2O_3	7.12 ± 0.10	9.34 ± 0.13	2.44	13.60
SiO_2	52.48 ± 1.32	29.70 ± 1.15	52.25	49.66
K_2O	1.07 ± 0.02	0.93 ± 0.02	2.04	0.25
CaO	0.59 ± 0.03	0.58 ± 0.03	0.47	10.73
MnO_2	1.77 ± 0.26	2.71 ± 0.33	0.78	0.22 (based on BCR)
Fe_2O_3	20.39 ± 1.05	42.53 ± 1.32	29.70	12.19
BaO	1.68 ± 0.11	0.20 ± 0.02	0.03	0.11 (based on BCR)
Σ	88.65	88.94	94.90	83.91

* Residue of (1X) 0.1N HC_2 + (1X) am. ox. Leach.

+ Based on INAA data, all other unmarked data from AAS work.

(1) Average values for smectites from Eklund (1973).

(2) Average values for basalts from Corliss et al. (1976).

the SiO_2 and CaO contents might be significantly increased. The SiO_2 and CaO concentrations, particularly in BBD, agree well with the given smectite composition and, therefore, a significant feldspar component seems unlikely in these samples. The x-ray diffractograms of this residue, moreover, do not show evidence of any well defined peaks attributable to a feldspar component.

A comparison of the BBD and RBD residue composition is made in Figure 27 with reported nontronite compositions from Ross and Hendricks (1945), Bischoff (1972), Eklund (1974), Müller and Förstner (1976), Isphording (1975), and Corliss et al. (1977, in preparation).

On the SiO_2 - Fe_2O_3 - MgO plot, all data show a close clustering along the SiO_2 - Fe_2O_3 axis. Both BBD and RBD lie within, or near, the literature data cluster with RBD at the extreme Fe_2O_3 end of the data envelope.

The SiO_2 - Fe_2O_3 - Al_2O_3 plot shows considerable scatter in reported nontronite compositions. In general, marine or hydrothermal nontronites (Eklund; Bischoff; Müller and Förstner; Corliss et al.) show quite low Al_2O_3 and, therefore, plot near the SiO_2 - Fe_2O_3 axis. Continental nontronites, including those with "excess" Fe_2O_3 (Ross and Hendricks), show considerably more scatter and tend toward the Al_2O_3 end member. These Al_2O_3 rich samples plot in the area between the marine nontronites and the montmorillonite-beidellite end members of the smectite group (Figure 27). The BBD and RBD residues plot within or near the field defined by marine and continental nontronites, and supports the contention that these samples represent the smectite component of the sediments.

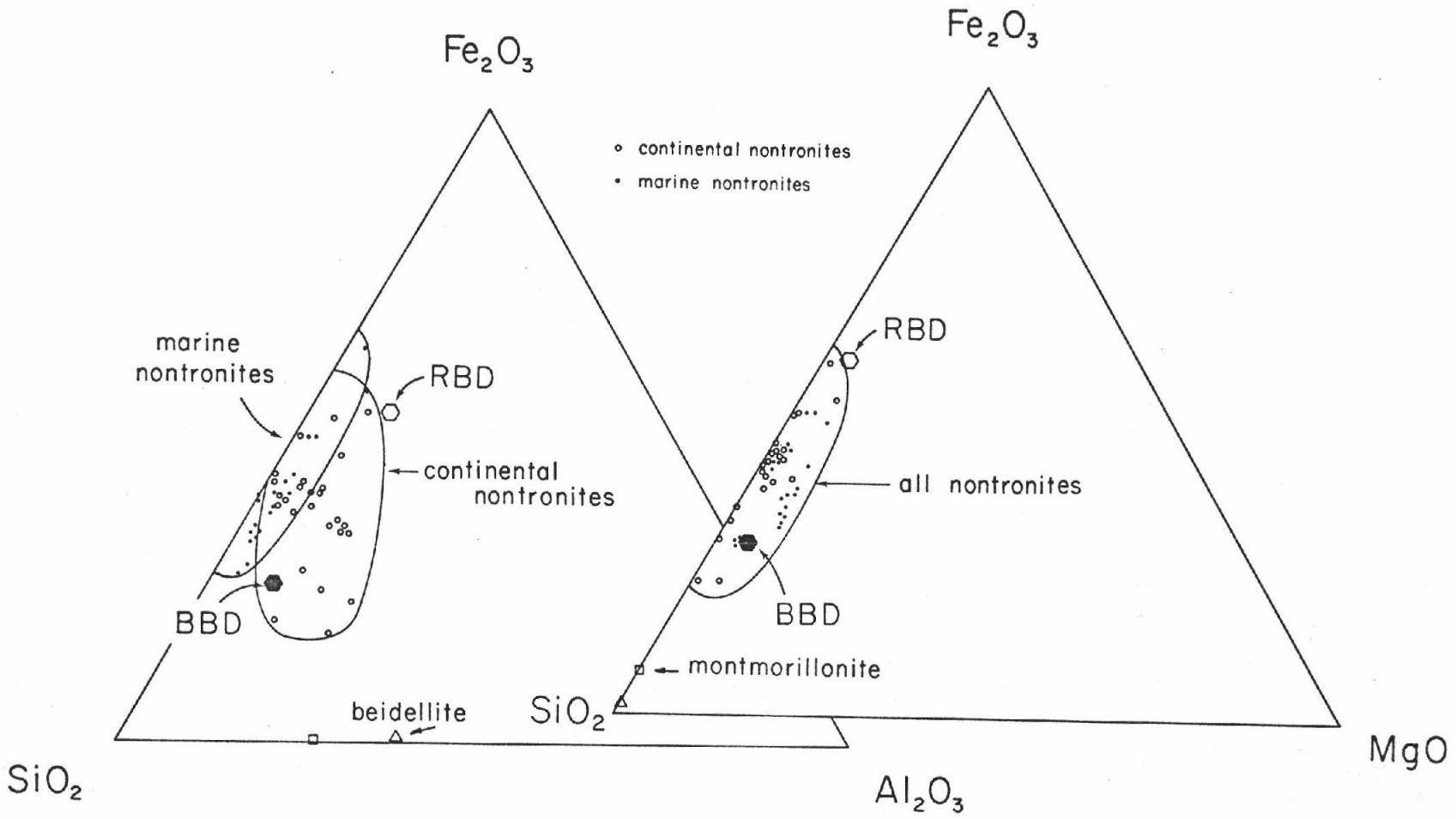

Figure 27. Fe_2O_3-SiO_2-Al_2O_3-MgO composition of the leach residue of BBD and RBD compared to marine and continental nontronites.

3.6 Calculated Smectite Composition of BBD and RBD Residues

Ross and Hendricks (1945) on the basis of extensive petrographic, x-ray, and chemical analyses of members of the montmorillonite group of clays provide a mathematical procedure for calculating structural formulas from known chemical analyses. I have used their method and applied the following limitations:

a) general structure

$X_{.67}Y_{4-6}Z_8O_{20}(OH)_4 \cdot nH_2O$ (MacEwan, 1961; Edklund, 1973)

X = charge balancing ions ($Ca^{+2}/2$, Na^+, K^+)

Y = octahedral ions (Al^{+3}, Fe^{+3}, Mg^{+2}, Mn^{+4})

Z = trioctahedral ions (Al^{+3}, Si^{+4})

b) unit cell of 44 equivalents

c) all Fe and Mn are in their highest normal oxidation states with all iron in the octahedral layer.

For BBD, the resultant structure is:

$$(Ca^{+2}/2, Na^+, K^+)_{.66}(Al^{+3}_{.92}, Fe^{+3}_{2.25}, Mg^{+2}_{.71}, Mn^{+4}_{.18})$$
$$(Al^{+3}_{.31}, Si^{+4}_{7.69})O_{20}(OH)_4 \cdot nH_2O$$

Applying this same method to the residue composition of RBD fails to give a real solution until the Fe_2O_3 content of the sample is reduced from the observed 42.53% to 23.01%. Under this new restriction, the resultant structural formula is:

$$(Ca^{+2}/2, Na^+, K^+)_{.65}(Al^{+3}_{.06}, Fe^{+3}_{3.43}, Mg^{+2}_{.76}, Mn^{+4}_{.37})$$
$$(Al^{+3}_{2.12}, Si^{+4}_{5.88})O_{20}(OH)_4 \cdot nH_2O$$

The designation $Ca^{+2}/2$ indicates that only half as many Ca^{+2} ions are required as Na^{+} or K^{+} to produce the same charge balance effect.

A comparison of the formulas indicates that in the Roggeveen Basin smectite there is a greater degree of substitution of Al for Si in the tetrahedral layer compared to the Bauer Basin sample. This is accompanied by a concomitent substitution of Fe^{+3} for Al^{+3} in the octahedral layer. It is then to be expected that nontronites developing in metalliferous sediment environments will show a considerable degree of compositional variation dependent on the availability of Fe, Al, and Si. The exact composition of these smectites would also show the inclusion of Ni, Cu, and Zn (Eklund, 1974), as well as As, Sb, and Hf substituting to a minor degree for Mg and Mn in the octahedral layer. In these structural formulas no iron has been inserted in the tetrahedral layer, although Bischoff (1972) indicates that this substitution does occur in Red Sea nontronites. In the preceeding formulas, it may be seen that an Fe-Al exchange can be made between the octahedral and tetrahedral layers without changing the overall composition of the sample. Since both ions have the same +3 charge, there would not be any change in the budget of charge balancing ions either.

Ross and Hendricks (1945) have found that the number of ions in octahedral coordination in smectites (Σ) did not exceed 4.40 except in a few of the samples they examined. They concluded that Σ values in excess of 4.40 indicated that part of the aluminum was external to the smectite lattice, i.e. an impurity. The Σ value for BBD is 4.19 and for RBD it is 4.62. The RBD residue composition used in addition to having

an excess of Fe_2O_3 may also include a small amount of detrital Al.

The x-ray diffractograms of the BBD and RBD smectite residue did not evidence a detrital component. However, the presence of such a component, rich in Al, may be indicated by the fact that both the BBD and RBD residue samples are displaced toward the Al_2O_3 apex of the SiO_2-Fe_2O_3-Al_2O_3 triangular plot (Figure 27) and away from the marine nontronite field shown. If it is assumed that part of the Al is in another than the smectite component a recalculation of the structural formula would require the displacement of iron from the octahedral to the tetrahedral layer. More extensive experimental work is required to resolve the question of the mineralogical nature of the oxalate + mild acid leached residues.

The structural formulas calculated agree reasonably well with the nontronite formula of Eklund (1974), derived from microprobe analyses of single smectite grains, and with the more general formulas of Ross and Hendricks (1945), and MacEwan (1961).

3.7 Calculation of the Phase Composition of the Salt Free Bulk Sediment Compositions of BBD and RBD

Based on the measured composition of phase separates and results from the leaching experiments, it is possible to estimate the composition of the Bauer and Roggeveen Basin samples in terms of the following components:

a) fish debris

b) carbonate

c) micronodules/amorphous oxyhydroxides

d) iron rich smectite

e) excess Fe_2O_3 (RBD only)

f) barite

All values are given on a salt free basis (SFB).

a) Fish Debris

Not having directly measured values of the lanthanides in the Fe-smectite of either the Bauer or Roggeveen Basins, it is not possible to determine by means of a set of simultaneous equations the weight percentage of each separate phase. Previous studies, however, have shown that the lanthanide contents of smectites is quite low (Toth, 1977; Corliss et al., 1977). Consequently, this phase as well as all other phases except fish debris may be ignored as contributors to the lanthanides concentratin of the bulk sediments (Table 15). This permits an estimate of the phosphatic fish debris content of BBD and RBD. Again, Ce is excluded here. These estimates are shown in the last column of Table 15. The range of values for BBD is 9.8 - 19.0% fish debris. The average value for BBD is 13.1%. The RBD sample shows a 5.7 - 7.3% range and an average value of 6.2%. These estimates are, of course, maximum values because of the assumptions made.

b) Carbonate

The carbonate content of BBD and RBD were measured by Leco analyses and are 2.3% in BBD and 1.0% in RBD (Table 10). As the carbonate component is removed along with the fish debris phase during mild acid treatment, the percent weight of these two components should compare well with the measured percent weight loss noted in Table 9. This com-

TABLE 15

Lanthanide Concentrations in the Major BBD and RBD Sediment Components and an Estimate of the % Fish Debris in BBD and RBD

Element	Core	Concentration in PPM in F.D.+	Mn-Micro	Fe-Sm*	Bulk++	Estimated % F.D.+
La	BBD	1,887	44.3	4.04	256	13.57
Nd	"	1,250	n.d.	n.d.	238	19.04
Sm	"	268	4.7	0.75	38.4	14.33
Eu	"	91.5	1.2	0.19	11.3	12.35
Tb	"	55.7	n.d.	0.13	6.0	10.77
Yb	"	370	n.d.	1.06	42.9	11.59
Lu	"	71.7	1.9	0.13	7.0	9.76
					range (9.8-19.0%); $\bar{X}$ = 13.1%	
La	RBD	3,279	n.d.	4.04	230	7.01
Nd	"	3,409	n.d.	n.d.	247	7.25
Sm	"	782	22.8	0.75	49.1	6.28
Eu	"	231	4.5	0.19	12.6	5.45
Tb	"	105	2.9	0.13	6.0	5.71
Yb	"	494	n.d.	1.06	30.4	6.15
Lu	"	89.9	5.9	0.13	4.7	5.23
					range (5.5-7.3%); $\bar{X}$ = 6.2%	

n.d. = not detected
+ Fish debris
++ Lanthanide concentrations in the salt free sediment, Appendix III.
* Average lanthanide values for 5 smectites from Galapagos hydrothermal deposits, Corliss et al. (1977).

parison is shown below:

		Estimated or Measured Content	
		BBD	RBD
Fish Debris		13.1%	6.2%
Carbonate		2.3%	1.0%
Σ	=	15.4%	7.2%
Measured Fraction Removed by Mild Acid (1X) Treatment (Table 9)		15.0%	9.4%

The greater degree of discrepancy for the estimated versus measured leachable fraction for the BBD material is most likely due to the presence of a larger fraction of amorphous component in the Roggeveen Basin material. It will be seen in the following section that the micronodule component in RBD is about twice as high as in BBD. Some of this oxalate leachable component is undoubtedly being removed by the mild acid leach.

c) Micronodules

Cobalt is highly concentrated in the micronodule phase compared to other sediment components (Tables 2-6). Various published Co values for smectites indicate quite low concentrations in this phase [0.02 ± 0.02% CoO (Eklund, 1974); 5.1 PPM (Toth, 1977); 4.3 PPM (Corliss et al., 1977, in press)]. Assuming that all other phases may be ignored as Co contributors, the micronodule phase content of each sample may be calculated

from the Co concentrations in the micronodules, and the salt free bulk sediment. This result is:

BBD = 25.5% micronodules

RBD = 43.9% micronodules

The total percent weight loss of each sample from a double leaching of ammonium oxalate is 24% for BBD and 41.6% for RBD (Table 9). The micronodule estimates are, of course, maximum values since I have assumed no other Co contributing components, but are in good agreement with the leach data. The close agreement between the calculated and experimentally determined values indicates that there is either no substantial fraction of amorphous component in the sediments, that any such amorphous material has been converted to a crystalline form during the freeze drying procedure, or that the composition of the amorphous component is very similar to that of the micronodule phase and is not readily distinguishable.

d) Smectite

I have already indicated that the residue of the combined oxalate and mild acid leach bears a close resemblance to known iron-rich smectites. The fraction of this residue remaining after leaching should then be a measure of the smectite fraction in the sediment. Based on the data of Table 9, it is found that the 59.4% of the Bauer Basin sample and 47.6% of the Roggeveen Basin samples are unaffected by a combined oxalate and acid treatment. Using the phase analysis data of Eklund (1974), Dymond and Eklund (in preparation) have calculated that the Bauer Basin sediment from which the phases were recovered consisted

of 70.1% smectite. This agrees well with the value of 59.4% determined in this work.

A correction is made in e) for the excess iron in RBD.

e) Excess Fe as Fe_2O_3 in RBD

It was noted in section 3.5 that in order to calculate a structural formula for the RBD sample, the iron content had to be reduced from 42.53% to 23.01% Fe_2O_3. The form of excess iron in this sample is most likely goethite or a similar oxyhydroxide but for convenience will be referred to as Fe_2O_3. Ross and Hendricks (1945), in working with nontronites, found that the analyses of certain samples which showed "no evidence of essential impurities" could not be reduced to structural formulas without first reducing their iron content. These authors suggest that the impurity is due to the presence of "a mixed-layer material." The condition for the formation of such a mixed layer structure may exist in the Roggeveen Basin where the development of smectites in the presence of a high iron concentration and a paucity of mobile organic silica may occlude iron oxide components in the clay structure. It is also possible that certain types of smectites may form with the considerable substitution of iron for aluminum in the tetrahedral as well as the octahedral layer. In either of the two cases indicated, the "excess" iron would not be subject to oxalate leaching and appear as part of the residue. The excess iron may also be present as a separate crystalline goethite phase which also would not be susceptible to oxalate leaching (Dymond et al., 1977). Indications of a separate goethite phase were noted in the x-ray diffractogram of the

RBD residue. Assuming that the "excess" iron is foreign to the smectite phase, the RBD residue then actually consists of 21.9% excess iron and 78.1% smectite. In terms of the salt free bulk sediment, the 57.6% smectite which the RBD residue represented actually reduces to 12.6% "excess" Fe_2O_3 and 45.0% smectite.

f) Barite

The data for BaO in the BBD and RBD residues (Table 14) shows that both values are considerably higher than the value given by Eklund (1974) for an iron rich smectite. By reducing the BaO concentration of each sample to the value of Eklund (0.03%) and changing the excess BaO to $BaSO_4$, an estimate may be made of the barite content of each sample. This estimate should be close to a mixture value and is found to be:

	BBD	RBD
% Barite	1.7	.2
% Smectite	57.7	57.4^{++}
Σ %	59.4^{+}	57.6^{+}

$^{+}$ These are the values determined in d) for the leach residue estimates.

$^{++}$ This value includes "excess" Fe_2O_3.

The higher fraction of barite in BBD is most probably a reflection of a greater degree of biogenic input from the equatorial high productivity zone into the Bauer Basin compared to the Roggeveen Basin.

g) Phase Composition of BBD and RBD

The phase composition of the salt free Bauer Basin and Roggeveen

Basin are compared in Table 16 and show that:

a) the sum of the fractions of the components is close to 100% and that, therefore, the phase composition estimates are reasonably good (In most cases, the estimates are maximum values.),

b) the higher fish debris, carbonate and barite contents of BBD reflect a greater degree of biological input to the Bauer Basin compared to the Roggeveen Basin,

c) the higher micronodules and the "excess" iron content of RBD reflects a higher degree of iron and manganese oxyhydroxide input to the Roggeveen Basin compared to the Bauer Basin,

d) the higher smectite fraction in the BBD sample may be due to the higher input of biological silica to the Bauer Basin permitting the more extensive development of an iron-rich smectite phase, as a result of the combination of biogenic silica with Fe and Mn oxyhydroxides to form smectites and todorokite (Lyle et al., 1977),

e) the near 100% value of Σ for BBD indicates that the components in this sediment are selectively leached by the various treatments used. In the RBD sediment, there is a greater degree of amorphous character and the leach treatments are, therefore, less phase specific, and

f) it is possible to estimate the phase composition of a metalliferous sediment on the basis of a few simple leaches.

TABLE 16

Phase Composition of BBD and RBD

		BBD	RBD
a)	Fish Debris	13.1%	6.2%
b)	Carbonate	2.3%	1.0%
c)	Micronodules and amorphous Fe and Mn oxyhydroxides	25.5%	43.9%
d)	Smectite	57.7%	45.0%
e)	Crystalline Fe-oxyhydroxides	none	12.6%
f)	Barite	1.7%	0.2%
	Σ	100.3%	108.9%

4.0 DISCUSSION OF RESULTS AND CONCLUSIONS

It was found that the Bauer and Roggeveen Basins bulk sediments responded in very similar manner to various chemical leachings. This implies that, in spite of being separated by over 4,000 kms and of differences in their overall chemical compositions, the sediments of these two areas bear considerable similarity to each other. Dymond et al. (1973), on the basis of extensive analyses of metalliferous sediments from the EPR, Bauer Basin, and several DSDP sites outside the Nazca Plate, suggested that all of these sediments had a common origin. The only satisfactory explanation was the precipitation of metal rich phases from hydrothermal fluids. This hypothesis was later refined by Heath and Dymond (1977) to incorporate contributions from detrital, hydrogenous, and biogenic materials as well as the important hydrothermal component. Lonsdale (1977) suggested that the chemical and mineralogical similarity between the EPR and Bauer Basin metalliferous sediments was strong evidence of a common origin. On the basis of hydrographic data and current measurements, Lonsdale described a pattern of bottom currents (Figure 1) capable of transporting fine grained precipitates eastward from the EPR into the Bauer Basin where these particles could "settle out in the slack water" of this area.

If, as seems reasonable, the EPR is the actual source of the metalliferous sediments of the Bauer Basin, then it is logical to assume that the very similar sediments of the Roggeveen Basin originate in the fracture zones of the South Chile Rise and are deposited in the "slack waters" of this area by the bottom currents described by Lonsdale (Figure

1). Francheteau et al. (1975) indicate that on the MAR transform fault troughs are prime sites for metal-rich hydrothermal emanations. The composition of surface sediment samples indicates a lobe of high Fe and Mn deposition extending eastward from the EPR at 25°S and of undefined southern extent (Corliss, unpublished data). Referring to the bottom water circulation over the Chile Rise, Lonsdale (1976) states "Figure 1 illustrates the dominance of inflow through this transform fault system. Other gaps in the Chile Rise may be effective passages at shallower levels." This is indicated by arrows through the fracture zones to the west of Lonsdale's main flow paths on the extreme east of the Chile Rise (Figure 1).

The influence of a strong bottom current moving north into the Roggeveen Basin from the Bellinghausen Basin through fracture zones where it could pick up significant quantities of hydrothermal components is indicated in the Roggeveen Basin by a higher sedimentation rate and a higher iron content compared with the Bauer Basin (Veeh, written communication).

In their study of ferromanganoan sediments from the Equatorial East Pacific, Sayles and Bischoff (1973) found that:

> "the major ion concentrations and the pH of the pore water fluids do not differ significantly from the overlying bottom water,"
>
> and that, therefore,
>
> "diagenetic reactions must occur primarily near the sea water sediment interface. Extensive reaction at depths of 20 cm. or more would affect the composition of the pore waters."

This may only be true for relative shallow sediment depths. Dymond

et al. (1977) have shown for sediments down to 110 m. in DSDP Site 319 that there are marked differences in major (Fe, Mn) and minor (Co, Cu, Ni, Zn) element compositions. These are attributed to changes in the relative contributions of elemental sources rather than to diagenetic changes in sediments derived from a single origin. M. Lyle (O.S.U. Ph.D. thesis, in progress) has found a decrease in the opal content down core in Y73-3-20P (a core in the Bauer Basin near the site of BBD). A corresponding increase in the crystallinity of the smectite component, as indicated by the full width at half maximum (of peak height) (FWHM), indicates a general growth down core of the smectite grain size. This recombination of opal, Fe, and Mn oxyhydroxides to form smectite and micronodules has been discussed by Dymond and Eklund (in preparation) and Lyle et al. (1977).

These ideas can help to explain the fact that there was virtually no biogenic silica in the BBD and RBD samples examined, as well as the absence of carbonate and phillipsite. In contrast, these components were found to be fairly common in BBS (the surface sample of the Bauer Basin) but were missing from BBD and RBD. Phillipsite, biogenic carbonate, and silica can then be considered as ephemeral components of metalliferous sediments of the Bauer and Roggeveen sediments.

Another characteristic of the metalliferous sediments examined is explainable on the basis of the above diagenetic model. Near surface and down core samples of the sediments were observed to have much the same size distribution of micronodules. This may be a manifestation of the widespread conversion of oxyhydroxides and opal to smectites and

micronodules. Micronodules are normally limited in size, usually < 63μ, and a suite of sizes above that are not evident indicating that the smectite formation occurs evenly throughout the surface sediments, i.e. many points of nucleation of the micronodules. The lack of evidence of an increase in the size of micronodules down core indicates that the diagenetic change occurs and is essentially completed at the sea water sediment interface, as indicated by Sayles and Bischoff (1973).

The ammonium oxalate leach, designed to remove amorphous Fe and Mn oxyhydroxide phases, show that for BBD a double treatment dissolved 24.0% of the sediment but removes an average of only 10% of the lanthanides present. In the case of RBD under the same condition, 41.6% of the sediment is dissolved while approximately 30% of the lanthanides are removed. This noticeable difference between the Bauer sample and the Roggeveen Basin sample is probably related to the fact that the sediments in RBD are accumulating at a higher rate than those of BBD and that a larger fraction of the lanthanides in the sediment are associated with the amorphous oxyhydroxide phase.

Arrhenius and Bonatti (1965) propose that phosphatic fish debris actively accumulates lanthanide elements with time in the sediments. The above results may be interpreted in the following manner. Phosphatic fish debris per se contains a high concentration of lanthanide elements as well as the capability of acquiring additional lanthanides, after being incorporated into the sediments. The formation and deposition of amorphous oxyhydroxide components over the Nazca Plate, or other similar areas, scavange, from either sea water or perhaps even hydro-

thermal fluids, available lanthanides and eventually carry these elements, as well as other trace elements, into the sediments. Here diagenetic changes reorganize the distribution of elements, the lanthanides being incorporated and stabilized in the phosphatic fish debris. In the Bauer Deep region, productivity is still high enough to provide a sufficient supply of fish debris to the sediments to fix the supply of oxyhydroxide-borne lanthanides. In the Roggeveen Basin area, the oxyhydroxide-borne lanthanide supply to the sediments outweighs the fish debris supply and, as such, a larger fraction of these lanthanides remain unfixed and, therefore, susceptible to dissolution by an ammonium oxalate leach. The above proposed redistribution of lanthanides would, moreover, help to explain the fact that the lanthanide imprint on metalliferous sediments has essentially a sea water pattern, and also why fish debris from different sources (core levels, or geographical area) have different lanthanide concentrations. It is also possible that the lower supply of silica vs. iron in the Roggeveen Basin inhibits the conversion of the iron oxyhydroxides to an iron-rich smectite, and that this in turn prevents the release of the lanthanides. This model can also help to explain why Ce shows a negative anomaly in the fish debris and positive anomaly in the micronodule component. Cerium, because of its +4 oxidation state, incorporates readily into the micronodule phase during formation and thus is unavailable to enter into the fish debris component (Dymond and Eklund, in preparation).

Dr. Herb Veeh (written communication, 1974) measured the sediment accumulation rates of the cores in question by the 230 Th/232Th disequi-

librium method (Koczy, 1961) and found the accumulation rate of BBD to be 1.9 mm/10^3 years, while that of RBD was 4.3 mm/10^3 years. Using a total-γ counting procedure, Mr. Chris Moser (O.S.U. Master's thesis, in progress) has determined accumulation rates of 1.4/10^3 years and 2.9 mm/10^3 years for BBD and RBD, respectively.

Bulk chemical data for the Roggeveen Basin sediment sample (RBD), in combination with the sediment accumulation rate values of Veeh, show that transition elements are accumulating at rates equal to or greater than those on the same parts of E.P.R. (Dymond and Veeh, 1975). In general, this data indicates that all elements analyzed are accumulating at a higher rate in the Roggeveen than in the Bauer Basin. These results are shown in Table 17.

The accumulation rate data can further be used to compute what may be called an enrichment factor. This is defined for my purposes as the rate at which elements are accumulating in the Bauer or Roggeveen Basins compared (divided by) to the rate at which these elements are supplied to the worlds oceans in a dissolved state. The calculations are made on a mg/cm^2/10^3 years basis and the factors calculated shown in Table 18. Dissolved lanthanide concentrations in river waters are limited to one value given for La. The enrichment factor for this element will be used as representative of other lanthanides except Ce. It is evident that the data show transition and lanthanide elements to be accumulating in BBD and RBD at rates much too high to be explained by a river water source. Corliss (1971) has shown that Mn, Fe, Co, and the lanthanides and other minor elements such as Sc to be depleted in the "slowly cooled interior portions (of pillow basalts from the MAR) relative to the

TABLE 17

Metal Accumulation Rates in the Bauer and Roggeveen Basins
($mg/cm^2/10^3$ years)

Element	BBD	RBD
Na	2.329	6.050
Mg	1.008	3.449
Al	1.289	6.754
Si	6.674	16.073
K	0.695	1.517
Ca	1.530	3.720
Sc	0.001	0.004
Cr	0.001	0.007
Mn	2.275	12.010
Fe	6.265	46.233
Co	0.010	0.043
Ni	0.030	0.253
Cu	0.049	0.325
Zn	0.018	0.099
As	0.003	0.063
Sb	0.001	0.003
Ba	0.704	0.903
La	0.009	0.038
Ce	0.003	0.027
Nd	0.009	0.042
Sm	0.001	0.008
Eu	0.0004	0.002
Tb	0.0002	0.001
Yb	0.002	0.005
Lu	0.0003	0.0008
Hf	0.0002	0.001
W	0.001	0.005
Th	0.001	0.001

quenched flow margins." This was suggested to be due to the fact "that these components . . . occupy accessible sites . . . in the hot solid rock mass, and are mobilized by dissolution . . . in sea water introduced along contraction cracks that form during cooling and solidification."

These results clearly indicate that there must be a local source for many of the elements considered or that by some unique mechanism a proportionate fraction of dissolved transition and lanthanide elements contributed by rivers end up in the metalliferous sediments of the Nazca Plate. A local source of these elements seems a more reasonable and satisfactory explanation in view of the tectonic activity along the EPR, and the South Chile Rise and the recently proven association of hydrothermal activity with the active Galapagos Rift. Not all elements showing an enrichment factor greater than 1 need be of hydrothermal origin. Al, Ni, and some Co could be of detrital origin while Si and Ba, particularly in the BBD sample, could be biogenic in origin. The source of various elements in Nazca Plate sediments has been discussed in detail by Heath and Dymond (1977). The high Mn and Fe enrichment factors in RBD and the low silica, and carbonate content of this sample indicate that the Roggeveen Basin may make an ideal area in which to study relatively pure hydrothermal sediments.

Dymond et al. (1973) have suggested on the basis of the similarity of the lanthanide patterns that the lanthanides in metalliferous sediments derive ultimately from sea water. The sea water normalized lanthanide patterns for the various components separated from BBS show con-

TABLE 18

Enrichment Factors

(Rate at which elements are accumulating in BBD and RBD compared to the rate at which these elements are supplied to the oceans as dissolved river matter.)

Element	BBD	RBD
Na	0.03	0.08
Mg	0.03	0.10
Al	0.36	1.91
Si	0.19	0.45
K	0.03	0.07
Ca	0.12	0.28
Sc	28.3	113.1
Cr	0.08	0.80
Mn	51.5	272
Fe	1.06	7.81
Co	5.66	24.3
Ni	11.3	95.4
Cu	1.11	7.35
Zn	0.20	1.12
As	0.34	7.13
Sb	0.06	0.34
Ba	7.96	10.22
La*	5.09	21.49
W	3.77	18.9
Th	0.11	1.13

* Taken as representative of all lanthanides as these are no data for other lanthanides in river water.

River water data from Riley and Chester (1971).

Average river runoff (3.2×10^{19} gms/year) from Garrels and MacKenzie (1971).

Total surface area of world ocean (3.62×10^{8} km^2) from Turekian (1968).

siderable deviation from a sea water pattern (Figure 2). The biogenic carbonate data of Spirn (1965) have been used because they are more complete than, but similar to, my own. Enrichments over sea water ranging from ~1 x 10^6 for the carbonate component to 2.5 x 10^8 for the fish debris fraction were found.

The brown aggregates which represent the bulk BBS sediment show the nearly horizontal normalized pattern indicative of a sea water pattern. This is also true of the yellow aggregates. The fish debris pattern shows a very marked negative Ce anomaly. The micronodule and carbonate patterns are both similar to that of the shales (Haskin and Haskins, 1966). These patterns show a marked positive Ce anomaly and a noticeable depletion of the heavy lanthanides; i.e. Tb, Yb, Lu. The phillipsite pattern shows a general shale pattern except for the marked negative Ce anomaly. In the absence of any other data, the nontronite lanthanide values of Corliss et al. (1977, in preparation) were used as representative of the iron rich smectites which constitute a major fraction of metalliferous sediments. This component shows a relatively flat pattern indicating a sea water source, a relatively low concentration of lanthanides as compared to other components, and a slight positive Ce anomaly.

It is evident that the sea water like pattern of BBS hides the complex patterns of the individual components in this sediment. Important also is that the fish debris component shows a ten fold enrichment in lanthanides over micronodules, the next most important sediment component, and a one hundred fold enrichment over the carbonate and nontronite phases.

Piper (1974) has indicated that the lanthanide pattern of river waters is similar to that of shales which is, of course, markedly different from that of sea water (Figure 28). This implies that, if river waters are the ultimate source of sea water lanthanides, a considerable degree of fractionation must take place in the ocean to reduce the shale input pattern to the observed sea water pattern. The lighter lanthanides (La to Eu) would have to be removed preferentially with respect to the heavier lanthanides (Tb to Lu). This is the pattern observed for the phillipsite, micronodule and phillipsite phases. Cerium is primarily removed by the micronodule and carbonate phases which show a marked positive Ce anomaly.

This work has attempted to elucidate the nature of the distribution of elements in the phases composing metalliferous sediments of the Bauer and Roggeveen Basins and to make estimates of the phase composition of the sediments themselves. An attempt has been made to suggest how these phases themselves originate and how they acquire their elemental composition. Numerous problems, however, remain unanswered. For example, although the biogenic input to the Roggeveen Basin is lower than for the Bauer Basin, the rate of accumulation of Ba in the Roggeveen Basin is higher than that for the Bauer Basin. This observation appears to conflict with the observation that Ba is enriched in the biogenic deposits of the Equatorial Pacific (Goldberg and Arrhenius, 1958). Recent results from the Galapagos Hydrothermal Area, however, indicate Ba to correlate well with the silica content of hot waters emanating from hydrothermal vents (Edmond, unpublished data). The leaching results indicate that Ba is quite mobile in the sediments and apparently not

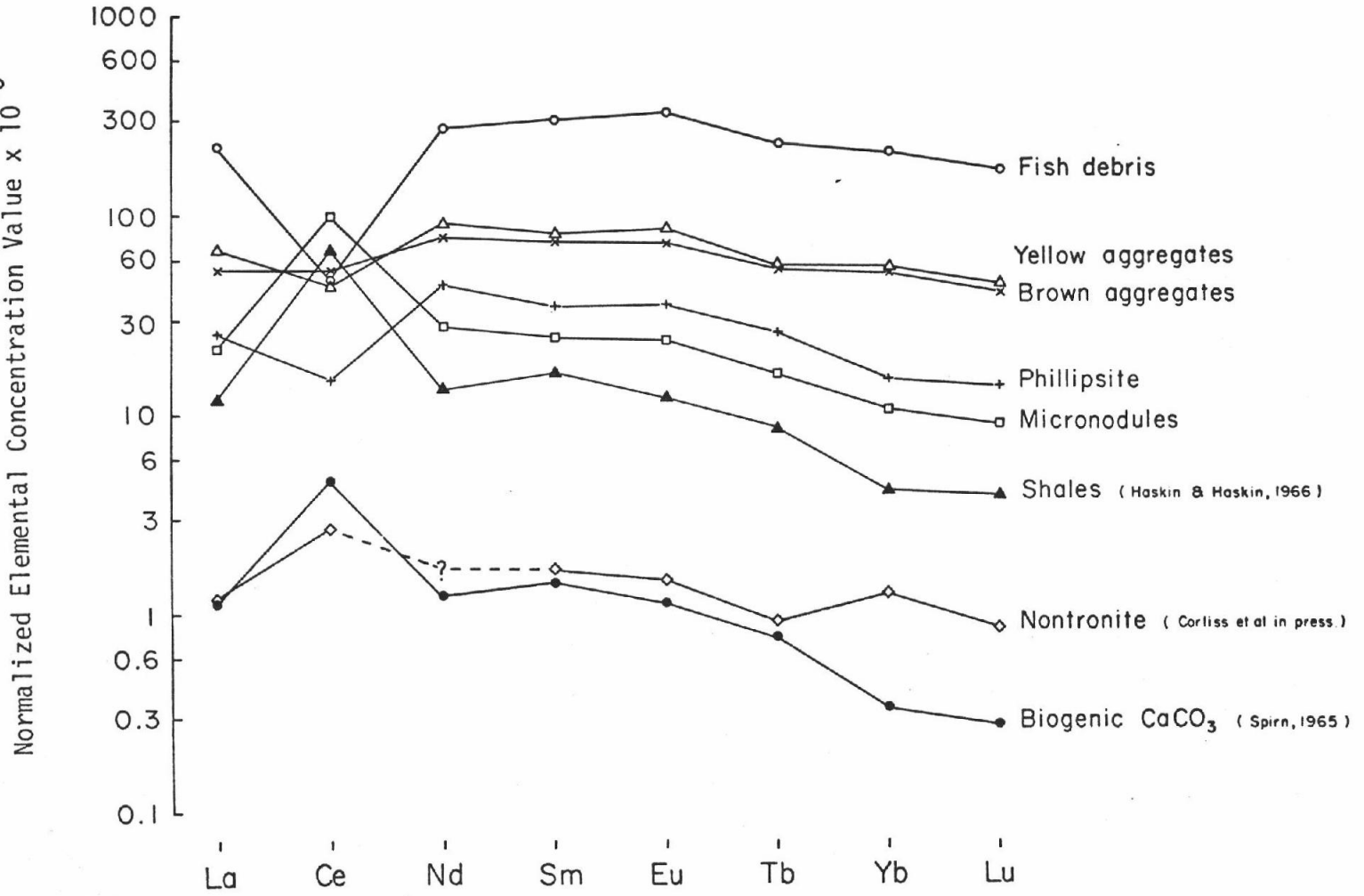

Figure 28. Lanthanide element concentrations in various metalliferous sediment components and shales compared by normalizing to sea water.

totally fixed in an insoluble barite phase.

Another element of considerable interest is aluminum. The leaching experiments indicate that this element exists in part in a mobile state in metalliferous sediments. Although the unleachable fraction of Al can be assumed to be in the smectite phase, it is not clear how the leachable Al is distributed. The phase distribution of this and other elements requires considerably more work along the lines of the work described in this thesis.

In completing this work, I would like to indicate a number of avenues of further research which would add significantly to our knowledge of the formation of metalliferous sediments. An important first step would be to carry out phase separation work of the type done here, on several surface samples from the Bauer, Yupanqui and Roggeveen Basins. Analyses of pure phases of biogenic silica, carbonate and fish debris as well as authigenic phillipsite, micronodules, and iron rich smectites would provide information on the areal distribution of these components, as well as establishing the variability of composition of such phases over the Nazca Plate. The chemical composition data in itself would be of considerable general interest given the paucity of such information available in the literature.

The next step would be to correlate leaching results on selected surface samples with the available phase composition data and then to use this information to interpret down core studies selected cores.

Of particular interest in this work would be the solution of the question of the major and trace element composition of the smectites in

metalliferous sediments. The positive identification of a smectite by x-ray or microprobe analyses would have to be correlated with its physical aspect under a low power microscope. This should then allow the recovery of sufficient smectite material to do both AAS and INAA studies.

5.0 SUMMARY

Major and minor element analyses of bulk, silt, and clay size fractions and of sand size components of metalliferous sediments from the Bauer and Roggeveen Basins of the western Nazca Plate indicate that:

a) although the elemental composition of the bulk sediments is different the individual elements appear to be distributed similarly in both basins among the sediment components,

b) the most important sediment components in each basin are an iron rich smectite (nontronite), micronodules, and fish debris,

c) in the Bauer Basin sample there is a small fraction of barite present, and that in the Roggeveen Basin a crystalline Fe-oxyhydroxide phase (possibly goethite) is present,

d) based on the similarity of response of some key elements (in the bulk, silt, and clay sized fractions of the two sediment samples) to oxalate, and mild acid leaches it appears that the distribution of sediment components is uniform from the coarsest to the finer sediment fractions,

e) that by examining the composition of the coarse sized components of metalliferous sediments it is possible to infer how elements are distributed among sediment components in the fine fractions of these deposits,

f) the micronodule component contains most of the Mn, Ni, Co, N, and Ce present in the sediments and a significant amount of the As, Sb, Fe, Hf, Sc, Cu, and Zn,

g) a fish debris component representing a small fraction of the total sediment contains most of the lanthanides, much of the Sc, and probably also much of the Ca, and most of the P,

h) an iron rich smectite probably eliminates the Fe, Si, and Al in the sediments and contains also a significant amount of As, Sb, Th, Hf, Cu, Ni, Zn, and Mg, and some Mn,

i) the lanthanide pattern of a surface metalliferous sediment resembles that of sea water yet results from the mixture of individual components whose lanthanide patterns differ markedly in concentration and shape from each other and from that of the final sediment, and

j) a diagenetic change occurs near the surface of metalliferous sediments in which opal and iron- and manganese-oxyhydroxides combine to produce an iron-rich smectite and micronodules.

6.0 BIBLIOGRAPHY

Arrhenius, G. and Bonatti, E., 1965. Neptunism and volcanism in the ocean. In: Progress in Oceanography, v. 3, Pergamon Press Ltd., p. 7-23.

Bernat, M. and Goldberg, E.D., 1969. Thorium isotopes in the marine environment. Earth Planet. Sci. Lett., v. 5, p. 308-312.

Bernat, M., Baria, R.H., Koide, M., Griffin, J.J., Goldberg, E.D., 1970. Uranium, thorium, potassium and argon in marine phillipsites, Geochim. Cosmochim. Acta, v. 34, p. 1053-1071.

Bischoff, T.L., 1972. A ferroan nontronite from the Red Sea geothermal system. Clays and Clay Min., v. 20, p. 217-223.

Blokh, A.M., 1961. Rare earths in the remains of Paleozoic fishes of the Russian platform. Geochemistry (USSR) English Transl., p. 404-415.

Bonatti, E., 1963. Zeolites in Pacific pelagic sediments. New York Acad. Sci. Trans., Ser. II, v. 25, p. 938-949.

Bonatti, E., 1965. Palagonite, hyaloclastites and alteration of volcanic glass in the ocean. Bulletin Volcanologique, v. 28, p. 3-15.

Bonatti, E., 1975. Metallogenesis at oceanic spreading centers. Annual Review of Earth and Planetary Sciences, v. 3, p. 401-431.

Bostrom, K. and Peterson, M.N.A., 1966. Precipitates from hydrothermal exhalations on the East Pacific Rise. Econ. Geol., v. 61, p. 1258-1265.

Bostrom, K. and Peterson, M.N.A., 1969. The origin of aluminum poor ferromanganoan sediments in areas of high heat flow on the East Pacific Rise, Mar. Geol., v. 7, p. 427-447.

Bostrom, K., Peterson, M.N.A., Toensuu, O., Fisher, D., 1969. Aluminum-poor ferromanganoan sediments on active oceanic ridges., Tour. Geophys. Res., v. 74, p. 3261-3270.

Church, T.M., 1970. Marine barite, Ph.D. Thesis, University of California at San Diego, 100 p.

Cloud, P.E., 1965. Carbonate precipitation and dissolution. In: Chemical Oceanography, J.P. Riley and G. Skirrow (eds.), Academic Press, 508 p.

Corliss, J.B. and Dymond, J., 1973. Preliminary shipboard report YALOC-73, Leg 4. O.S.U. School of Oceanography, unpublished report.

Corliss, J.B., Dymond, J., Lopez, C., 1976. Elemental abundance patterms in Leg 34 rocks. In: Initial Reports of DSDP, v. 34, R.S. Yeats and S.R. Hart (ed.), U.S. Government Printing Office, p. 293-300.

Corliss, J.B., Lyle, M., Dymond, J., Crane, K., 1977. Sediment mounds, hydrothermal ferromanganese deposits near the Galapagos Rift, (in preparation).

Cronan, D.S., 1972. Basal ferriginous sediments cored during Leg 16, Deep Sea Drilling Project. In: Initial Reports of the DSDP, v. 16, T.H. van Andel and G.R. Heath (eds.), U.S. Government Printing Office, p. 601-608.

Cronan, D.S. and Tooms, J.S., 1969. The geochemistry of manganese nodules and associated pelagic deposits from the Pacific and Indian Oceans. Deep-Sea Research, v. 16, p. 335-359.

Dasch, E.J., Dymond, J.R., Heath, G.R., 1971. Isotopic analysis of metalliferous sediment from the East Pacific Rise, Earth Planet. Sci. Lett., v. 13, p. 175-180.

Dymond, J., and Eklund, W., 1977. A microprobe study of metalliferous sediment components, (in preparation).

Dymond, J., Veeh, H.H., 1975. Metal accumulation rates in the Southeast Pacific and the origin of metalliferous sediments. Earth Planet. Sci. Lett., v. 27, p. 241-248.

Dymond, J., Corliss, J.B., Heath, G.R., 1977. History of metalliferous sedimentation at DSDP Site 319, in theSoutheast Pacific. Geochim. Cosmochim. Acta, v. 41, p. 741-753.

Dymond, J., Corliss, J.B., Stillinger, R., 1976. Chemical composition and metal accumulation rates of metalliferous sediments from Sites 319, 320B, and 321. In: Initial Reports of DSDP, v. 34, R.S. Yeats and S.R. Hart (eds.), U.S. Government Printing Office, p. 575-588.

Dymond, J., Corliss, J.B., Heath, G.R., Field, C.W., Dasch, E.J., Veeh, H.H., 1973. Origin of metalliferous sediments from the Pacific Ocean. Geol. Soc. Am. Bull., v. 84, p. 3355-3372.

Eklund, W., 1974. A microprobe study of metalliferous sediment components. Unpublished M.S. Thesis, Oregon State University, 77 p.

Emilani, C., 1955. Mineralogical and chemical composition of the tests of certain pelagic foraminifera. Micropaleontology, v. 1, p. 377-380.

Fewkes, R.H., 1973. External and internal features of marine manganese nodules as seen with the SEM and their implications in nodule origin. In: The Origin and the Distribution of Manganese Nodules in the Pacific and Prospects for Exploration. M. Morgenstein (ed.), Hawaii Inst. of Geophysics Press, Honolulu, p. 21-29.

Francheteau, J., et al., 1975. Transform fault and rift valley geology by bathyscaph and diving saucer, Science, v. 190, p. 108-110.

Friedrich, G.H., 1976. Manganese micronodules in deep sea sediments and their relation to manganese nodule fields. In: Tech. Bull. No. 2, U.N. Economic and Social Commission for Asia and the Pacific (CCOP/SOPAC), G.P. Glasby and H.R. Katz (eds.), U.S. Government Printing Office, p. 39-53.

Garrels, R.M. and Mackenzie, F.T., 1971. Evolution of sedimentary rocks, W.W. Norton and Co., 397 p.

Glover, E.D., 1977. Characterization of a marine birnessite. Amer. Miner., v. 62, p. 278-285.

Goldberg, E.D., 1961. Chemical and mineralogical aspects of deep-sea sediments. In: Physics and Chemistry of the Earth, v. 4, L.H. Ahrens, F. Press, S.K. Runcorn, and H.C. Urey (eds.), Pergamnon Press, p. 281-302.

Goldberg, E.D., Arrhenius, G.O.S., 1958. Chemistry of Pacific pelagic sediments, Geochim. Cosmochim. Acta, v. 13, p. 153-212.

Gordon, C.E., Randle, K., Goles, G.C., Corliss, J.B., Beesen, M.H., Oxley, S.S., 1968. Instrumental activation analysis of standard rocks with high resolution x-ray detectors. Geochim. Cosmochim. Acta, v. 32, p. 364-396.

Haskin, M.A., and Haskin, L.A., 1966. Rare-earths in European shales: a redetermination. Science, v. 154, p. 507-509.

Heath, G.R., 1973. Preliminary shipboard report, YALOC-73, Leg 3. O.S.U. School of Oceanography, unpublished report.

Heath, G.R. and Dymond, J., 1977. Genesis transformation of metalliferrous sediments from the East Pacific Rise, Bauer Deep and Central Basin, Northwest Nazca Plate. Geol. Soc. Am. Bull., v. 88, p. 723-733.

Hermann, A.G., 1972. Yttrium and lanthanides, biogeochemistry. In: Handbook of Geochemistry, v. II/3, K.H. Wedepohl (ed.), Springer Verlag, p. 39, 57-71 (L-1 to L-3).

Herron, E.M., 1972. Sea floor spreading and the Cenozoic history of the East Central Pacific. Geol. Soc. Am. Bull., v. 83, p. 1671-1692.

Høgdahl, Ø., Melson, S., Bowen. V., 1968. Neutron activation analysis of lanthanide elements in sea-water. Advances in Chemistry, v. 73, p. 308-325.

Isphording, W.C., 1975. Primary nontronite from the Venezuelan guayana. Amer. Miner., v. 60, p. 840-848.

Kochenov, A.V. and Zinov'ev, V.V., 1960. Distribution of rare earth elements in phosphatic remains of fish from the Maikop deposits. Geochemistry (USSR), English Transl., p. 860-873.

Koczy, F.F., 1961. Age determinations in sediments by natural radioactivity. In: The Sea, v. 3, M.N. Hill (ed.), John Wiley and Sons, p. 816-831.

Krinsley, D., 1960. Trace elements in the tests of planktonic foraminifera. Micropaleontology, v. 6, p. 297-300.

Ku, T.L. and Broecker, W.S., 1969. Radiochemical studies on manganese nodules of deep sea origin. Deep Sea Research, v. 16, p. 625-637.

Landa, E.R. and Gast, R.G., 1973. Evaluation of crystallinity in hydrated ferric oxides. Clays and Clay Minerals, v. 21, p. 121-130.

Lipps, J.H. and Ribbe, P.H., 1967. Electroprobe microanalysis of planktonic foraminifera. J. of Paleont., v. 41, p. 492-496.

Lonsdale, Peter, 1976. Abyssal circulation of the S.E. Pacific and some geological implications, J. Geol. Res., v. 87. p. 1163-1176.

Lyle, M., Dymond, J., Heath, G.R., 1977. Copper-nickel enriched ferromanganese nodules and associated crusts from theBauer Basin, northwest Nazca Plate, Earth Planet. Sci. Lett., v. 35, p. 55-64.

MacEwan, D.M.C., 1961. Montmorillonite minerals. In: The X-ray Identification and Crystal Structures of Clay Minerals, G. Brown (ed.), Mineral. Soc. London, p. 143-207.

Martin, J.H. and Knauer, G.A., 1973. The elemental composition of plankton. Geochim. Cosmochim. Acta, v. 37, p. 1639-1653.

Müller, C. and Förstner, V., 1976. Primary nontronite from the Venezuelan guayana: additional primary occurrences (Red Sea, Lake Malawi), Amer. Miner., v. 61, p. 500-501.

Murray, J. and Renard, A.F., 1891. Deep-sea deposits. In: Report on the Scientific Results of the Voyage of H.M.S. Challenger during the years 1873-76, Her Majesty, Government, London, 1608 p.

Piper, D.Z., 1974. Rare earth elements in ferromanganese nodules and other marine phases. Geochim. Cosmochim. Acta, v. 38, p. 1007-1022.

Raab, W., 1972. Physical and chemical features of Pacific deep-sea manganese nodules and their implications to the gensis of nodules. In: Ferromanganese Deposits on the Ocean Floor. D. Horn (ed.), Nat. Sci. Found., p. 31-49.

Riley, J.P. and Chester, R., 1971. The components of deep-sea sediments. In: Introduction to Marine Chemistry. J.P. Riley and R. Chester (eds.), Academic Press, 465 p.

Rancitelli, L.A. and Perkins, R.W., 1973. Major and minor elemental composition of manganese nodules. In: Inter-University Program of Research on Ferromanganese Deposits of the Ocean Floor, Phase I Report, Nat. Sci. Found.

Reshetnjak, V.V., 1971. Occurrence of Phaeodarian radiolaria in recent sediments and Tertiary deposits. In: The Micropaleontology of Oceans, v. 24, B.M. Funnel and W.R. Ridel (eds.), p. 343-349.

Rex, R.W., 1967. Authigenic silicates formed from basaltic glass by more than 6 x 10^7 years contact with sea-water, Sylvania Guyot, Marshall Islands. Clay and Clay Minerals, v. 27, p. 195-203.

Riley, J.P. and Sinhaseni, P., 1958. Chemical composition of 3 manganese nodules from the Pacific Ocean, J. Mar. Res., v. 17, p. 466-482.

Ross, C.S. and Hendricks, S.B., 1945. Minerals of the Montmorillonite group. USGS Prof. Paper 205-B, 85 p.

Sayles, F.L. and Bischoff, J.L., 1973. Ferromanganoan sediments in the equatorial East Pacific. Earth Planet. Sci. Lett., v. 19, p. 330-336.

Sayles, F.L., Ku, T.L., Bowker, P.C., 1975. Chemistry of ferromanganoan sediment of theBauer Deep. Geol. Soc. Am. Bull., v. 86. p. 1423-1431.

Sheppard, R.A., Gude, A.J. II, Girffin, J.J., 1970. Chemical composition and physical properties of phillipsite from the Pacific and Indian Oceans. The Amer. Mineral., v. 55, p. 2053-2062.

Skornyakova, N.S., Andruschenko, P.F., Fomina, L.S., 1962. Chemical composition of Pacific Ocean iron-manganese concretions, Okeanologiya, v. 2, p. 264-277.

Spirn, R.V., 1965. Rare earth distributions in the marine environment. Ph.D. Thesis, M.I.T., Dept. of Geology and Geophysics, 165 p.

Stanley, Edith M., 1973. Minor element abundance in radiolarian tests, unpublished data presented 1973 Section Meeting of Geol. Soc. Am., Minneapolis.

Stumm, W. and Morgan, J.J., 1970. Aquatic chemistry. Wiley-Interscience, 583 p.

Thompson, G., Bowen, V.T., 1969. Analyses of coccolith ooze from the deep tropical Atlantic. J. Mar. Res., v. 27, p. 32-38.

Toth, John R., 1977. Deposition of submarine hydrothermal manganese and iron, and evidence for hydrothermal input by volatile elements to the ocean. Unpublished M.S. Thesis, Oregon State University, 79 p.

Turekian, K.K., 1968. Oceans. Prentice Hall, Inc., 120 p.

Turekian, K.K., Katz, A., Chan, L., 1973. Trace element trapping in pteropod tests. Limn. Oceanog., v. 18, p. 240-249.

Volkov, I.I. and Fomina, L.S., 1973. New data on the geochemistry of the rare earths in Pacific Ocean sediments. Geochemistry International, p. 1178-1187.

von der Borch, C.C. and Rex, R.W., 1970. Amorphous iron oxide precipitates in sediments cored during Leg 5, Deep Sea Drilling Project. In: Initial Reports of the DSDP, v. 5, D.A. McManus and R.E. Burns (eds.), U.S. Government Printing Office, p. 541-544.

von der Borch, C.C., Nesteroff, W.D., Galenhouse, J., 1971. Iron-rich sediments cored during Leg 8 of the Deep Sea Drilling Project. In: Initial Reports of the DSDP, v. 8, J.I. Tracey and G.H. Sutton (eds.), U.S. Government Printing Office, p. 829-835.

APPENDIX I

Detailed Methodology

I.1 Phase Separations

The initial and most complete phase separation work was effected on the sediments of BBS. Various biogenic and authigenic phases were recovered in the manner described below:

a) Approximately 3/4 to 1 kg of sediment was fluidized by tumbling for several hours with 1 gallon of filtered distilled water.

b) The slurry was sieved first through a large diameter (10") 250 μ sieve.

c) Sediment fractions retained on the sieve were washed with the jet from a wash bottle using water recycled from the slurry which passed through the sieve.

d) The material retained on the sieve was transferred to a glass beaker and sonic treated in order to break up loose aggregates. The cleaned fraction was resieved, and air dried for further work.

e) The dispersed sediment was further sieved through 177 μ, and 63 μ sieves, and the retained fraction treated as above.

f) Fish debris and carbonate tests and most manganese micronodules were recovered primarily from the > 177 μ size, sonic cleaned fraction.

g) The 63-177 μ size fraction provided the material for the phillipsite separation.

h) In order to accelerate the phase separation work the > 177 μ size fraction was split into magnetic and non-magnetic fractions consisting primarily of a manganese-micronodule phase,

and a biogenic phase respectively, by means of Frantz Isodynamic Magnetic Separator. The only phase to be chemically treated during this work was the siliceous fraction. Due to its low concentration and low bulk density, a sufficient quantity of this siliceous material could only be collected by removing the acid soluble carbonate and fish debris component from a much larger amount of the non-magnetic fraction mentioned above; 0.5N HCl acid was used for this purpose. The resultant residue contained a few grains of foreign matter, most probably detrital components, and, of course the acid resistant biogenic silica phase. These foreign particles were removed prior to analysis.

i) In addition to the distinctly authigenic or biogenic phases mentioned above, two additional components were separated out. One will be referred to as yellow particles and the other as brown particles. The two have very similar external appearances except for their color. The brown particles are of a light chocolate brown color and likely represent the bulk sediment, while the yellow particles have a pale canary yellow color and appear generally to represent the bulk sediment composition as influenced by the presence of some organic matter.

The problem of obtaining pure fractions of sediment components could only be overcome by the tedious method of hand picking the various components under the microscope. As indicated above the fragile biogenic components -- fish debris, and carbonate foram tests were recovered primarily from the sediment fraction retained on the > 177 μ sieve.

The manganese micronodules were recovered from this same fraction by sonic treatment, once the fragile components had been removed. In the case of the micronodules it was possible to concentrate a magnetic fraction consisting of almost pure micronodules and to separate this from a non-magnetic fraction of fish debris, organic carbonate, and a small fraction of non-magnetic, possibly detrital material. The magnetic concentration of the micronodules made the cleaning and concentration of a pure phase considerably easier.

I.2 Wet Sieving and Particle Size Settling

The bulk material from the core catchers of the two main cores used in this work, i.e., BBD and RBD, were treated in exactly the same way. Several hundred grams of material were removed from the bulk material and mixed with enough double distilled water to convert the mixture into a thin slurry by tumbling. In spite of the high water content of the sediments (>65% in each case) these samples were quite firm and required 5 to 6 times their own weight of water in order to obtain a slurry. Once the sediment had been sufficiently broken up, the resultant slurry was wet sieved successively through 354, 250, 177, 105, 63, and 44 μ size 3" diameter brass sieves. The material retained on each sieve was rinsed on the sieve with recycled water recovered from the filtrate. This was possible because of the rapidity with which the material sieved, settled out, thus leaving a rather clear supernatant. Recycling the rinse water was aimed at reducing the chemical leaching effect of using excessive double distilled water, and reduced the total volume of sample that had to be dealt with.

The sediment from BBD showed a tendency to form small clumps and considerably more fine material in the form of clumps was retained on each sieve, than did the RBD sediment which showed very little tendency to clump. The material which passed through the 44 μ sieve was used to settle out three size fractions, i.e., < 4 μ; 4-20 μ, and 20-44 μ. In order to recover the various fractions the sediment was concentrated using candle filters and the concentrates freeze dried.

Each of the size fractions > 354 μ, 250-354 μ, 177-250 μ, 105-177 μ, 63-105 μ, and 44-63 μ, recovered, air dried and weighed. The fractions > 177 μ were used for separating out the Mn micronodule, and fish debris components. Once these fractions had been picked clean of the fragile fish debris component, the > 177 μ fraction was sonic treated in water in order to remove the fine material which had been retained on the screens as lumps. The coarse component of this treatment was recovered on a 44 μ sieve, dried, and used for the recovery of manganese micronodules.

One of the main purposes of using the many sieves indicated above was to help break up the bulk sediment without resorting to a sonic treatment of the samples. Since these samples were to be size settled it was desirable to avoid biasing the composition of the smaller size fractions, i.e., 20-44 μ, 4-20 μ, and < 4 μ by artifically contributing fragments from larger sized components.

I.3 BBD and RBD Bulk Sediment Water Content

As a preliminary step to carrying out the various leaching experiments it was required to know the water content of the bulk sediment.

This measurement would be used for estimating the salt content of each core sample. The moisture content was determined by measuring the weight loss of approximately 150 grams of wet bulk sediment, freeze dried as two separate portions.

I.4 Sediment Wet Bulk Densities

Essential to the future calculation of sediment mass and metal accumulation rates is a knowledge of the sediment density. As the samples of material of BBD and RBD were quite large, 10-15 lbs each, the sediment mass was sampled in various places in order to minimize errors due to compositional variations.

The bulk densities were determined by penetrating the sediment with a thin stainless steel ring of known volume and weight. When the ring was full it is removed, the outside carefully cleaned of excess material, and the sediment and ring re-weighed. During the measurements, care was exercised to avoid packing the sediment, including voids in the sample, or allowing the physical limits of the ring to be exceeded by the volume of sediment. The sample wet bulk density is calculated from the known sample weight and ring volume. The dry bulk density was later calculated from the measured wet bulk density and known sample water content.

I.5 Chemical Leachings

The procedure consists of treating a sample of sediment with a pH 3.0 solution of 0.2 M ammonium oxalate and 0.2 M oxalic acid. Using a sample to leach ratio of 50-100 mg/100 ml of leach. The treatment is

carried out for two hours in the dark under mild agitation.

All samples were treated in the same manner before being leached i.e., sample splits were dried at 110°C for ~8 hours, cooled in a dessicator for several hours before weighing out ~450-500 mg. In each case the sample was leached with 500 ml of leach. Agitation was effected by means of a shaker table lent by Vern Smith of the O.S.U. Radiation Center. The samples were treated in 750 ml wide mouth dark bottles. Filtrations were carried out with 47 mm Ø, 0.45 μ Millipore filters. The residue recovered was then washed with an equal volume of water (~500 ml), and then transferred either back to the jar for a second leach or to a centrifuge tube. Centrifuging the final residue from each leach permitted freeze drying the samples within a short time of their recovery as most of the accompanying water could immediately be decanted off. The leaching experiments were carried out at least twice for each treatment. In the first case the leachate was discarded and the residue used for INAA work. In the second case the leachate volume was closely controlled (made up to 1 liter) and the various leachates and corresponding residues analyzed by AAS for major and minor elements. A third set of leaching experiments was carried out after dosing the bulk sediment with some 5-7% of pure quartz for X-ray purposes. An attempt to prepare differential diffractograms from this last set of samples proved fruitless because of problems with the computer program designed to scale and subtract pairs of diffractograms based on the quartz content of the samples.

I.6 Atomic Absorption Spectroscopy (AAS)

The AAS methodology used on the residue samples analyzed has been fully described in Dymond et al. (1973). In brief, it consists of dissolving a dried, weighed sample in a teflon bomb at 125°, using HNO_3 and HF. The dissolved sample is then neutralized with boric acid and made up to volume with double distilled water. Various dilutions are prepared for metalliferous sediments in order to reduce the concentrations of certain elements (Fe, Mn, Si, etc.) to measurable levels. The matrix of the standards is matched with that of the unknowns in order to eliminate analytical errors due to chemical differences. In the case where leachates were analyzed complete sets of new standards were prepared using a matrix corresponding to that of the unknowns, i.e., d.d. H_2O, 0.1N HCl, 2N HCl, and acidified ammonium oxlate. The results of these analyses are presented in Appendix II.

I.7 Instrumental Neutron Activation Analysis I.N.A.A.

The analytical procedure used has been described in Gordon et al. (1968) and Dymond et al. (1973). Data accumulation and reduction were effected by means of a computerized ND 812 multi-channel (4096) analyzer system. Standard rocks W-1, BCR-1, G-2, AGV, and GSP were used in the various experiments for most major and trace elements. Additionally, however, it was found necessary to prepare liquid standards for As, Br, and W. These were prepared from 1000 PPM As - Atomic Adsorption Liquid Standards, high purity NaBr, and pure Tungsten metal, respectively. The final data reduction was carried out on the O.S.U. CDC-3300 computer using an internal Marine Geochemistry program.

I.8 X-Ray Diffraction Work

Diffraction work was done on both bulk sediments, and on several pure separates. This work was done on the O.S.U. Marine Geology Group's Phillips X-Ray Instrument, using a collimated Cu K α beam. Oriented and random mount samples were run as prescribed by the nature and/or size of the samples. Scans were made for most samples from 4° to 65° 2θ at rates of 300-800 secs/per degree 2θ in steps of 2/100 of a degree. The slower scans were used for bulk sediments and the more rapid scans for pure fractions. The data was digitally recorded on magnetic tapes and scaled diffractograms prepared from these tapes on the O.S.U. CDC-3300 Computer. The programs to perform these operations and data extraction are available in the Marine Geology Group (O.S.U.) x-ray tape library. See also I.5.

I.9 S.E.M. and Micrography Photography Work

The scanning electron microscope results presented in this paper were obtained on an International Scientific Instrument Model MSM-2 Mini-S.E.M. operated by the Department of Biology of O.S.U. All other photomicrographs were taken with a Nikon Microflex Model AFM Automatic Photomicrographic System or with a Wild M4A Binocular Microscope with Pentax camera adapter. These latter two microscope systems permitted a systematic black and white and/or color photographic record of sediment phases or size fractions to be kept, in the enlargement range 16X to 400X. The S.E.M. system permitted observation of the various individual phases at magnifications up to 10,000X. Good reliable photographic documentation was not possible, however, much above 2,000X with

the available system.

I.10 Weight Losses for Bulk Sediments of BBD and RBD Produced by Single and Multiple Leaches

The effect (% of weight loss) of each leach was estimated as follows:

a) The effect of a water leach on the sediment is known experimentally (15.5% in the case of BBD; 9.7% for RBD).

b) The effect of a given single (1X) leach is also known experimentally, and is always higher than the effect of the simple water leach. The average for (1X) 0.1N HCl leaches is 28.2%.

c) Assuming that the leaching effect of the water matrix is constant, the effect of the acid in the acid leach is calculated as a simple difference (i.e., 28.2-15.5 = 12.7% weight loss due to the acid fraction of the 0.1N HCl leach). Similarly for the ammonium oxalate leaches.

d) In similar manner the effect of a second leach is estimated. Here, however, it is assumed that the water matrix has no additional effect, and that the total weight loss is due to the acid or oxalate present in the solution.

Noted that the total weight loss values of Table 9 Column T represent the sample weight losses based on the original weight of the sample and therefore, includes a substantial portion of water soluble "salts." Columns L_1 and L_2 give the % weight loss for each leach treatment, corrected for salt content. The upper figures are based on the original weight of the sample, while the lower figure in parentheses represents

this same value recalculated to a "salt free" sediment basis. This conversion is calculated as:

$$L_1 \Big/ 1 - \frac{L_W}{100} = \frac{L_1}{0.845} \qquad \text{(for BBD)}$$

$$= \frac{L_1}{.903} \qquad \text{(for RBD)}$$

It is important to note that the weight losses presented in Table are based on the most consistent weight loss data for repeated leachings of the same sample. In cases where the averaged leach results subtended an error of more than $\pm$ 3-4%, a new sample was treated in similar manner and the most consistent 2 of 3 values are used for the data given in Table 9. In the cases where new samples had to be prepared due to subsequent sample loss, all three leached weight values were used if the agreement between samples was within the above indicated limit of error. The leaching procedures involve transfering the sediment samples numerous times from:

i) weighing vial -- leaching bottle

ii) leaching bottle -- filtration paper

iii) filtration paper -- centrifuge tube

iv) centrifuge tube (after freeze drying) -- weighing vial

In the case of double leachings, two additional sample transfers took place, i.e.,

ii) a) filtration paper -- leaching bottle

b) leaching bottle -- second filtration paper

APPENDIX II

Atomic Absorption Data on Leachates and Residues of Chemically Treated Y73-3-21K (BBD) and Y73-4-64K (RBD) Bulk Sediments

In these AAS data tables the column headings 1L, 2L, etc. represent the following:

1L: elemental concentration in the bulk sediment removed by the first leach

2L: elemental concentration in the bulk sediment removed by the second leach

R: elemental concentration in the residue remaining after one, or two leaches

R/B: elemental concentration in the residue re-calculated to the bulk sediment, i.e., corrected for sample weight loss due to leaching

1L + 2L + R/B: sum of elemental concentrations in the fractions making up the bulk sediment

Table II - 1

% Aluminum - BBD

Chemical Leach	Concentration in				
	1L	2L	R	R/B	1L + 2L + R/B
none (bulk sediment)	-	-		2.84 ±.06	2.84 ±.06
d.d. water	n.d.	-	3.40 ±.07	2.88 ±.06	2.88 ±.06
(1X)- .1N HCl	0.53 ±.02	-	3.32 ±.10	2.38 ±.07	2.91 ±.08
(2X)- .1N HCl	0.50 ±.02	0.09 ±.01	3.41 ±.09	2.36 ±.06	2.95 ±.06
(1X)- 2N HCl	1.17 ±.03	-	2.92 ±.08	1.60 ±.04	2.77 ±.05
(1X)- Am. Ox.	0.22 ±.02	-	3.93 ±.07	2.63 ±.04	2.84 ±.05
(2X)- Am. Ox.	0.21 ±.02	0.02 ±.01	3.95 ±.05	2.64 ±.04	2.88 ±.04
(1X)- Am. Ox. + (1X)- .1N HCl	0.21 ±.03	0.45 ±.03	3.77 ±.05	2.05 ±.03	2.71 ±.05

Table II - 2

% Barium - BBD

Chemical Leach	Concentration in				
	1L	2L	R	R/B	1L + 2L + R/B
none (bulk sediment)	-	-		1.63 ±.09	1.63 ±.09
d.d. water	0.01 ±.01	-	1.91 ±.11	1.62 ±.09	1.63 ±.09
(1X)- .1N HCl	0.40 ±.04	-	1.49 ±.09	1.07 ±.06	1.47 ±.08
(2X)- .1N HCl	0.40 ±.02	1.00 ±.05	0.56 ±.07	0.39 ±.05	1.76 ±.07
(1X)- 2N HCl	0.76 ±.04	-	0.25 ±.01	0.13 ±.01	0.90 ±.04
(1X)- Am. Ox.	0.17 ±.01	-	2.25 ±.14	1.51 ±.09	1.67 ±.09
(2X)- Am. Ox.	0.18 ±.01	0.32 ±.02	1.80 ±.10	1.21 ±.06	1.71 ±.07
(1X)- Am. Ox. + (1X)- .1N HCl	0.13 ±.01	0.77 ±.18	1.51 ±.10	0.82 ±.06	1.72 ±.19

Table II - 3

% Calcium - BBD

Chemical Leach	Concentration in				
	1L	2L	R	R/B	1L + 2L + R/B
none (bulk sediment)	-	-		3.37 ±.07	3.37 ±.07
d.d. water	0.16 ±.00	-	3.77 ±.09	3.20 ±.07	3.36 ±.07
(1X)- .1N HCl	2.88 ±.03	-	2.11 ±.04	1.51 ±.03	4.39 ±.04
(2X)- .1N HCl	2.92 ±.03	0.04 ±.00	0.45 ±.02	0.31 ±.01	3.27 ±.03
(1X)- 2N HCl	2.82 ±.07	-	0.59 ±.03	0.32 ±.01	3.20 ±.07
(1X)- Am. Ox.	0.17 ±.01	-	3.94 ±.08	2.64 ±.05	2.81 ±.05
(2X)- Am. Ox.	0.14 ±.01	0.90 ±.00	3.86 ±.08	2.59 ±.06	2.81 ±.06
(1X)- Am. Ox. + (1X)- .1N HCl	0.09 ±.00	2.96 ±.04	0.42 ±.02	0.23 ±.01	3.27 ±.04

Table II - 4

PPM Cobalt - BBD

Chemical Leach	Concentration in				
	1L	2L	R	R/B	1L + 2L + R/B
none (bulk sediment)	-	-		208 ±19	208 ±19
d.d. water	n.d.	-	275 ±23	233 ±19	233 ±19
(1X)- .1N HCl	n.d.	-	312 ±28	224 ±20	224 ±20
(2X)- .1N HCl	n.d.	n.d.	297 ±25	206 ±17	206 ±17
(1X)- 2N HCl	65 ±22	-	183 ±37	100 ±20	165 ±30
(1X)- Am. Ox.	235 ±63	-	n.d.	n.d.	235 ±63
(2X)- Am. Ox.	217 ±57	n.d.	n.d.	n.d.	217 ±57
(1X)- Am. Ox. + (1X)- .1N HCl	216 ±90	n.d.	51 ±33	28 ±18	244 ±92

Table II - 5

PPM Copper - BBD

Chemical Leach	Concentration in				
	1L	2L	R	R/B	1L + 2L + R/B
none (bulk sediment)	-	-		1,081 ±30	1,081 ±30
d.d. water	n.d.	-	1,310 ±32	1,110 ±27	1,110 ±27
(1X)- .1N HCl	374 ±14	-	951 ±42	681 ±30	1,055 ±33
(2X)- .1N HCl	333 ±15	43 ±11	973 ±39	675 ±27	1,051 ±33
(1X)- 2N HCl	496 ±7	-	943 ±8	515 ±4	1,011 ±8
(1X)- Am. Ox.	492 ±12	-	804 ±6	538 ±4	1,030 ±13
(2X)- Am. Ox.	502 ±12	25 ±7	771 ±6	516 ±4	1,043 ±14
(1X)- Am. Ox. + (1X)- .1N HCl	479 ±10	21 ±8	934 ±9	507 ±5	1,007 ±14

Table II - 6

% Iron - BBD

Chemical Leach	Concentration in				
	1L	2L	R	R/B	1L + 2L + R/B
none (bulk sediment)	-	-		13.59 ±.47	13.59 ±.47
d.d. water	n.d.	-	16.77 ±.42	14.21 ±.36	14.21 ±.36
(1X)- .1N HCl	0.94 ±.03		18.19 ±.49	13.03 ±.35	13.98 ±.35
(2X)- .1N HCl	0.94 ±.02	0.32 ±.02	20.09 ±.59	13.93 ±.41	15.19 ±.41
(1X)- 2N HCl	4.51 ±.27	-	14.00 ±.83	7.65 ±.45	12.17 ±.53
(1X)- Am. Ox.	4.61 ±.09	-	14.59 ±.97	9.76 ±.65	14.37 ±.66
(2X)- Am. Ox.	4.62 ±.10	0.56 ±.09	14.54 ±.95	9.73 ±.63	14.91 ±.65
(1X)- Am. Ox. + (1X)- .1N HCl	4.62 ±.09	0.37 ±.02	14.26 ±.73	7.75 ±.40	12.73 ±.41

Table II - 7

% Potassium - BBD

Chemical Leach	Concentration in				
	1L	2L	R	R/B	1L + 2L + R/B
none (bulk sediment)	-	-		1.53 ±.05	1.53 ±.05
d.d. water	0.30 ±.01	-	1.40 ±.05	1.18 ±.04	1.49 ±.04
(1X)- .1N HCl	0.94 ±.01	-	0.76 ±.07	0.54 ±.05	1.48 ±.05
(2X)- .1N HCl	0.95 ±.02	0.06 ±.00	0.64 ±.05	0.44 ±.37	1.45 ±.04
(1X)- 2N HCl	1.00 ±.03	-	0.83 ±.02	0.45 ±.01	1.46 ±.03
(1X)- Am. Ox.	0.95 ±.02	-	0.83 ±.02	0.56 ±.01	1.51 ±.03
(2X)- Am. Ox.	0.91 ±.04	0.03 ±.00	0.79 ±.02	0.53 ±.01	1.47 ±.04
(1X)- Am. Ox. + (1X)- .1N HCl	0.93 ±.02	0.06 ±.00	0.89 ±.02	0.48 ±.01	1.47 ±.03

Table II - 8

% Magnesium - BBD

Chemical Leach	Concentration in				
	1L	2L	R	R/B	1L + 2L + R/B
none (bulk sediment)	-	-		2.22 ±.02	2.22 ±.02
d.d. water	0.28 ±.00	-	2.25 ±.02	1.90 ±.02	2.19 ±.02
(1X)- .1N HCl	0.98 ±.01	-	1.73 ±.04	1.24 ±.03	2.22 ±.03
(2X)- .1N HCl	1.03 ±.01	0.07 ±.00	1.80 ±.04	1.25 ±.03	2.34 ±.03
(1X)- 2N HCl	1.25 ±.02	-	1.71 ±.02	0.94 ±.01	2.19 ±.02
(1X)- Am. Ox.	0.96 ±.02	-	1.81 ±.02	1.21 ±.01	2.18 ±.02
(2X)- Am. Ox.	0.95 ±.02	0.03 ±.01	1.76 ±.02	1.18 ±.01	2.16 ±.03
(1X)- Am. Ox. + (1X)- .1N HCl	0.96 ±.05	0.11 ±.00	1.97 ±.02	1.07 ±.01	2.14 ±.05

Table II - 9

% Manganese - BBD

Chemical Leach	Concentration in				
	1L	2L	R	R/B	1L + 2L + R/B
none (bulk sediment)	-	-		5.01 ±.18	5.01 ±.18
d.d. water	n.d.	-	5.51 ±.21	4.67 ±.18	4.67 ±.18
(1X)- .1N HCl	0.15 ±.00	-	6.43 ±.25	4.61 ±.18	4.75 ±.18
(2X)- .1N HCl	0.15 ±.00	0.02 ±.00	6.97 ±.20	4.83 ±.14	5.00 ±.14
(1X)- 2N HCl	2.31 ±.02	-	4.58 ±.22	2.51 ±.12	4.81 ±.12
(1X)- Am. Ox.	4.86 ±.04	-	1.20 ±.16	0.80 ±.11	5.66 ±.12
(2X)- Am. Ox.	4.85 ±.04	0.02 ±.01	0.90 ±.23	0.60 ±.15	5.47 ±.16
(1X)- Am. Ox. + (1X)- .1N HCl	4.81 ±.04	0.03 ±.00	1.12 ±.16	0.61 ±.09	5.44 ±.10

Table II - 10

PPM Nickel - BBD

Chemical Leach	Concentration in				
	1L	2L	R	R/B	1L + 2L + R/B
none (bulk sediment)	-	-		661 ±164	661 ±164
d.d. water	n.d.	-	943 ±201	799 ±170	799 ±170
(1X)- .1N HCl	242 ±22	-	712 ±215	510 ±154	752 ±156
(2X)- .1N HCl	234 ±33	168 ±31	671 ±195	465 ±135	867 ±142
(1X)- 2N HCl	414 ±35	-	610 ±122	333 ±67	747 ±76
(1X)- Am. Ox.	639 ±95	-	51 ±9	34 ±6	673 ±95
(2X)- Am. Ox.	625 ±91	n.d.	49 ±9	33 ±6	658 ±91
(1X)- Am. Ox. + (1X)- .1N HCl	667 ±110	n.d.	42 ±10	23 ±5	690 ±110

Table II - 11

% Silicon - BBD

Chemical Leach	Concentration in				
	1L	2L	R	R/B	1L + 2L + R/B
none (bulk sediment)	-	-		14.66 ±.48	14.66 ±.48
d.d. water	n.d.	-	16.80 ±.59	14.23 ±.50	14.23 ±.50
(1X)- .1N HCl	0.22 ±.16	-	19.73 ±.66	14.14 ±.47	14.36 ±.50
(2X)- .1N HCl	0.19 ±.16	n.d.	20.58 ±.64	14.28 ±.44	14.47 ±.47
(1X)- 2N HCl	1.40 ±.16	-	22.92 ±.57	12.53 ±.31	13.93 ±.35
(1X)- Am. Ox.	0.68 ±.09	-	20.49 ±.58	13.71 ±.39	14.39 ±.40
(2X)- Am. Ox.	0.74 ±.60	0.17 ±.05	21.22 ±.65	14.20 ±.43	15.11 ±.44
(1X)- Am. Ox. + (1X)- .1N HCl	0.61 ±.05	n.d.	24.52 ±.62	13.32 ±.33	13.93 ±.34

Table II - 12

PPM Zinc - BBD

Chemical Leach	Concentration in				
	1L	2L	R	R/B	1L + 2L + R/B
none (bulk sediment)	-	-		399 ±15	399 ±15
d.d. water	n.d.	-	498 ±18	422 ±15	422 ±15
(1X)- .1N HCl	127 ±8	-	723 ±25	518 ±18	645 ±20
(2X)- .1N HCl	136 ±9	8 ±5	521 ±19	361 ±13	505 ±17
(1X)- .2N HCl	227 ±4	-	299 ±9	163 ±5	390 ±6
(1X)- Am. Ox.	185 ±9	-	356 ±13	238 ±9	423 ±13
(2X)- Am. Ox.	180 ±13	7 ±5	321 ±8	215 ±5	402 ±15
(1X)- Am. Ox. + (1X)- .1N HCl	163 ±29	12 ±8	315 ±89	171 ±48	346 ±57

Table II - 13

% Aluminum - RBD

Chemical Leach	Concentration in				
	1L	2L	R	R/B	1L + 2L + R/B
none (bulk sediment)	-	-		3.74 ±.08	3.74 ±.08
d.d. water	n.d.	-	4.31 ±.08	3.92 ±.07	3.92 ±.07
(1X)- .1N HCl	0.49 ±.03	-	4.01 ±.07	3.32 ±.06	3.81 ±.07
(2X)- .1N HCl	0.47 ±.02	0.08 ±.02	3.97 ±.07	3.21 ±.06	3.76 ±.07
(1X)- 2N HCl	1.06 ±.03	-	4.38 ±.07	2.55 ±.04	3.61 ±.05
(1X)- Am. Ox.	0.68 ±.05	-	4.95 ±.06	3.01 ±.04	3.69 ±.07
(2X)- Am. Ox.	0.66 ±.05	0.18 ±.02	4.97 ±.07	2.75 ±.04	3.58 ±.07
(1X)- Am. Ox. + (1X)- .1N HCl	0.62 ±.05	0.29 ±.02	4.94 ±.07	2.70 ±.04	3.61 ±.07

Table II - 14

% Barium - RBD

Chemical Leach	Concentration in				
	1L	2L	R	R/B	1L + 2L + R/B
none (bulk sediment)	-	-		0.50 ±.03	0.50 ±.03
d.d. water	n.d.	-	0.55 ±.05	0.50 ±.05	0.50 ±.05
(1X)- .1N HCl	0.33 ±.03	-	0.21 ±.04	0.17 ±.03	0.50 ±.05
(2X)- .1N HCl	0.31 ±.02	0.13 ±.01	0.05 ±.00	0.04 ±.00	0.47 ±.02
(1X)- 2N HCl	0.44 ±.09	-	0.02 ±.00	0.01 ±.00	0.46 ±.09
(1X)- Am. Ox.	0.16 ±.01	-	0.65 ±.04	0.40 ±.03	0.56 ±.03
(2X)- Am. Ox.	0.15 ±.01	0.18 ±.02	0.36 ±.06	0.20 ±.04	0.54 ±.04
(1X)- Am. Ox. + (1X)- .1N HCl	0.13 ±.01	0.32 ±.03	0.18 ±.01	0.10 ±.01	0.55 ±.03

Table II - 15

% Calcium - RBD

Chemical Leach	Concentration in				
	1L	2L	R	R/B	1L + 2L + R/B
none (bulk sediment)	-	-		2.06 ±.05	2.06 ±.05
d.d. water	0.15 ±.002	- -	2.04 ±.06	1.85 ±.06	2.01 ±.06
(1X)- .1N HCl	2.27 ±.03	-	1.29 ±.01	1.07 ±.01	3.34 ±.12
(2X)- .1N HCl	2.86 ±.03	0.02 ±.00	0.46 ±.02	0.37 ±.02	3.25 ±.04
(1X)- 2N HCl	1.68 ±.06	-	0.34 ±.03	0.20 ±.02	1.88 ±.06
(1X)- Am. Ox.	0.22 ±.01	-	2.59 ±.06	1.58 ±.04	1.80 ±.04
(2X)- Am. Ox.	0.16 ±.01	0.17 ±.01	2.71 ±.09	1.50 ±.05	1.83 ±.05
(1X)- Am. Ox. + (1X)- .1N HCl	0.15 ±.01	1.50 ±.03	0.41 ±.02	0.23 ±.01	1.87 ±.03

Table II - 16

PPM Cobalt - RBD

Chemical Leach	Concentration in				
	1L	2L	R	R/B	1L + 2L + R/B
none (bulk sediment)	-	-		239 ±22	239 ±22
d.d. water	n.d.	-	272 ±27	248 ±25	248 ±25
(1X)- .1N HCl	n.d.	-	285 ±22	236 ±18	236 ±18
(2X)- .1N HCl	n.d.	n.d.	290 ±17	235 ±14	235 ±14
(1X)- 2N HCl	89 ±22	- -	160 ±30	93 ±17	182 ±28
(1X)- Am. Ox.	210 ±82	-	46 ±34	28 ±21	238 ±85
(2X)- Am. Ox.	207 ±65	n.d.	n.d.	-	207 ±65
(1X)- Am. Ox. + (1X)- .1N HCl	202 ±92	n.d.	44 ±33	24 ±18	226 ±94

Table II - 17

PPM Copper - RBD

Chemical Leach	Concentration in				
	1L	2L	R	R/B	1L + 2L + R/B
none (bulk sediment)	-	-		1,803 ±51	1,803 ±51
d.d. water	n.d.	-	1,972 ±43	1,795 ±39	1,795 ±39
(1X)- .1N HCl	570 ±13	-	1,478 ±40	1,225 ±33	1,795 ±35
(2X)- .1N HCl	527 ±12	144 ±13	1,477 ±45	1,197 ±36	1,868 ±40
(1X)- 2N HCl	920 ±10	-	1,396 ±17	811 ±10	1,731 ±14
(1X)- Am. Ox.	877 ±15	-	1,447 ±8	880 ±5	1,757 ±16
(2X)- Am. Ox.	869 ±14	112 ±7	1,400 ±8	774 ±4	1,755 ±16
(1X)- Am. Ox. + (1X)- .1N HCl	824 ±17	72 ±9	1,552 ±20	848 ±11	1,744 ±22

Table II - 18

% Iron - RBD

Chemical Leach	Concentration in				
	1L	2L	R	R/B	1L + 2L + R/B
none (bulk sediment)	-	-		25.72 ±.45	25.72 ±.45
d.d. water	0.004 ±.003	-	25.10 ±.65	22.84 ±.59	22.85 ±.59
(1X)- .1N HCl	1.27 ±.02	-	28.25 ±.75	23.41 ±.62	24.68 ±.62
(2X)- .1N HCl	1.22 ±.02	0.38 ±.02	30.40 ±.50	24.64 ±.40	26.23 ±.40
(1X)- 2N HCl	8.56 ±.19	-	27.85 ±.84	16.19 ±.49	24.75 ±.52
(1X)- Am. Ox.	8.18 ±.10	-	26.93 ±.89	16.38 ±.54	24.56 ±.55
(2X)- Am. Ox.	7.98 ±.08	2.17 ±.09	26.04 ±1.06	14.40 ±.59	24.56 ±.60
(1X)- Am. Ox. + (1X)- .1N HCl	7.47 ±.08	0.53 ±.02	29.75 ±.92	16.25 ±.50	24.25 ±.51

Table II - 19

% Potassium - RBD

Chemical Leach	Concentration in				
	1L	2L	R	R/B	1L + 2L + R/B
none (bulk sediment)	-	-		0.84 ±.04	0.84 ±.04
d.d. water	0.18 ±.01	-	0.69 ±.07	0.63 ±.06	0.81 ±.06
(1X)- .1N HCl	0.43 ±.01	-	0.52 ±.04	0.43 ±.04	0.87 ±.04
(2X)- .1N HCl	0.44 ±.01	0.03 ±.00	0.50 ±.04	0.41 ±.03	0.87 ±.03
(1X)- 2N HCl	0.43 ±.03	-	0.69 ±.02	0.40 ±.01	0.83 ±.04
(1X)- Am. Ox.	0.38 ±.01	-	0.75 ±.02	0.46 ±.01	0.84 ±.02
(2X)- Am. Ox.	0.37 ±.01	0.01 ±.00	0.82 ±.02	0.45 ±.01	0.84 ±.02
(1X)- Am. Ox. + (1X)- .1N HCl	0.38 ±.01	0.03 ±.00	0.77 ±.02	0.42 ±.01	0.83 ±.01

Table II - 20

% Magnesium - RBD

Chemical Leach	Concentration in				
	1L	2L	R	R/B	1L + 2L + R/B
none (bulk sediment)	-	-		1.91 ±.02	1.91 ±.02
d.d. water	0.19 ±.00	-	1.90 ±.02	1.73 ±.01	1.91 ±.01
(1X)- .1N HCl	0.88 ±.01	-	1.45 ±.02	1.20 ±.02	2.07 ±.02
(2X)- .1N HCl	0.86 ±.01	0.08	1.34 ±.02	1.09 ±.02	2.02 ±.02
(1X)- 2N HCl	1.17 ±.02		1.30 ±.02	0.75 ±.01	1.93 ±.02
(1X)- Am. Ox.	1.00 ±.05		1.48 ±.02	0.90 ±.01	1.90 ±.05
(2X)- Am. Ox.	0.97 ±.02	0.07 ±.02	1.47 ±.02	0.81 ±.01	1.86 ±.03
(1X)- Am. Ox. + (1X)- .1N HCl	0.96 ±.05	0.07 ±.00	1.55 ±.02	0.85 ±.01	1.88 ±.05

Table II - 21

% Manganese - RBD

Chemical Leach	Concentration in				
	1L	2L	R	R/B	1L + 2L + R/B
none (bulk sediment)	-	-		6.65 ±.20	6.65 ±.20
d.d. water	n.d.	-	7.61 ±.18	6.93 ±.16	6.93 ±.16
(1X)- .1N HCl	0.15 ±.00	-	8.09 ±.24	6.70 ±.20	6.85 ±.20
(2X)- .1N HCl	0.15 ±.00	0.02 ±.00	8.00 ±.21	6.49 ±.17	6.66 ±.17
(1X)- 2N HCl	2.93 ±.03	-	6.14 ±.26	3.57 ±.15	6.50 ±.15
(1X)- Am Ox.	6.60 ±.10	-	2.28 ±.17	1.38 ±.11	7.98 ±.14
(2X)- Am. Ox.	6.50 ±.05	0.03 ±.01	1.51 ±.27	0.84 ±.15	7.36 ±.16
(1X)- Am. Ox. + (1X)- .1N HCl	6.46 ±.05	0.04 ±.00	1.71 ±.21	0.93 ±.11	7.43 ±.12

Table II - 22

PPM Nickel - RBD

Chemical Leach	Concentration in				
	1L	2L	R	R/B	1L + 2L + R/B
none (bulk sediment)	-	-		1,439 ±160	1,439 ±160
d.d. water	n.d.	-	1,616 ±195	1,471 ±177	1,471 ±177
(1X)- .1N HCl	326 ±27	-	1,563 ±167	1,295 ±138	1,621 ±141
(2X)- .1N HCl	282 ±38	168 ±31	1,395 ±157	1,131 ±127	1,581 ±136
(1X)- 2N HCl	864 ±56	-	1,184 ±140	688 ±81	1,552 ±98
(1X)- Am. Ox.	1,103 ±63	-	78 ±11	47 ±7	1,150 ±63
(2X)- Am. Ox.	1,115 ±61	n.d.	80 ±11	44 ±6	1,159 ±61
(1X)- Am. Ox. + (1X)- .1N HCl	1,089 ±69	51 ±18	79 ±9	43 ±5	1,183 ±71

Table II - 23

% Silicon - RBD

Chemical Leach	Concentration in				
	1L	2L	R	R/B	1L + 2L + R/B
none (bulk sediment)	-	-		8.91 ±.39	8.91 ±.39
d.d. water	n.d.	-	8.86 ±.38	8.07 ±.34	8.07 ±.34
(1X)- .1N HCl	0.27 ±.20	-	9.74 ±.40	8.07 ±.33	8.34 ±.39
(2X)- .1N HCl	0.27 ±.19	n.d.	10.09 ±.42	8.18 ±.34	8.44 ±.39
(1X)- 2N HCl	1.97 ±.32	-	12.41 ±.51	7.21 ±.30	9.18 ±.44
(1X)- Am. Ox.	0.72 ±.08	-	12.86 ±.51	7.82 ±.31	8.54 ±.32
(2X)- Am. Ox.	0.81 ±.09	0.13 ±.01	14.22 ±.48	7.87 ±.27	8.81 ±.28
(1X)- Am. Ox. + (1X)- .1N HCl	0.60 ±.07	n.d.	13.88 ±.54	7.58 ±.29	8.18 ±.30

Table II - 24

PPM Zinc - RBD

Chemical Leach	Concentration in				
	1L	2L	R	R/B	1L + 2L + R/B
none (bulk sediment)	-	-		552 ±23	552 ±23
d.d. water	n.d.	-	555 ±20	505 ±18	505 ±18
(1X)- .1N HCl	174 ±6	-	437 ±18	362 ±15	536 ±16
(2X)- .1N HCl	200 ±6	n.d.	392 ±20	318 ±16	518 ±17
(1X)- 2N HCl	298 ±7	-	464 ±9	270 ±5	568 ±9
(1X)- Am. Ox.	240 ±5	-	519 ±17	316 ±10	556 ±11
(2X)- Am. Ox.	247 ±42	28 ±6	491 ±14	272 ±8	547 ±43
(1X)- Am. Ox. + (1X)- .1N HCl	237 ±5	13 ±6	532 ±12	291 ±7	541 ±10

Elemental Oxide Balances of AAS Chemical Analyses

Table II-25 presents the AAS analyses for BBD and RBD bulk samples in their raw form and as the corresponding oxides. The sodium content is converted to NaCl as this is the most important Na phase present in the freeze-dried bulk sediment. It is seen that the sum of the oxides + NaCl add up to about 90% for each case. This figure incorporates errors such as incomplete analyses of all elements present, errors of analysis, and the fact that the presence of water of hydration has not been included. Including the weight loss values determined at 500°C during the LECO carbonate analyses, the mass balance figures approach more closely a complete analysis. The heating at 500°C is probably strong enough to drive off part of the sample and so the weight loss figures given are somewhat high estimates of water content. The final figures for sum of oxides NaCl + volatiles indicate that all major elements present in the samples have been analyzed and that the analytical technique was good. This is an important confirmation, as most analyses given in this work are presented as ppm or % of the metallic element rather than as oxides.

Comparison of the results listed under column (1L + 2L + R/B) in Tables II-1 through II-24 indicates quite good agreement for most analyses and most elements. Some discrepancies are evident and these are undoubtedly due to analytical errors in the leachate fractions. It should be kept in mind that all leach residues were analyzed in exactly the same manner and with the same matrix. The leachates on the other hand varied quite markedly in matrix composition, i.e., d.d. water,

Table II - 25

Atomic Absorption Data for Bulk Sediments
BBD and RBD Recalculated to
the Oxides

	BBD (Y73-3-21K)		RBD (Y73-3-64K)	
Element	% Element	% Oxide	% Element	% Oxide
Al	2.84	5.37	3.74	7.07
Ba	1.63	1.82	0.50	0.56
Ca	3.37	4.72	2.06	2.88
Co	0.02	0.03	0.02	0.03
Cu	0.11	0.14	0.18	0.23
Fe	13.59	19.43	25.72	36.77
K	1.53	1.84	.84	1.01
Mg	2.22	3.68	1.91	3.17
Mn	5.01	7.93	6.65	10.52
Na	5.13	13.04*	3.38	8.59*
Ni	0.07	0.09	0.14	0.18
Si	14.66	31.38	8.91	19.07
Zn	0.04	0.05	0.06	0.07
Lanthanides	∿.06	∿.07	∿.07	∿.08
% Loss @ 500% C (H_2O)		10.33		13.31
Sum of Oxides + NaCl		89.6%		90.2%
Sum of Oxides + NaCl + Volatiles		99.9%		103.5%

*as the chloride

.1N HCl, 2N HCl; and ammonium oxalate-oxalic acid. No previous experience has been collected at our labs in the area of doing AAS work with such different matrices. One problem which became quite obvious immediately was that Ba, and probably Ca standards could not be prepared with an oxalic acid matrix due to immediate precipitation of the insoluble BaOX and CaOx. What other elements may have been affected to a greater or lesser degree by such effects or by other effects such as stable complex formations and how these reactions could effect the AAS results is unknown. It will be noted, for example, that the results in the final column of the 2N HCl leach treatment vary most often and most widely from neighboring values.

The interpretation of the data are primarily based on the residue analyses and so variations in leachate results are more complementary than primary in value. These data tend to lend support to leach effects observed in the residues rather than acting as primary evidence of such effects. That most of the data show consistent leaching patterns adds support to the quality of the AAS results.

APPENDIX III

Concentrations of Unleachable Elements in the Sediments of BBD and RBD Based on AAS and INAA Analysis

Code for Column Headings for Appendix III Tables

a. - residue of d.d. water leach

b. - residue of (1X) - .1N HCl leach

c. - residue of (2X) - .1N HCl leach

d. - residue of (1X) - 2N HCl leach

e. - residue of (1X) - am. ox. leach

f. - residue of (2X) - am. ox. leach

g. - residue of (1X) - am. ox. leach + (1X) .1N HCl leach

The data presented have been adjusted for the sample weight loss due to leaching, and the original bulk sample "salt content". Values given in the tables are then the unleachable concentration, of the given element present in the "salt free" sediment.

The concentration values in Tables III-1 to III-2, and III-4 to III-5, are further reduced to unleachable elemental ratios in Tables III-3, and III-6 respectively. These ratios are the result of dividing the concentration value in any given column by the corresponding value listed in column (a) of that same table.

Example:

The fraction of (1X) am. ox. unleachable Cu in RBD is found by dividing 974 PPM (Table III-4, column (e)) by 1,972 PPM (Table III-4, column (a)) to obtain 0.49 (value given in Table III-6, column (e)) for this element.

Table III-1

AAS Data for Y73-3-21K (BBD) Given on a Salt Free Sediment Basis

Element	Treatment (a)	(b)	(c)	(d)
Al	3.40±2.2	2.82±3.0	2.80±2.5	1.89±2.6
Ba	1.91±5.8	1.27±5.8	0.46±11.8	0.16±5.5
Ca	3.77±2.3	1.79±1.9	0.37±4.7	0.38±4.3
Co	275±8.4	265±9.0	244±8.4	118±20.2
Cu	1,310±2.4	806±4.4	799±4.0	610±0.85
Fe	16.77±2.5	15.43±2.7	16.49±2.9	9.06±5.9
K	1.40±3.3	0.64±9.1	0.52±8.4	0.54±2.1
Mg	2.25±0.89	1.46±2.1	1.47±2.2	1.11±1.2
Mn	5.51±3.8	5.45±3.9	5.72±2.9	2.97±4.8
Ni	780±21.3	604±30.2	551±29.1	395±20.0
Si	16.80±3.5	16.73±3.4	16.89±3.1	14.83±2.5
Zn	498±3.6	613±3.5	428±3.7	193±3.0

Note: 1) all error terms given as % of element concentration shown

2) all elemental concentrations are given in % except for Co, Cu, Ni, and Zn which are given in PPM

Table III-1
Continued

Element	(e)	(f)	(g)
Al	3.11±1.1	3.03±1.4	2.42±1.4
Ba	1.78±6.1	1.38±5.3	0.97±6.8
Ca	3.12±2.0	2.96±2.2	2.70±5.8
Co	n.d.	n.d.	32.8±64.7
Cu	637±0.75	591±.078	600±1.0
Fe	11.55±6.7	11.15±6.5	9.17±5.2
K	0.66±1.9	0.60±2.3	0.57±1.9
Mg	1.44±1.0	1.35±1.0	1.26±1.0
Mn	0.95±13.7	0.69±25.4	0.72±14.6
Ni	40.4±17.7	37.6±18.4	27.0±23.8
Si	16.23±2.8	16.27±3.1	15.76±2.5
Zn	282±3.7	246±2.5	202±28.3

Table III-2

INAA Data for Y73-3-21K BBD Given on a Salt Free Sediment Basis

Element	Treatment			
	(a)	(b)	(c)	(d)
As	92.6±2.4	98.5±1.9	94.3±1.9	75.2±2.0
Ba	18,178±2.1	15,197±2.2	4,842±2.7	547±5.8
Ce	71.1±1.3	53.7±1.5	50.0±1.6	17.6±2.5
Co	289±1.0	295±1.0	309±1.0	219±1.1
Cr	15.6±4.8	18.2±4.5	13.2±5.4	15.6±4.7
Eu	11.3±4.7	2.2±7.0	1.0±9.3	n.d.
Fe	17.48±0.7	17.24±0.7	16.06±0.7	13.39±0.7
Hf	4.8±3.5	5.8±2.7	4.8±3.0	2.9±4.7
K	n.d.	6,394±13.0	5,666±13.0	6,009±11.9
La	256±1.4	47.4±2.1	26.9±2.7	5.4±5.4
Lu	7.0±4.1	1.3±4.9	0.6±5.8	n.d.
Na	6,219±2.1	2,659±1.8	2,458±1.8	2,455±1.7
Nd	238±1.9	70.4±3.2	n.d.	n.d.
Sb	12.1±8.1	12.3±8.1	11.4±8.4	7.1±9.3
Sc	27.7±0.5	17.7±0.6	14.5±0.6	10.8±0.6
Sm	38.4±0.5	7.4±0.8	3.6±1.1	0.6±2.3
Tb	6.0±1.4	1.0±2.8	0.6±3.7	n.d.
Th	3.6±2.6	4.6±2.3	3.9±2.5	1.4±4.0
W	n.d.	9.0±6.9	8.5±6.9	8.3±6.6
Yb	42.9±3.3	7.7±4.5	3.5±5.9	n.d.

1) All values except Fe given in PPM
2) Iron value given as percentage
3) All error terms given as % of value shown

Table III-2 (Cont.)

Element	(e)	(f)	(g)
As	38.2±2.7	28.9±3.1	32.6±2.5
Ba	16,304±2.1	12,507±2.2	11,328±2.3
Ce	33.1±1.7	22.1±2.4	12.6±3.0
Co	4.6±5.2	3.9±6.3	2.8±7.2
Cr	20.3±3.8	17.2±4.6	20.1±4.2
Eu	11.2±4.6	9.6±4.8	4.2±5.7
Fe	12.51±0.7	11.43±0.9	11.45±0.8
Hf	2.4±3.7	2.4±4.2	2.8±3.8
K	n.d.	n.d.	n.d.
La	252±1.3	229±1.4	94.3±1.6
Lu	5.8±4.0	5.3±4.2	1.9±4.5
Na	3,174±2.0	3,242±2.0	2,389±1.8
Nd	243±1.7	208±2.0	94.3±2.8
Sb	3.8±10.8	4.9±10.8	5.0±10.4
Sc	20.8±0.5	20.7±0.5	11.7±0.7
Sm	36.9±0.5	33.9±0.5	15.7±0.6
Tb	5.0±1.4	4.6±1.5	2.0±2.0
Th	2.2±3.0	2.4±3.2	1.7±3.7
W	n.d.	n.d.	n.d.
Yb	36.3±3.3	34.4±3.4	13.7±3.8

1) All values except Fe given in PPM
2) Iron value given as percentage
3) All error terms given as % of value shown

Table III-3

Unleachable Fraction of Element Present in the Salt Free Sediment of Y73-3-21K (BBD)

Element	Leach Treatment					
	(b)	(c)	(d)	(e)	(f)	(g)
Al	.83	.82	.56	.91	.89	.71
As	1.06	1.02	.81	.41	.31	.35
Ba	.87	.28	n.d.	.94	.71	.63
Ca	.47	.10	.10	.83	.78	.07
Ce	.76	.70	.25	.47	.31	.18
Co	1.02	1.07	.76	.02	.01	.01
Cr	1.17	.85	1.00	1.30	1.10	1.29
Cu	.62	.61	.47	.49	.45	.46
Eu	.19	.09	.00	.99	.85	.37
Fe	.92	.98	.54	.69	.67	.55
Hf	1.21	1.00	.60	.50	.50	.58
K	.46	.37	.38	.47	.43	.41
La	.19	.11	.02	.98	.89	.37
Lu	.16	.05	n.d.	.75	.69	.29
Mg	.65	.66	.49	.64	.60	.56
Mn	.99	1.04	.54	.17	.13	.13
Na	.43	.40	.39	.51	.52	.38
Nd	.30	n.d.	n.d.	1.02	.87	.40
Ni	.77	.71	.51	.05	.05	.03
Sb	1.02	.94	.59	.31	.40	.41
Sc	.64	.52	.39	.75	.75	.42
Si	1.00	1.01	.88	.97	.97	.94
Sm	.19	.09	.02	.96	.88	.41
Tb	.17	.10	.00	.83	.77	.33
Th	1.28	1.08	.39	.61	.67	.47
W			not detected			
Yb	.18	.08	n.d.	.85	.80	.32
Zn	1.23	.86	.39	.57	.49	.41

n.d. = not detected

Table III-4

AAS Data for Y73-4-64K (RBD)

Given on a Salt Free Sediment Basis

Element	Treatment			
	(a)	(b)	(c)	(d)
Al	4.31±1.8	3.68±1.8	3.56±1.9	2.82±1.6
Ba	0.55±9.0	0.19±18.0	0.04±7.2	0.02±18.1
Ca	2.04±3.0	1.18±11.3	0.41±4.8	0.22±7.7
Co	272±9.9	261±7.7	260±5.9	103±18.8
Cu	1,972±2.2	1,356±2.7	1,326±3.1	898±1.2
Fe	25.10±2.6	25.92±2.7	27.28±1.6	17.92±3.0
K	0.69±9.5	0.48±8.2	0.45±7.8	0.45±2.2
Mg	1.90±0.8	1.33±1.7	1.21±1.4	0.83±1.4
Mn	7.61±2.4	7.43±2.9	7.18±2.7	3.95±4.2
Ni	1,616±12.1	1,434±10.7	1,252±11.3	762±11.8
Si	8.86±4.3	8.93±4.1	9.05±4.2	7.98±4.1
Zn	555±3.6	401±4.1	352±5.1	299±1.9

Note: 1) all error terms given as % of element concentration shown

2) all elemental concentrations are given in % except for Co, Cu, Ni, and Zn which are given in PPM

Table III-4

(cont.)

Element	(e)	(f)	(g)
Al	3.33±1.3	3.05±1.4	2.99±1.4
Ba	0.44±6.6	0.22±17.5	0.11±8.0
Ca	1.75±2.3	1.66±3.3	0.25±5.4
Co	31±73.9	n.d.	27±75.0
Cu	974±0.55	858±0.57	939±1.3
Fe	18.14±3.3	15.95±4.1	18.00±3.1
K	0.51±2.2	0.50±2.6	0.47±2.4
Mg	1.00±1.1	0.90±1.2	0.94±1.1
Mn	1.53±7.6	0.93±17.7	1.03±12.1
Ni	52±14.1	49±13.8	47.8±11.4
Si	8.66±4.0	8.71±3.4	8.40±3.9
Zn	350±3.3	301±2.9	322±2.3

Table III-5

INAA Data for Y73-4-64K (RBD) Given on a Salt Free Sediment Basis

Element	Treatment			
	(a)	(b)	(c)	(d)
As	387±1.7	387±1.6	386±1.6	328±1.6
Ba	5,163±2.5	2,231±3.0	1,056±3.9	-
Br	7.8±6.0	8.3±5.3	7.6±5.3	9.6±5.3
Ce	163±0.8	117±0.9	114±0.9	29.2±1.7
Co	275±1.0	272±1.0	272±1.0	204±1.0
Cr	26.3±3.4	20.8±3.8	23.8±3.5	17.3±3.8
Eu	12.6±4.5	1.8±7.1	1.0±8.9	-
Fe	28.05±0.6	28.00±0.6	25.53±0.6	21.23±0.6
Hf	7.6±2.5	7.4±2.2	7.2±2.2	4.2±2.6
K	n.d.	n.d.	n.d.	n.d.
La	230±1.4	42.7±2.3	26.4±2.7	8.6±4.2
Lu	4.7±4.2	0.9±5.4	0.6±5.4	0.4±6.3
Na	4,597±1.8	3,358±1.7	3,397±1.7	4,255±1.7
Nd	247±1.7	-	-	-
Sb	19.0±7.2	20.2±7.1	18.9±7.2	13.4±7.4
Sc	27.6±0.4	19.5±0.5	18.1±0.5	11.5±0.6
Sm	49.1±0.5	6.8±0.8	3.8±1.0	1.3±1.6
Tb	6.0±1.3	1.1±2.6	0.9±2.8	0.1±6.9
Th	7.1±1.9	7.1±1.7	6.8±1.7	1.7±3.0
W	33.8±7.3	26.4±5.2	25.0±5.2	27.0±5.0
Yb	30.4±3.5	3.3±5.6	4.7±5.0	1.6±7.2

1) All values except Fe in PPM
2) Iron values given in %
3) All error terms given in % of value shown

Table III-5 (cont.)

Element	(e)	(f)	(g)
As	214±1.8	192±1.7	233±1.6
Ba	3,688±2.5	2,915±2.6	1,141±3.5
Br	9.1±5.3	7.1±4.9	6.3±5.1
Ce	51.3±1.2	34.8±1.4	21.9±1.9
Co	5.6±4.2	5.1±4.4	5.2±4.6
Cr	23.9±3.1	28.1±2.8	20.6±3.5
Eu	9.8±4.5	7.5±4.7	3.1±5.7
Fe	17.86±0.6	16.25±0.6	19.48±0.6
Hf	3.4±2.8	2.7±3.1	3.7±2.8
K	n.d.	n.d.	n.d.
La	172±1.4	152±1.3	55.6±1.8
Lu	2.9±4.2	2.5±4.3	1.0±4.8
Na	3,494±2.2	3,356±1.7	3,117±1.6
Nd	207±1.6	175±1.7	83.5±2.3
Sb	8.6±7.9	7.7±8.1	10.6±7.7
Sc	16.1±0.5	14.7±0.5	12.9±0.6
Sm	38.1±0.5	33.4±0.5	13.8±0.6
Tb	4.0±1.4	3.5±1.4	1.4±2.1
Th	2.3±2.5	1.9±2.8	2.1±2.8
W	n.d.	n.d.	n.d.
Yb	20.1±3.5	17.6±3.5	8.2±4.0

1) All values except Fe in PPM
2) Iron values given in %
3) All error terms given in % of value shown

Table III-6

Unleachable Fraction of Element Present in the Salt Free Sediment of Y73-4-64K (RBD)

Element	Leach Treatment					
	(b)	(c)	(d)	(e)	(f)	(g)
Al	.85	.83	.65	.77	.71	.69
As	1.00	1.00	.85	.55	.50	.60
Ba	.43	.20	n.d.	.71	.56	.22
Ca	.58	.20	.11	.86	.81	.12
Ce	.72	.70	.18	.31	.21	.13
Co	.99	.99	.74	.02	.02	.02
Cr	.79	.90	.66	.91	1.07	.78
Cu	.69	.67	.46	.49	.44	.48
Eu	.14	.08	n.d.	.78	.60	.25
Fe	1.00	.91	.76	.64	.58	.69
Hf	.97	.95	.55	.45	.36	.49
K	.69	.65	.64	.73	.77	.67
La	.19	.11	.04	.75	.66	.24
Lu	.18	.10	.06	.62	.56	.22
Mg	.70	.64	.44	.53	.48	.49
Mn	.98	.94	.52	.20	.12	.14
Na	.73	.74	.93	.76	.73	.68
Nd	n.d.	n.d.	n.d.	.84	.71	.34
Ni	.89	.77	.47	.03	.03	.03
Sb	1.06	.99	.71	.45	.41	.56
Sc	.71	.66	.42	.58	.53	.47
Si	1.01	1.02	.90	.98	.98	.95
Sm	.14	.08	.03	.78	.68	.28
Tb	.18	.15	.02	.67	.58	.23
Th	1.00	.96	.24	.32	.27	.30
W	.78	.74	.80	n.d.	n.d.	n.d.
Yb	.11	.15	.05	.66	.58	.27
Zn	.72	.63	.54	.63	.54	.58

n.d. = not detected